Characterization of Anatid herpesvirus 1 (vaccine strain) and understanding the role of viperin and cholesterol in its infection

A Thesis
Submitted in partial fulfillment of the requirements for the Degree of

DOCTOR OF PHILOSOPHY

by

Manisha Pandey

(156106007)

Department of Biosciences and Bioengineering
Indian Institute of Technology Guwahati
Guwahati – 781039, Assam, India
February 2021

Dedicated to My Parents

INDIAN INSTITUTE OF TECHNOLOGY GUWAHATI

DEPARTMENT OF BIOSCIENCES & BIOENGINEERING

DECLARATION

I do hereby declare that the content embodied in this thesis entitled **"Characterization of Anatid herpesvirus 1 (vaccine strain) and understanding the role of viperin and cholesterol in its infection"** is the result of investigations carried out by me in the Department of Biosciences and Bioengineering, Indian Institute of Technology Guwahati, Guwahati, India under the guidance of Dr. Sachin Kumar and Dr. Nitin Chaudhary.

In keeping with the general practice of reporting scientific observations, due acknowledgments have been made wherever the work described is based on the findings of other investigators are referred to.

February 2021

Manisha Pandey

Roll no.156106007

INDIAN INSTITUTE OF TECHNOLOGY GUWAHATI

DEPARTMENT OF BIOSCIENCES & BIOENGINEERING

CERTIFICATE

It is certified that the work described in this thesis entitled **"Characterization of Anatid herpesvirus 1 (vaccine strain) and understanding the role of viperin and cholesterol in its infection"** by Manisha Pandey (Roll No. 156106007) for the award of the degree of Doctor of Philosophy is an authentic record of the results obtained from the research work carried out under my supervision at the Department of Biosciences & Bioengineering, Indian Institute of Technology Guwahati, Guwahati, India, and this work has not been submitted elsewhere for a degree or diploma.

February 2021

Dr. Sachin Kumar
Associate Professor
Thesis Supervisor
Department of Biosciences & Bioengineering
Indian Institute of Technology Guwahati, Assam, India

Dr. Nitin Chaudhary
Associate Professor
Thesis Co-Supervisor
Department of Biosciences & Bioengineering
Indian Institute of Technology Guwahati, Assam, India

Supervisors

Dr. Sachin Kumar

Department of Biosciences & Bioengineering

Indian Institute of Technology Guwahati

Dr. Nitin Chaudhary

Department of Biosciences & Bioengineering

Indian Institute of Technology Guwahati

Doctoral Committee

Prof. Arun Goyal, Chairman

Department of Biosciences & Bioengineering

Indian Institute of Technology Guwahati

Dr. Shankar Prasad Kanaujia

Department of Biosciences & Bioengineering

Indian Institute of Technology Guwahati

Dr. Sunanda Chatterjee

Department of Chemistry

Indian Institute of Technology Guwahati

Characterization of Anatid herpesvirus 1 (vaccine strain) and understanding the role of viperin and cholesterol in its infection

Ph.D. Thesis, Manisha Pandey, 2021

ACKNOWLEDGEMENTS

Working towards the accomplishment of this endeavor has been an incredible journey of my life, which would not have been possible without the encouragement and support of my supervisor, doctoral committee members, my family, friends, and colleagues.

With immense pleasure, I would like to express my sincere gratitude to my supervisors ***Dr. Sachin Kumar*** *and* ***Dr. Nitin Chaudhary****. I wish to thank and acknowledge for their excellent guidance, unwavering support, motivation, and providing me with an excellent atmosphere for carrying out my research work. Without their valuable suggestions and constructive criticism, this work couldn't have been assumed in its current form.*

I would like to thank my Doctoral committee: ***Prof. Arun Goyal, Dr. Shankar Prasad Kanaujia, Dr. Sunanda Chatterjee*** *for their constant review of my Ph.D. work and insightful comments during different phases which helped in the proper execution of this work. I am grateful to Prof. Arun Goyal for providing me access to their lab facilities and suggestions during manuscript writing.*

I would like to extend my thanks to the present and former heads of the Department of Biosciences & Bioengineering, IIT Guwahati, ***Prof. Latha Rangan****,* ***Prof. K. Pakshirajan****, and* ***Prof. Venkata. V. Dasu*** *for providing me with the necessary infrastructure and facilities.*

Sincere gratefulness is expressed to ***Dr. Pankaj Deka****,* ***Dr. N.N. Barman*** *from College of Veterinary Sciences, Khanapara, Assam, India, and* ***Dr. Puro*** *from ICAR-NEH, Barapani, Meghalaya, India for providing AnHV-1 related studies and their immense help in conducting animal studies. I am also thankful to* ***Dr. R. Iorio*** *from the University of Massachusetts, USA, for providing a monoclonal antibody against HN protein of NDV.*

I am thankful to the Department of Biosciences & Bioengineering and Central Instrumentation Facility (CIF), IITG for providing me instruments for my research work. I am also thankful to the Ministry of Human Resource and Development, Govt. of India for providing fellowship throughout my Ph.D.

I wish to acknowledge the support received from other teaching and non-teaching staff of the Department of Biosciences and Bioengineering, IIT Guwahati.

My humble thankfulness to all the past and present lab members for the support and advice offered by them. My heartfelt thanks to ***Sudhir Morla, Barnali Nath, Vishnu Kumar, MSK Bharadwaj, Yoya Vashi, Anjali Gupta, Kamal Shokeen, Shambhavi Pandey, Shubham Gaurav, Vipin Jagrit, Poonam Lamba, and Neta Venkatesh*** *for their needful help and cooperation throughout my work. I am thankful to my friends* ***S. Sanjana, Sunanda Chhetry,*** *and* ***Ganesh. N*** *who has been my family on the campus and* ***Prajakta Deshpande*** *for constructive discussion and motivation.*

Finally, I would like to express my deepest sense of gratitude and affection to ***My parents*** *and my elder sister* ***Nisha Shah*** *for their blessings and immense belief in me and have encouraged me to go ahead in my career. I will always be indebted to them for their daily support, sacrifice, and selfless love. My humble thanks to my brother,* ***Alok Shah,*** *and my niece* ***Vidhi*** *for relieving my stress and cheering me up during difficult times, my thanks equally go to my* ***parents-in-law*** *for their encouragement.*

I owe greatly to my husband, ***Vinay Shankar Pandey****. I am highly thankful for his relentless support, understanding, perpetuated encouragement, and listening to my problems, and providing perspective during my Ph.D. endeavor. I immensely value his contribution and faith in me.*

Manisha Pandey

February 2021

Table of Contents

Abbreviations

µm	Micromolar
µl	Microliter
mM	Millimolar
ANOVA	Analysis of variance
AnHV-1	Anatid Herpesvirus 1
ATCC	American type culture collection
Bp	Base pairs
BoHV-1	Bovine Herpesvirus 1
CEF	Chicken embryo fibroblast
cDNA	Complementary DNA
CPE	Cytopathic effect
dpi	Days post-infection
DVE	Duck viral enteritis
DEF	Duck embryo fibroblast
DEL	Duck embryo liver
DF-1	Continuous chicken fibroblast cell line
DMEM	Dulbecco's modified Eagle's medium
DNA	Deoxyribonucleic acid
F	Fusion protein of NDV
FBS	Fetal bovine serum
FITC	Fluorescein isothiocyanate
FPPS	Farnesyl pyrophosphate synthase
gC	Glycoprotein C of AnHV-1
GAPDH	Glyceraldehyde 3-phosphate dehydrogenase
GM-CSF	Granulocyte-macrophage colony-stimulating factor
hpi	Hours post-infection
HIV	Human immunodeficiency virus
HCV	Hepatitis virus
HEp-2	Human epithelial type 2 cells
HDV	Hepatitis delta virus
HN	Hemagglutinin-Neuraminidase protein of NDV
HMG-CoA	3-hydroxy-3-methylglutaryl-CoA

HSV-1	Herpes Simplex Virus 1
HSPG	Heparan sulfate proteoglycans
ICPI	Intracerebral pathogenicity index
ICTV	International Committee on Taxonomy of Viruses
IIFA	Indirect immunofluorescence assay
IFN	Interferon
ISG	Interferon stimulated gene
ILTV	Infectious Laryngotracheitis
IFIT	IFN-induced proteins with tetratricopeptide repeats
I-TASSER	Iterative threading assembly refinement
Kb	Kilobase
L	RNA dependent RNA polymerase of NDV
LDs	Lipid droplets
M	Matrix protein of NDV
MDT	Mean death time
MOI	Multiplicity of infection
MDCK	Madin-Darby Canine Kidney
MDV	Marek Disease Virus
MβCD	Methyl-beta-cyclodextrin
MVA/T7	Recombinant modified vaccinia virus Ankara bearing T7 gene
MTT	3-(4,5-dimethylthiazol-2-yl)-2,5-diphenyl tetrazolium bromide
Mx 1	Myxovirus resistance 1
NDV	Newcastle Disease Virus
N	Nucleoprotein of NDV
NI	Neutralisation indices
NCBI	National center for biotechnology information
NCCS	National center for cell science
OIE	World Organisation for Animal Health
ORF	Open reading frame
OAS	2′-5′-oligoadenylate synthetase
P	Phosphoprotein of Newcastle Disease Virus
PBS	Phosphate buffered saline
PBST	Phosphate buffered saline Tween-20

PCR	Polymerase chain reaction
PBMC	Peripheral blood mononuclear cells
pNDV	rNDV full length expression plasmid
pNDV.viperin	Plasmid bearing chicken viperin gene
PRV	Pseudorabies virus
PRR	Pattern recognition receptor
PKR	Protein kinase R
QT-35	Japanese quail fibrosarcoma cell line
qRT-PCR	Quantitative PCR
rpm	Revolutions per minute
RNA	Ribonucleic acid
RMSD	Root Mean Square Deviation
RSAD 2	Radical S-adenosyl methionine domain-containing protein 2
rNDV	Recombinant NDV
rNDV.viperin	rNDV expressing viperin
rNDV.GFP	rNDV expressing green fluorescent protein
SD	Standard deviation
SPF	Specific pathogen-free
TCID50	Tissue culture infectious dose
TG	Trigeminal ganglia
TEM	Transmission electron microscopy
TLR	Toll-like receptor
Vero	African green monkey kidney
Viperin	Virus inhibitory protein, endoplasmic reticulum associated, IFN Inducible
VZV	Varicella-Zoster virus
VSV	Vesicular stomatitis virus
WNV	West Nile Virus
ZAP	Zinc-finger antiviral protein

List of figures

Page no.

base 2. The results were statistically analyzed using one-way ANOVA (Dunnett's multiple comparisons test, GraphPad Prism 8). An asterisk indicates a significant difference (*), (**), (***) of $P < 0.05$; $P < 0.01$; $P < 0.001$ respectively (B). The cell lysates were prepared at 48 h post-transfection and analyzed for viperin protein by an immune blot. The β-actin was used as a loading control (C).

Figure 4.4. The expression of the AnHV-1, UL30 gene was analyzed by the semi-quantitative PCR in DF-1 cells transfected with pcDNA3.1 and pcDNA.viperin (A) The mRNA expression of gC gene of AnHV-1 was analyzed by the qRT-PCR, and mRNA levels were normalized to GAPDH mRNA and represented as mean fold expression with respect to control. The fold change in gene expression was calculated by $2^{-\Delta\Delta Ct}$ and the data were transformed in log base 2. The results were statistically analyzed using one-way ANOVA (Dunnett's multiple comparisons test, GraphPad Prism 8). (B). The DF-1cells were transfected with pcDNA3.1 and pcDNA.viperin, and cell lysates were analyzed for AnHV-1 protein by western blot at 72hpi. The β-actin was used as a loading control. (C). The pcDNA3.1 and pcDNA.viperin transfected cells were infected with AnHV-1, and virus yield was calculated by $TCID_{50}$ (D). The data represent the mean ± standard deviation of three independent experiments. Statistical significance difference was determined by using one-way ANOVA (Dunnett's multiple comparisons test, GraphPad Prism 8). An asterisk indicates a significant difference (*), (**), (***) of $P < 0.05$; $P < 0.01$; $P < 0.001$ respectively. 66

Figure 4.5. Cellular localization of viperin and lipid droplets. The DF-1 cells were seeded over coverslip, and the cells have been transiently transfected with viperin. The cells were analyzed by immunofluorescence for localization to lipid droplets using BODIPY lipid droplet marker and mouse anti-FLAG antibody for viperin expression after 48 h post-transfection. Representative images represent DF-1 cells stained with anti-viperin (red channel) and lipid droplets (green channel). The merged panel shows the co-localization of viperin and lipid droplets. Cell nuclei were stained with DAPI (blue channel). Samples were visualized under confocal microscopy with a magnification of 63X. (A). DF-1 cells were transfected with pcDNA3.1 and pcDNA.viperin, and the amount of cholesterol was determined in comparison to untreated cells using an Amplex red cholesterol assay kit (B). Statistical significance difference was determined by using one-way ANOVA (Dunnett's multiple comparisons test, GraphPad Prism 8) A p-value of less than 0.001 is flagged with three stars (***) and p-valve of more than 0.05 is labeled as non-significant (ns). 67

Figure 4.6. Construction of recombinant plasmid pNDV.viperin (A). The upper strand represents pNDV (T7 promoter, NP, P, M, F-, HN, L, and HDR- hepatitis delta ribozyme) and the lower strand represents pNDV.viperin. The viperin cloned at AscI site between the P and M genes of the NDV antigenomic cDNA. The ORF of viperin has a flanking sequence of NDV gene end (GE), and intergenic T nucleotide, and a gene start (GS). The confirmation of pNDV.viperin full-length clone (B). Lane M: DNA ladder; lane 1: undigested pNDV; lane 2: AscI digested pNDV; lane 3: undigested pNDV.viperin; lane 4: AscI digested pNDV.viperin showing the release of a 1065 bp gene. The PCR confirmation of rNDV.viperin (C). Lane M: DNA ladder; lane 1: amplification by the forward primer of pNDV vector and reverse primer of the viperin gene; lane 2: amplification by viperin gene-specific primer; lane 3: amplification by pNDV specific primers. The western blot analysis for the confirmation of NDV and viperin protein expressions by rNDV.viperin using the monoclonal antibody of HN and polyclonal antibody of viperin, respectively (D). 68

Chapter 5. Role of cholesterol in AnHV-1 infection

concentrations of MβCD, followed by exogenous cholesterol replenishment (C). Real-time analysis of viral mRNA using gC gene-specific amplification. The DF-1 cells were treated with varying concentrations of MβCD and replenished with cholesterol, followed by AnHV-1 infection and analyzed for their relative mRNA levels. The data presented are the average of three independent experiments and were shown as the mean ± S.D. The mRNA determinations were performed by qRT-PCR, and mRNA levels were normalized to GAPDH mRNA and represented as mean fold expression concerning control. Statistical significance difference was determined by using one-way ANOVA (Dunnett's multiple comparisons test, GraphPad Prism 8). A p-value of less than 0.001 is flagged with three stars (***), and a p-value of more than 0.05 is labeled as non-significant (ns) (D). Viral titer was determined after the replenishment of cholesterol by $TCID_{50}$. The data represent the mean ± standard deviation of three independent experiments. Statistical significance difference was determined by using one-way ANOVA (Dunnett's multiple comparisons test, GraphPad Prism 8). A p-value of less than 0.01 is flagged with two stars (**) and a p-value more than 0.05 is labeled as non-significant (ns) (E).

Figure 5.3. Lovastatin blocks AnHV-1 infection by inhibiting cholesterol biosynthesis. Cytotoxicity analyses of lovastatin using MTT assay in DF-1 cells after 48 h. The data represent the mean ± standard deviation of three independent experiments (A). DF-1 cells were treated with 4μM of lovastatin, and the cholesterol content was measured. Statistical significance difference was determined by using one-way ANOVA (Dunnett's multiple comparisons test, GraphPad Prism 8). A p-value of less than 0.05 is flagged with one star (*) (B). The expression of a viral gene (gC) of AnHV-1 was determined by the qRT-PCR and normalized to GAPDH mRNA and represented as mean fold expression concerning control. Statistical significance difference was determined by using one-way ANOVA (Dunnett's multiple comparisons test, GraphPad Prism 8). A p-value of less than 0.01 is flagged with two stars (**) (C). AnHV-1 infectivity post lovastatin treatment was determined with virus titration in DF-1 cells. The data represent the mean ± standard deviation of three independent experiments. Statistical significance difference was determined by using one-way ANOVA (Dunnett's multiple comparisons test, GraphPad Prism 8). A p-value of less than 0.01 is flagged with two stars (**) (D). 84

Figure 5.4. Removal of viral envelope cholesterol affects virus infection. The purified virions were treated with 20 mM MβCD and compared with untreated virion (A). The image shows a single virion comprising of an intact viral envelope (i), and disruption of the viral envelope was observed in MβCD treated virion as indicated by an arrow Samples were visualized under a transmission electron microscopy with a magnification of X 60,000. Virus suspension treated with MβCD was used to infect DF-1 cells, and mRNA expression of viral gC gene was determined by qRT-PCR, and mRNA levels were normalized to GAPDH mRNA and represented as mean fold expression concerning control. Statistical significance difference was determined by using one-way ANOVA (Dunnett's multiple comparisons test, GraphPad Prism 8). A p-value of less than 0.01 is flagged with two stars (**) (B). DF- 1 cell were infected with viral suspension treated with MβCD and untreated control, and virus titer was measured. The data represent the mean ± standard deviation of three independent experiments. Statistical significance difference was determined by using one-way ANOVA (Dunnett's multiple comparisons test, GraphPad Prism 8). A p-value of less than 0.05 is flagged with one star (*) (C). 85

List of tables

Page no.

Chapter 3. The immune response of AnHV-1 immunization in ducks

Chapter 4. Understanding the role of viperin in AnHV-1 infection

Abstract

Anatid herpesvirus 1 (AnHV-1) is the causative agent of duck viral enteritis (DVE) of the *Anatidae* family contains the majority of species in the order of *Anseriformes*. The disease is a highly contagious disease characterized by high mortality rates, , decreased egg production among domestic and wild ducks, swans, geese, and other waterfowl of different ages and thus can cause significant economic losses and posing major to traditional agriculture across the globe. The etiological agent of the disease AnHV-1 is a member of the family *Herpesviridae,* genus *Mardivirus,* and subfamily *Alphaherpesvirinae.*

The disease is controlled by vaccination to the flock with chick embryo adapted attenuated vaccine in developed countries. We propagated and characterized the vaccine strain of AnHV-1 in continuous cell lines Vero, DF-1, QT-35, and MDCK. The study was carried out in a comparative manner using CEF since they are most widely used for AnHV-1 propagation and isolation and observed an enhanced replication of the virus in different cell lines. Compared to chick embryo adapted live vaccine virus, heterologous cell culture system will provide a system devoid of other avian infectious agents and it can be used for propagation and cultivation of AnHV-1 vaccine strain for developing cell culture-based vaccines on a mass scale. A hallmark of a viral infection is a profound reaction by infected cells. Cytokines are released mainly secreted by immune cells in response to infection and help synchronize immune system response and, their concentration varies during infection and function as immunomodulatory. We systemically explored the expression profile of cytokines in different organs and peripheral blood mononuclear cells (PBMC). Our results showed that AnHV-1 could replicate in several tissues and the expression of several cytokines were up-regulated especially in the brain and spleen of infected ducks and well in PBMC. Modulation of innate immune-related genes upon infection with vaccine strain will provide information regarding the protective efficacy of vaccination.

Interferon (IFN) response is the first line of defence against viral infection, which activate the induction of a broad array of antiviral proteins. Virus inhibitory protein, endoplasmic reticulum-associated, IFN-inducible (Viperin) is an IFN-induced protein that obstructs the replication of a variety of viruses by diverse mechanisms. We modeled the structure of chicken viperin protein and showed IFN-induced antiviral protein viperin inhibits AnHV-1 and localizes to lipid droplets in DF-1 cells. It has also been found that the concentration of cholesterol was reduced in viperin overexpressed cells. In addition, a recombinant virus expressing viperin was constructed and recovered using the Newcastle disease virus vector to interrogate its function in viral infection and another therapeutic potential.

Cholesterol is an essential component of the cell membrane and involves in the life cycle of several viruses. During the infection, the immune response also targets the lipid pathway as an approach for virus elimination. The inhibitory function of viperin is related to reduce cholesterol on the membrane of DF-1 cells. We examined the role of cholesterol for both the target cell membrane and the viral envelope. We observed that cholesterol depletion from the cellular membrane results in the inhibition of AnHV-1 infection. The inhibitory effect was moderately restored by exogenous replenishment of cholesterol. Furthermore, the inhibition of endogenous cholesterol synthesis by a statin drug also inhibited the infectivity of AnHV-1. Presumably, the removal of cholesterol from the AnHV-1 envelope might be disrupting the viral envelope resulting in its diminished infectivity. Our finding highlights the engagement of cholesterol in AnHV-1 infectivity and the cellular cholesterol level could be exploited as a potential antiviral against viral infections.

Chapter 1.

Introduction and Review of Literature

1.1 Introduction

The poultry industry constitutes a significant and thriving sector of agriculture worldwide. Poultry is one of the rapidly growing segments of the agriculture sector in India and has undergone an evolution from mere backyard activity to a major commercial activity. In this emerging scenario, queries are being raised about the impact of viral diseases on poultry. Traditionally, the term poultry is used for wildfowl (Galliformes) and waterfowl (Anseriformes). Viral infectious agents such as Newcastle Disease Virus (NDV), Avian Influenza virus (AIV), Infectious Laryngotracheitis Virus (ILTV), Marek Disease Virus (MDV), and Anatid herpesvirus-1 (AnHV-1) the major constraint affecting the poultry industry (Swayne D, 2013). There are approximately 146 species in the family *Anatidae* and they are distributed on every continent of the world. This family is predominantly adapted to an aquatic environment and most commonly referred to as waterfowl. The majority of the species are migratory and play an important ecological role as a part of the food chain. A few species have been domesticated for agriculture, egg, meat, and liver production, and many others are hunted for food and recreation, some members act as vectors for zoonosis such as avian influenza.

1.1.1 Duck viral enteritis

DVE is a highly infectious and contagious disease of *Anatidae* family. It is an acute herpes virus infection of ducks, geese, swans, and other domestic and wild waterfowls (Swayne D, 2013). Bird-to-bird contact with the virus that has contaminated the environment perpetuates an outbreak (Sandhu and Shawky, 2003, Burgess and Yuill, 1983). The disease is responsible for high mortality rates among domestic and wild ducks, swans, geese, and other waterfowl. The infection is accompanied by carcass condemnation, reduction of egg production and hatchability causing significant economic losses to the duck rearing industry across the globe

(Jansen, 1968, Leibovitz and Hwang, 1968, Walker et al., 1969). The disease is known to have global distribution, wherein migratory waterfowl plays a crucial role in disease transmission within and between continents (Brand and Docherty, 1984, Spieker et al., 1996, Wozniakowski and Samorek-Salamonowicz, 2014). Either of sexes from varying age groups of ducks are vulnerable to DVE. It can establish infection in the birds that survive exposure to it; a state referred to as latency. The virus is capable of exhibiting latent infection in trigeminal ganglia and lymphoid tissue after primary infection. During latency, the virus cannot be detected by the standard method, and hence, from this site, re-activation of the virus can occur that results in disease outburst (Shawky and Schat, 2002).

1.1.2 Virus

The etiological agent of DVE is AnHV-1, as per taxonomic classification by the International Committee on Taxonomy of Viruses (ICTV), AnHV-1 belongs to order *Herpesvirales*, family *Herpesviridae*, subfamily *Alphaherpesvirinae*, and genus *Mardivirus* (Walker et al.,2020, Roizmann et al. 1992). It is an enveloped virus that has a diameter of 120-130 nm with a globular shape (Gardner et al., 1993, Yuan et al., 2005). The viral genome is double-stranded DNA of approximately 158-162kb in length (Li et al., 2009, Wuet al., 2012) which encodes for 78 open reading frames (ORFs). The virion has a complex structure consisting of four structural components: a bilayer-lipid envelope, tegument, an icosahedral capsid, and a linear double-stranded DNA (Grunewald et al., 2003, Yuan et al., 2005). The complete genome is composed of unique long and unique short (Byrne and Kousoulas 1995) regions bracketed by the internal and terminal inverted repeat sequences (IRS and TRS), respectively (Roizmann et al., 1992, Wu et al., 2012). The genome organization of AnHV-1 is similar to other alpha herpes viruses (Li et al, 2009, Fukuchi et al., 1984, Gardner et al., 1993). Out of 78, 74 genes are located within the unique region as a single copy and two genes (ICP4 and ICP22) are located in a repeat region, and thus each has two copies in the genome (Li et al., 2009). Major glycoproteins

are gL, gM, gH, gB, gC, gN, gK, gG, gD, gI and gE. Among these glycoproteins, gB, gC, gD, gH, and gL are involved in viral entry into the host cell, whereas gK, gM is involved in viral egress. Some proteins like gN are envelope protein, it is a type I membrane protein found in complex with gM. In addition, gI and gE are also type I membrane protein complexed with each other and plays role in cell to cell spread of virus. According to a recent study, gE has shown to play crucial role in virion morphology hence, the deletion of gE reduces the viral titer significantly (Liu et al., 2020) A recent study has reported the role of gI protein in viral cell-to-cell spread (Liu et al., 2020).

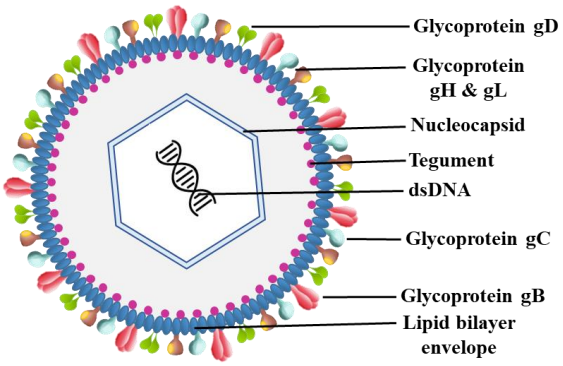

Figure 1.1 The schematic representation of Anatid herpesvirus 1.

1.1.3 Virus Replication

In a vulnerable host, AnHV-1 replication takes place in the mucosa of the digestive tract and continues to spread to the bursa of Fabricius, thymus, spleen, and liver (Islam and Khan 1995, Xuefeng et al., 2008). The epithelial cell and lymphocytes are the main site of virus replication (Xuefeng et al., 2008). Virus attachment to the host cell receptor is mediated by surface glycoproteins. AnHV-1 utilizes glycoprotein gB, gC, gD, gH, and gL to enter the host cell (Johnson et al.,1990, Spear et al., 2000). Glycoprotein B is essential for attachment and penetration of free virions (Byrne and Kousoulas, 1995) involving fusion between the viral envelope and cellular plasma membrane and helps in the transmission of infectivity from

primary infected cells to neighbouring non-infected cells (Li, et al. 1997). Glycoprotein C is a major component of the virion envelope and is proved to be a multifunctional protein (Lian, Xu et al. 2010). Its homologs of herpes simplex virus type 1 (HSV-1), pseudorabies virus (PRV), and bovine herpesvirus type 1 (BHV-1) helps in virion attachment, interacting with cell surface heparan sulfate proteoglycans (HSPG), thus mediating efficient virus attachment to the cells (Li et al., 1995, Tal-Singeret et al., 1995, Flynn and Ryan, 1996, Trybala et al., 1998, Mardberg et al., 2001, Rue and Ryan, 2002). Glycoprotein D mediates viral entry into the host (Fuller and Spear, 1987, Highlander et al., 1987). After binding the viral envelope fuses with the plasma membrane of the host and allows the entry of nucleocapsid into the host cytoplasm. DNA and protein complex are separated from the nucleocapsid and enter into the nucleus. After infection, genes are expressed as immediate-early IE, early (E) and late (L). The IE genes encode for regulatory proteins. Upon infection, IE genes are transcribed immediately, whereas early genes are transcribed before viral DNA replication and finally, transcription of late gene starts after synthesis of viral DNA and protein (Liu et al., 2015). Viral DNA replicates in the nucleus, and newly synthesized DNA is coiled and encapsulate into pre-formed immature capsids. Nucleocapsid and the inner layer of the nuclear envelope encapsidate to form a mature virion particle. Mature virion buds through the nuclear membrane and accumulates into the vacuoles within the cytoplasm of infected cells and are released by exocytosis (Everett, 2000, Flemington, 2001).

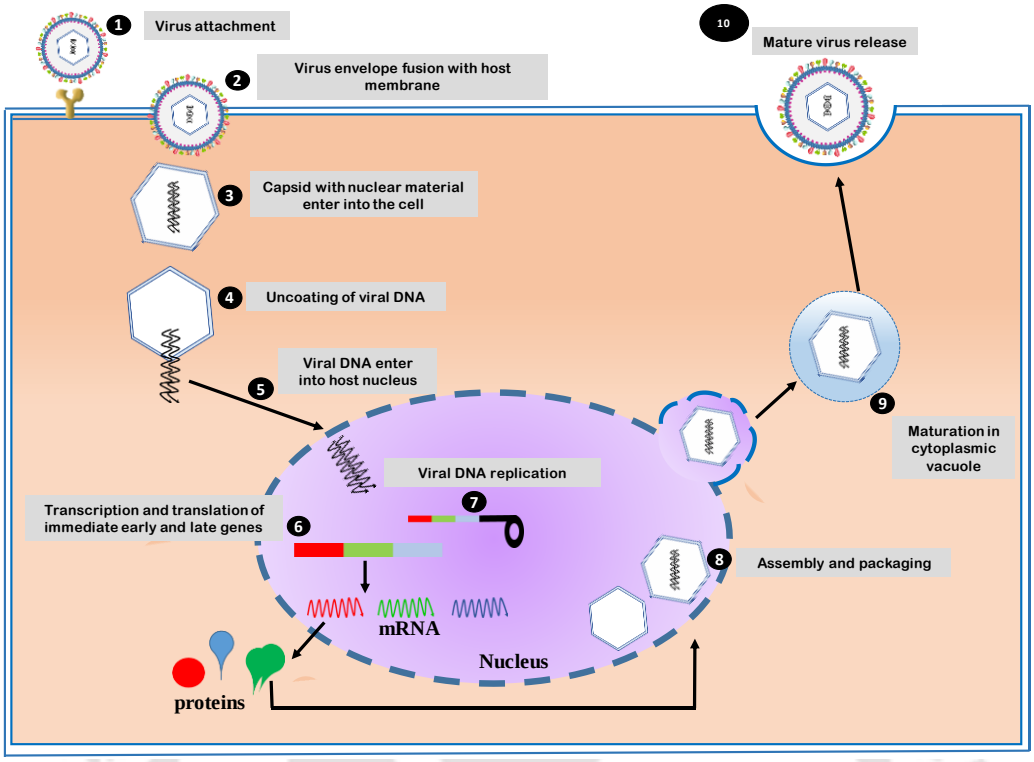

Figure 1.2 The replication cycle of Anatid herpesvirus 1.

1.1.4 Transmission

The susceptible population is mainly waterfowls; transmission through water appears to be a prime source. They may get exposed both by direct contact with the infected bird and indirectly from a virus-contaminated environment (Richter, 1993). The convalescent birds may become carriers and shed virus into the environment for a prolonged period (Burgess and Yuill, 1983, Shawky and Schat, 2002). Latency and re-activation of the virus have been responsible for outbreaks in domestic as well as migrating waterfowl. Migratory birds have been reported as carriers of AnHV-1 during many outbreaks (Van Dorssen, 1955, Dardiri and Hess, 1967, Brand and Docherty, 1984, Wozniakowski and Samorek-Salamonowicz, 2014). The principal mode of viral dissemination is horizontal transmission; however, vertical transmission also plays a significant role in disease spread (Burgess and Yuill 1981, Sandhu and Shawky, 2003).

1.1.5 Signs and Symptoms

The incubation period ranges from 3–7 days and varies according to species, age, sex, immune status of the affected bird, and the strain of AnHV-1 involved (Fenner et al., 1993, Sandhu and Metawally, 2008, OIE 2012). Clinical symptoms include sudden death, depression, loss of appetite, increased thirst, dehydration, weakness, ruffled feather, nasal discharge, ataxia, photophobia, tremor of head and neck, greenish and watery diarrhoea, and soiled vent has been observed in the flocks (Hanson and Willis, 1976, Richter, 1993, Campagnoloe et al., 2001, Sandhu, 2003, Gough, 2008). Infected birds exhibit swelling of the head and neck, swollen eyelids and tearing, hemorrhage of the esophageal mucosa, trachea, and bursa of Fabricius, and splenomegaly. Gross lesions are necrosis of the mucosa and submucosa of the gastrointestinal tract and lymphoid tissues. Vascular damage and internal haemorrhages in digestive mucosal tissue, lesions of lymphoid organs, and degenerative changes in parenchymatous tissues have been observed in infected birds (Leibovitz and Hwang, 1968, Montgomery et al., 1981, Wobeser, 1987, Gough and Alexander, 1990, Converse and Kidd, 2001, Li et al., 2016). In infected cells, AnHV-1 induces the formation of intracellular inclusion bodies which are characteristic of herpesvirus and have been visualized in hepatic and epithelial cells of infected birds (Dardiri and Gailunas, 1969). Inclusion bodies are an intracellular assembly of virions or viral parts in the nucleus or cytoplasm of an infected cell (Barr et al., 1992).

1.1.6 Diagnosis

Fluorescent antibody testing can be used to detect viral proteins (Tantaswasdi et al., 1988) in infected cells, and immunofluorescence can be useful for screening large numbers of sera. Several antibody-based diagnostic tests like serum neutralization in embryonated eggs and cell culture have been used to monitor antibodies (OIE 2012). ELISA (enzyme-linked immune sorbent assay) has been developed for AnHV-1 diagnosis (Pan et al., 2008, Jia et al., 2009, Wen et al., 2010, Wu et al., 2011). The antibody developed in birds may be diagnosed by virus

neutralization (VN). Neutralization indices between 0 and 1.5 were detected in domestic and wild waterfowl that had not been exposed to AnHV-1, NI of 1.75 or greater was considered to be evidence of prior exposure to the virus (Dardiri and Hess, 1967). Molecular diagnostic tools such as polymerase chain reaction (PCR) (Plummer et al., 1998, Hansen et al., 1999) using genes such as UL30 is used for confirmation of the virus, in addition PCR targeting UL2 gene has been used for detecting attenuated and virulent strains of AnHV-1 (Xie et al.,2017). Quantitative real-time PCR (qRT-PCR) has also been reported to be used in diagnosis (Yang et al., 2005, Qi et al., 2009, Wu et al., 2011).

1.1.7 Vaccination

Attenuated and naturally apathogenic strains of the virus have been used for immunizing the animals against clinical AnHV-1 infection (Hess and Dardiri, 1968, Jansen, 1968, Lin et al., 1984). Live attenuated and inactive vaccines have been used commercially (Shawky and Sandhu, 1997, Kulkarni et al., 1998). Effective protection induced by attenuated vaccine depends on the strain used and concentration of the virus (Kulkarni et al., 1998). In India, a chick embryo adapted AnHV-1 vaccines strain are being used commercially. Currently, in most of the European countries and the USA, both live attenuated and killed vaccines are being used in broiler and breeder ducks of two weeks old (Shawky and Sandhu, 1997, Sandhu and Metwally, 2008, Yang et al., 2015). AnHV-1 VAC strain attenuated by serial passage in chicken embryo cells is used as a commercial vaccine strain in China (Li et al., 2009). Attenuated AnHV-1 of the C-KCE strain from the embryonated chicken egg has also been used as a live vaccine in ducks (Liu et al., 2011, Wu et al,. 2012). Furthermore, gC deleted AnHV-1 has been used to develop a vectored AnHV-1 vaccine for AIV expressing hemagglutinin (H5) protein of AIV (Wang and Osterrieder., 2011). AnHV-1 has been used as a recombinant vector for Duck hepatitis A virus type 1 (DHAV-1) and shown to work as bivalent vaccine for and AnHV-1 Chinese challenge strain and DHAV-1 (Niu et al, 2020).

1.2 Review of Literature

1.2.1 History and global scenario

DVE, historically known as duck plague was first described in domestic waterfowl in the Netherlands in 1923 and was reported as the strain of fowl plague virus (avian influenza) adapted for ducks (Baudet, 1923). In 1949 the virus was isolated and shown to be different from other known bird viruses and named as duck plague in XIVth International Veterinary Congress in London (Jansen, 1968). The disease has a worldwide distribution and has caused several documented outbreaks in the anatid family. The first documented outbreak was reported in North America in commercial ducks in long island, New York in 1967 (Leibovitz and Hwang, 1968). DVE has become a concern for wild waterfowls in the United States since the late 1960s (Sandhu, 1997, Friend, 1999). Subsequently, several outbreaks have been reported in different states of the USA such as Maryland, Illinois Pennsylvania, and California (Hwang et al., 1975, Brand and Docherty, 1984, Davison et al., 1993, Campagnolo et al., 2001, Converse and Kidd, 2001). Surviving waterfowls after infection acted as virus carriers providing virus reservoirs for further outbreaks (Burgess et al., 1979) and cause the spread of disease in the wildlife population. The disease was reported in wild birds as well (Ziedler and Hlinak,1992). A recent study reported the occurrence of the virus in free-ranging water birds in Poland (Wozniakowski and Samorek-Salamonowicz, 2014). Commercially duck operations in Europe and Asia are affected due to AnHV-1 outbreaks. Catastrophic outbreaks have caused mass mortality and provoke major economic consequences in Asia (Jansen, 1964). European countries including England (Hall and Simmons, 1972, Gough and Alexander, 1990), Germany (Kaleta et al., 2007), Denmark (Prip et al., 1983) have reported the outbreak. Among Asian countries that have reported duck plague are China (Wang et al., 2013), Vietnam (Pritchard et al., 1999), Bangladesh (Ahamed, 2015), and India (Mukerji, et al., 1965). In 2016, a major

DVE outbreak was reported in Egypt, which killed 20-60% of affected birds (El-Tholoth et al,. 2019).

1.2.2 Indian scenario

In India, the first case of DVE was reported in 1963 in West Bengal (Mukerji et al., 1965). Several cases have been reported from other states like Kerala, Karnataka (Bulbule, 1982), and Assam (Konch, 2009). Recently, an outbreak has been reported in the Tamil Nadu state of India in Chara-Chemballi ducks (an indigenous breed of Kerala State) with a mortality rate of 44.4% (Pazhanivel et al., 2019). Assam, the leading North-eastern state, is the 2nd ranked duck state in India after West Bengal, with 12.01 (million) ducks in backyard poultry. Assam shares international boundaries with Bangladesh and Bhutan and interstate boundaries with West Bengal, Arunachal Pradesh, Meghalaya, Manipur, Mizoram, Tripura, and Nagaland. Assam also hosts wildlife sanctuaries which attract a lot of migratory birds during their migration season. All these factors lead to an increased risk of the introduction of pathogens. Frequent outbreaks of the AnHV-1 are reported from Assam, West Bengal (Chambal, 2009, Jana, 2014).

1.2.3 Interferon stimulated genes

IFNs were discovered in chicken in 1957 (Isaacs and Lindenmann, 1957) and the first chicken IFN (chIFN) gene was cloned and characterized in 1994 (Sekellick et al., 1994). For potential replication and infection, viruses have to breach the host immune system. The IFN response is one of the robust hosts' innate immune responses against viruses by acting upon cells to provide resistance to viruses (Isaacs and Lindenmann, 1957). Viral infection triggers a first-line host defense through the production of IFNs. IFNs are groups of cytokines grouped into three classes, Type I, II, and III IFNs, according to their amino acid sequence and function (Isaacs and Lindenmann, 1957). Type I IFN was discovered in 1957 because their antiviral activity against the influenza virus (Isaacs and Lindenmann, 1987) are broadly acting antiviral

cytokines and inflammatory cytokines (Randall and Goodbourn, 2008). IFNs activate signal transduction pathways that trigger the transcription of a set of genes to exhibit an antiviral response against the viral infection. These genes are referred to as interferon-stimulated genes (ISG) (Zhu et al., 1997, De Veer et al., 2001, Sen and Sarkar, 2007). Some IFN-inducible protein such as Mx1 GTPase (Myxovirus resistance 1), protein kinase R (PKR), 2′-5′-oligoadenylate synthetase (OAS), zinc finger antiviral protein (ZAP), viperin, and IFIT (IFN-induced proteins with tetratricopeptide repeats) have been characterized as antiviral (Gao et al., 2002, Haller et al., 2007, Sadler and Williams, 2007, Daffiset al., 2010, Hayakawa et al,. 2011, Pichlmairet al., 2011, Tag-El-Din-Hassan, et al., 2012). Virus inhibitory protein, endoplasmic reticulum-associated, interferon-inducible (Viperin) is an ISG that exhibits antiviral potential upon induction by type I and II IFN (Chin and Cresswell, 2001). Viperin was first identified in fish as a virus-induced gene (vig1); it is shown to be induced during infection of rainbow trout leukocytes with viral haemorrhagic septicemia virus, a fish rhabdovirus (Boudinot et al., 2000). Its human homolog is also known as radical SAM domain-containing 2 (RSAD2) and cytomegalovirus inducible gene5 (Cig5) was discovered as an inducible gene in fibroblasts upon cytomegalovirus infection and was named for virus inhibitory protein, endoplasmic reticulum-associated, IFN-inducible (Chin and Cresswell, 2001). Viperin exhibits antiviral against a broad spectrum of DNA and RNA viruses including herpesviruses (HCMV), flaviviruses (HCV, WNV), an orthomyxovirus (Influenza A virus), a paramyxovirus (Sendai virus), a rhabdovirus (VSV), and a retrovirus (HIV-1) (Zhu et al,. 1997, Rivieccioet al., 2006, Wang et al., 2007, Jiang et al., 2008, Jiang et al., 2010, Stirnweiss et al., 2010). During influenza infection, viperin expression exerts its effect at a later stage of the viral life cycle by inhibiting budding and release of virus by disrupting lipid raft microdomain on the plasma membrane. It is shown to bind and inhibit farnesyl diphosphate synthase (FPPS), an enzyme involved in the synthesis of multiple isoprenoid-derived lipids and cholesterol, thus may alter

the lipid content and hence affecting plasma membrane fluidity (Wang et al., 2007). Recently, viperin has shown to catalyse the conversion of cytidine triphosphate (CTP) to 3′-deoxy-3′,4′-didehydro-CTP (ddhCTP) which is first identified antiviral ribonucleoside in humans (Rivera-Serrano et al.,2020).

1.2.4 Role of cholesterol metabolic pathway in viruses

Cholesterol is one of the major sterols of mammalian cells and is required to maintain cell viability, membrane permeability, and involvement in cell signaling (Mukherjee et al., 1998, Goluszko and Nowicki, 2005, Ikonen, 2008). In the plasma membrane, most of the cholesterol is preferentially localized in lipid rafts. Membrane lipid rafts are microdomain present in extracellular leaflets of plasma membrane intracellular organelles such as Golgi body and endosomes it is highly rich in cholesterol and sphingomyelin (Brown and London, 2000, Simons and Toomre 2000,). Many viruses, both enveloped and non-enveloped, use lipid raft to enter and exit target cells (Takahashi and Suzuki, 2011). Herpesvirus requires multiple host and viral determinants. Pathogens cannot synthesize cholesterol and salvaging host cholesterol helps in synthesizing cholesterol-rich membranes and assembly platforms. The effect of viruses on cellular metabolism was studied, it was observed that the addition of glucose accelerated the release of poliovirus from infected HeLa cells (Eagle and Habel, 1956). It has been revealed that glycolysis, fatty acid synthesis, and glutaminolysis are commonly altered metabolic pathways by various viruses including dengue virus (Fontaine et al., 2015), human herpesvirus type 8 (Yogev et al., 2014), hepatitis C virus (Diamond et al., 2010), vaccinia virus (Fontaine et al., 2014), HIV-1 (Hegedus et al., 2014), HCMV and HSV-1 (Vastag et al., 2011) utilizing different mechanism to facilitate viral infection. Enveloped viruses derive their envelope from the host cellular membrane, Golgi body, or endoplasmic reticular during their budding. The involvement of lipid raft in virus entry has been studied by the effect of cholesterol-removing

reagents such as methyl-β-cyclodextrin (MβCD) (Takahashi and Suzuki, 2011). β-cyclodextrin has the highest affinity for the inclusion of cholesterol and most efficient in extracting cholesterol (Ohtani et al., 1989, Irie et al., 1992, Ohvo and Slotte, 1996). Lipid rafts have been implicated in the assembly and release of viruses including HIV, Ebola, Marburg, NDV, and VSV (Pessin and Glaser, 1980, Aloia et al., 1993, Luan et al., 1995, Chan et al., 2001, Freed, 2002, Pornillos et al,. 2002, Laliberte et al., 2006), it is also thought to be the site of virus release. It has been reported that lipid lowering drugs disturb the infectivity of Coronaviruses (Katsiki et al., 2020). Lowering the membrane cholesterol may curtain the attachment and internalization of Severe Acute Respiratory Syndrome Coronavirus 2 (SARS-CoV-2) (Abu-Farha et al., 2020, Radenkovic et al., 2020). In case of chronic HCV infection, it has been observed that statin drugs enhance viral clearance from blood (Ali et al., 2013). Cellular and systemic cholesterol metabolism play a vital role in regulating immune cell activity (Tall and Yvan-Charvet, 2015). It has been studied that lipid rafts provide requisite structure and scaffolding for recruitment and signaling of immune receptors (Yaqoob, 2009, Eich et al,. 2016). Depletion of cellular cholesterol has been shown to disrupt lipid raft and suppress T cell receptor (TCR)-mediated immune response and proinflammatory cytokine signaling. In contrast, these responses are augmented by cholesterol addition (Bensinger et al., 2008, Zhu et al., 2008, Armstronget al,. 2010, Surlset al., 2012, Zhu et al., 2012).

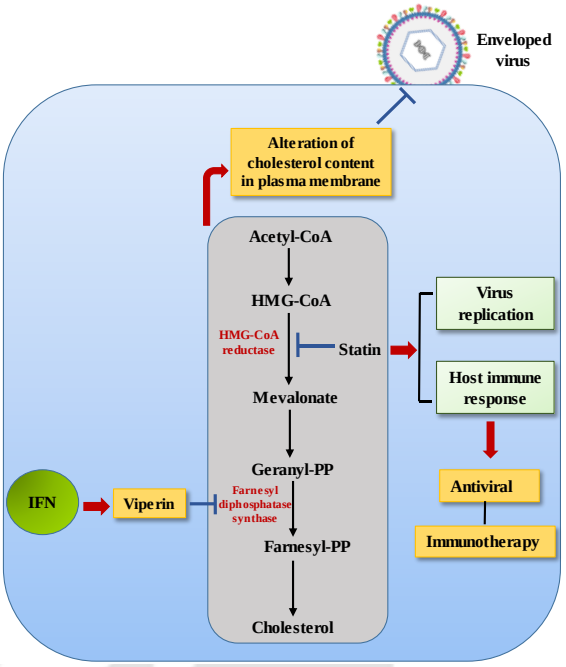

Figure 1.3. The schematic representation showing the effect of modulation in the cholesterol pathway on viral infectivity.

1.2.5 Newcastle disease virus as a vector for foreign gene expression

NDV is a single-stranded non-segmented negative-sense RNA virus and is a member of genus *Avulavirus* in the family *Paramyxoviridae*. The genome is about 15kbs and encodes six structural proteins, nucleoprotein (NP), phosphoprotein (P), matrix protein (M), fusion protein (F), hemagglutinin-neuraminidase (HN), and the large protein (L) (Krishnamurthy and Samal 1998). NDV is one of the naturally occurring oncolytic viruses inherently able to trigger lysis of tumor cells and have potential for cancer therapy (Reichard et al., 1992, Vigil et al., 2007) and is also an excellent recombinant viral vector. NDV can selectively replicate in and impair several human tumor cells without affecting normal cells (Reichard et al., 1992, Vigil et al., 2008, Schirrmacher and Fournier, 2009), NDV has been used as an oncolytic agent (Vigil et al., 2008) and as a gene delivery vector to express the therapeutic or immune regulatory genes (Janke et al., 2007). It is now possible to generate recombinant NDV entirely from cloned cDNA using a reverse genetics technique (Roberts and Rose, 1998, Peeterset al., 1999). The development of recombinant NDV facilitates the expression of the foreign gene to study the

function and potential of a specific gene. NDV has been used to express IL-15 (Xu et al., 2017), IL-2 (Wuet al., 2016), p53 (Fan et al., 2018), tumor necrosis factor-related apoptosis-inducing ligand (Wu et al., 2017), and granulocyte/macrophage colony-stimulating factor (GM-CSF) (Janke et al., 2007) in cancer immunotherapy. Genetically engineered NDV expressing human IFN-λ1 has been studied as a potential antitumor agent (Bu et al., 2016). NDV has also been used as a vaccine vector for immunization against several emerging pathogens (DiNapoli et al., 2007, Ge et al., 2007, Khattar et al,. 2011, Kim and Khattar, 2016).

1.3 Rationale for the study

Indian poultry sector has undergone a paradigm shift from being a mere backward activity to a major commercial agriculture-based industry. It is one of the important and rapidly growing agriculture sectors in India. This sector mainly consists of chicken, ducks, turkey, and geese for meat and egg production, and among them, duck production is 8.5% of the total. Viral infections are today one of the major threats to avian husbandry and causes a considerable impact on the economy. AnHV-1, despite being the most serious virus to the duck rearing industry is not well studied. The chick embryo adapted live AnHV-1 vaccine is the most widespread commercial used vaccine in India. However, the risk of contamination by other avian pathogens in the eggs or microbial contaminants during processing has obstructed vaccine supplies and depends on a continuous supply of egg which could be limited in the period of pandemic and extreme conditions of weather (Wong and Webby, 2013). Its economic impact in developing countries is substantial and there is a need to understand the cell culture spectrum of the virus to produce its vaccine on a mass scale. Therefore, investigating probable cell lines for developing a continuous cell culture-based vaccine against AnHV-1 infection will be advantageous. Vaccination of the only preventive measure for AnHV-1 infection. Thus, studying the regulation of different cytokine, innate immune-related genes upon immunization will provide information regarding the protective efficacy of vaccination and will help to

understand pathodynamics of the virus. Despite, vaccination AnHV-1 outbreaks have been reported.. This work focuses on exploring the role of host molecules that plays a critical role in the infectivity of the virus. Viperin is IFN stimulated protein that inhibits some virus infection via IFN-dependent or IFN-independent pathways. However, the role of viperin in AnHV-1 infection is not well understood. This study will provide information on the poultry's innate immune system, which could help developing novel antiviral therapies against AnHV-1 infection. Also, cholesterol is a crucial component of the plasma membrane and lipid raft which compartmentalize cellular processes in the host cell (Pike, 2006). Removal of cholesterol from the plasma membrane leads to affect the infectivity of some viruses. Many viruses such as HIV (Viard, et al., 2002), HSV (Bender et al., 2003), poliovirus (Danthi and Chow, 2004), human herpesvirus 6 (Huang et al., 2006), vaccinia virus (Chung et al., 2005) and foot and mouth disease (Martin-Acebes et al., 2007) virus has been reported to depend upon plasma membrane for its entry into the host. However, there is a limited study about the possible role of cholesterol in AnHV-1 infectivity. Cholesterol in the viral envelope can sustain the integrity of virus particles and helps in entry and exit from the host cell. The infectivity may be altered by destroyed viral envelope integrity owing to depletion of cholesterol.

1.4 Objectives

i. Adaptation and characterization of AnHV-1 in different cell lines.

ii. The immune response of AnHV-1 immunization in ducks.

iii. Understanding the role of viperin and cholesterol against AnHV-1.

Chapter 2.

Adaptation and characterization of AnHV-1 in different cell line

Chapter 2

2.1 Abstract

DVE is an acute, contagious and highly fatal infection of *Anatidae* family members. The disease is caused by AnHV-1. The infection of AnHV-1 is controlled by vaccination to the flock with chick embryo adapted attenuated vaccine in developed countries. In the present study, the permissiveness of AnHV-1 for different cells was analyzed. The AnHV-1 showed enhanced replication following its serial passage in CEF, DF-1, Vero, MDCK, and QT-35 cells. The CPE of rounding and clumping of cells were observed in CEF, DF-1, Vero, and QT-35 cell lines. The infectivity and viral replication were highest in CEF, DF-1, Vero, and QT-35 cells. In contrast, the results suggested that MDCK cells are less permissive for AnHV-1 infection with negligible CPE and reduced viral replication. Heterologous cell culture systems other than CEF may provide a system devoid of other avian infectious agents to adapt live vaccine viruses. Moreover, it can be used for the propagation and cultivation of AnHV-1 vaccine strain for developing cell culture-based vaccines with high titer and could be an economical alternative for the existing options.

2.2 Introduction

AnHV-1 infection is one of the most widespread and devastating diseases of waterfowl and has severely affected the waterfowl industry because of the relatively high mortality could be observed. The primary, diploid, and continuous cell culture systems were used for the production of cell culture-based vaccine (Briggs, 2007). Primary cell culture is acknowledged as the appropriate way since they support a wide range of viruses (Peterson et al., 1988, She et al., 2006, Leland and Ginocchio, 2007, Wozniakowski and Samorek-Salamonowicz, 2014). However, primary cells have a limited lifespan and their characteristics may change with subsequent passages (Rekha et al., 2014). In contrast, continuous cell lines have acquired the ability to proliferate indefinitely and, are more robust and easier to maintain as compared to

the primary cells (MacDonald, 1990, Kaur and Dufour, 2012). Continuous cell lines are widely used for propagation, adaptation, and attenuation of diverse viruses for the development of cell culture bases vaccines (Vidor et al., 1997, Groth et al., 2009, Kaur and Dufour, 2012). AnHV-1 is known to propagate in primary cell culture of avian origin and a homologous system like cell lines of duck origin, duck embryo fibroblast (DEF-CCL-141), and duck embryo liver (Wolf et al,. 1974, Dardiri, 1975, Kocan, 1976, Mondalet al., 2010). Vaccination is an extensive approach for the prevention and control of the AnHV-1 infection. To date, AnHV-1 has been propagated in primary cell lines of avian origin. Recently, the adaptation of the virulent strain of AnHV-1 has been studied in the Vero cell line (Aravind et al., 2015). AnHV-1 remains highly cell-associated which may require rigorous freeze-thaw cycle to rupture cell membrane and the limited studies of its propagation in continuous cell line make it difficult to work with. In the present work, we conducted a study to propagate the vaccine strain of AnHV-1 in four different continuous cell lines along with primary cells by studying characteristic CPE, viral infectivity and replication kinetics, and its gene expression.

2.3 Materials and Methods

2.3.1 Cell and virus

The Vero, QT-35, and MDCK cell lines were procured from the National Centre for Cell Science (NCCS), Pune, India. DF-1 was procured from ATCC (Manassas, VA, USA, ATCC CRL-12203). The primary chicken fibroblast cell CEF was made from nine days old embryonated chicken eggs as per standard protocol (Goldman, 2006). All the cells were maintained in Dulbecco's Modified Eagle Medium (DMEM) with 10% fetal bovine serum (FBS) except QT-35, which was maintained in RPMI-1640 supplemented with 10% FBS (Invitrogen, Grand Island, NY) at 37°C in 5% CO_2. Additional 1% non-essential amino acid (Gibco, Invitrogen) was added in media for the QT-35 cell line. The CEF cells were used for

the initial propagation of the vaccine strain of AnHV-1. The CEF monolayer was grown in a cell culture flask (75cm^2) in 10% DMEM 37°C in 5% CO_2. The vaccine strain of AnHV-1 was procured from the college of veterinary and animal sciences, Khanapara, Guwahati, India. The monolayer was infected with a vaccine strain of AnHV-1 and observed for CPE and harvested 96 hours post-infection (hpi) by freeze-thaw. Virus titration was done at the 5th passage in CEF cells using the standard method (OIE 2012). The harvested virus was stored at -80°C for further use.

2.3.2 Adaptation of AnHV-1 in different cell line

The CEF, DF-1, Vero, QT-35, and MDCK cells were grown to 80% confluence in a cell culture flask (Nunc, USA). The CEF propagated virus (10^5TCID$_{50}$/ml) was added to the mentioned cell culture monolayer and incubated at 37^{o}C for 1h for viral adsorption. After washing with PBS, the cells were maintained in DMEM with 2% FBS. The cells were incubated at 37^{o}C in a CO_2 incubator and examined regularly for the appearance of CPE. The virus was harvested at 96hpi by freeze-thaw. The harvested virus was clarified and used for further subsequent passages in all the cell lines. A total of 10 passages were given to all the cells. The observed CPE in the infected cells was imaged along with mock uninfected control at 72 hpi.

2.3.3 Indirect immunofluorescence assay

The indirect immunofluorescence assay (IIFA) was done for the detection of AnHV-1 antigen in infected cell lines. The CEF, DF-1 Vero, QT-35, and MDCK cells grown on a coverslip in a six-well culture plate were infected with virus propagated in the respective cell lines. The cells were harvested 72hpi and fixed with 4% formaldehyde for 20 min at room temperature. The fixed cells were treated with 0.2% Triton X-100 for 10min to increase cell permeability after washing thrice with PBS. The cells were blocked with 5% bovine serum albumin in PBS for 1h at 37^{o}C. The cells were washed again thrice with PBS containing Tween-20 (PBST) and

incubated with AnHV-1 polyclonal antibody raised in chicken for 4h at 37°C. The cells were washed again thrice with PBST and incubated with fluorescein isothiocyanate (FITC)-conjugated rabbit anti-chicken IgG antibodies (Cat no. AP162F, Merck) for 1h at 37°C. The cells were examined for fluorescence under 20X objective (FLoid cell imaging station, Invitrogen USA).

2.3.4 Detection of AnHV-1 DNA in infected cell culture by PCR

Genomic DNA from the virus-infected and control CEF, DF-1 Vero, QT-35, and MDCK cells was isolated using a standard protocol (OIE 2012). The extracted DNA was subjected to PCR amplification for the DNA polymerase (UL30) gene of AnHV-1. The sequence of the AnHV-1 UL30 gene was extracted from GenBank (Accession number: NC_013036.1) for primer designing. The gene-specific primers (forward 5'- GAAGGCGGGTATGTAATGTA - 3') and (reverse 5'- CAAGGCTCTATTCGGTAAT - 3') were used for the amplification of the UL30 gene from the extracted DNA.

2.3.5 Viral gene expression by Quantitative PCR (qRT-PCR)

The qRT-PCR was also employed to detect the mRNA expression of the AnHV-1 glycoprotein C (gC) gene. Total RNA was isolated from mock and AnHV-1 infected cells 72hpi using RNAiso Plus (TaKaRa, Japan) according to the manufacturer's protocol. RNA was quantified at 260nm absorbance, and purity was checked by the A260/280 ratio (>1.8). The cDNA was synthesized using the PrimeScript first-strand cDNA synthesis kit (TaKaRa, Japan). The qRT-PCR was performed using the SYBR Green PCR Master Mix (Applied Biosystems, USA) with AnHV-1 gC gene-specific primers (gC forward 5′ - GGAATGCAGTATGATCCCGT- 3′) (gC reverse 5′ - TCTTCGGTCGGTTCAAACCC - 3′). The transcript level of the target gene was relatively quantified using the $2^{-\Delta\Delta Ct}$ method. The relative amount of viral gene mRNA was normalized to that of GAPDH mRNA (GAPDH forward 5′ - ATGGAGAAGGCTGGGGCT

CA - 3′) (GAPDH reverse 5′- GTTGTCATGGATGACCTTGGC - 3′) in the same sample, which was used as an internal reference. The qRT-PCR reaction consisted of 40 cycles with the following conditions: 95°C for 30 s, followed by a two-step PCR reaction of 95°C for 15 s and 60°C for 30 s.

2.3.6 Protein expression analysis

Cells were infected and harvested 72hpi and the lysate was prepared to check the expression of the viral protein. The blots were developed using anti-AnHV-1 polyclonal and anti-β actin monoclonal antibodies (Invitrogen, USA). The signals obtained in the western blot assay were visualized using the ECL reagent (Thermo Fisher Scientific, USA).

2.3.7 Growth kinetics of AnHV-1 in different cell lines

The growth kinetics of AnHV-1 propagated in CEF, DF-1 Vero, QT-35, and MDCK cell line was determined by multi-cycle growth analysis based on virus titers at the 10^{th} passage. The cells were grown in triplicate in a 96 well plate and infected with AnHV-1 at MOI of 0.1. After 1h of virus adsorption, the cells were washed and maintained in DMEM with 2% FBS. The cell culture supernatant was collected and replaced with an equal volume of fresh media at 12, 24, 36, 48, 60, 72, 84, 96, 108, 120 h. The virus titers in 50% endpoint tissue culture infectious dose ($TCID_{50}$) units/µl were determined using Reed and Muench (Reed, 1938) method as also reported (Shah and Kumar, 2020).

2.3.8 Statistical analysis

All data were statistically expressed as mean $\pm$ SD of three independent experiments and analyzed with one-way ANOVA (Dunnett's multiple comparisons test, GraphPad Prism 8).

2.4 Results

2.4.1 Passage and Adaptation of AnHV-1 in different cell line

AnHV-1 infected CEF, DF-1 Vero, QT-35 and MDCK showed no characteristic CPE during initial passages. From the 5th passage onwards, the gradual development of CPE was observed in CEF, DF-1, Vero, and QT-35 cell line whereas no visible CPE was observed in MDCK cells. Following 48h of infection, the CEF and DF-1 cells started showing CPE and a prominent bulging and aggregation with clusters of affected cells were evident as early as 3 days post-infection (dpi) followed by the clumping of rounded cells and formation of intracellular vesicles leads to death and detachment of cells. In Vero and QT-35 lines, rounding and clumping of cells were observed after 3-4 dpi (Figure 2.1A).

2.4.2 IIFA for detection of AnHV-1 antigen in infected cells

IIFA of infected cells showed an AnHV-1 antigen in CEF, DF-1, Vero, and QT-35 cells. Green fluorescence appeared in the infected cell whereas, no signal appeared in mock uninfected cells. In contrast, no fluorescence appeared in MDCK cells following infection (Figure 2.1B).

2.4.3 PCR confirmation of AnHV-1 DNA in infected cell culture

The purity of extracted DNA from infected cell lines was checked by measuring the absorbance 260/280 ratio, which was 1.8. The PCR amplification using DNA polymerase (UL30) gene primers reveal a viral-specific amplicon size of 450 bp. (Figure 2.2A). Band intensity of UL30 PCR amplification was compared for all the cell lines using ImageJ software. Maximum viral gene band intensity was observed in CEF followed by DF-1, Vero, and QT-35 infected cells whereas, a faint band appeared in MDCK infected cells (Figure 2.2 B).

2.4.4 Expression of gC gene of AnHV-1 in infected cells

The expression of gC gene was examined in the infected cell line using qRT-PCR. The result showed that the expression of gC was greatly up regulated in CEF cells as reported earlier in other studies (Figure 2.2 C). The expression was elevated by 22.9 fold in CEF. Furthermore, the expression level of gC was higher in DF-1, Vero, and QT-35 cells. The expression of gC

was relatively low in the MDCK cell line with a fold change of 3.4, in particular, the expression of gC was diminished by 6.7 fold in the MDCK cell line compared to CEF cells. The mRNA levels of gC were normalized to GAPDH mRNA and represented as mean fold expression concerning control. The fold change in gene expression was calculated by $2^{-\Delta\Delta Ct}$.

2.4.5 Protein expression analysis

In western blot assay, the highest intensity of AnHV-1 specific protein bands was observed in AnHV-1 infected CEF cells. The protein expression of AnHV-1 was observed in the infected DF-1, Vero, and QT-35 cells. No band was observed in MDCK cells infected with AnHV-1. The β- actin was used as an internal control for all the experiments (Figure 2.2 D).

2.4.6 Viral growth kinetics of AnHV-1 in different cell lines

Multi-cycle growth kinetics were performed in different cell lines 12, 24, 36, 48, 60, 72, 84, 96, 108, and 120 hpi at the 10^{th} passage level. Distinct CPE was not visible in initial few passages, however enhanced CPE was observed in 10^{th} passage following its passage in permissive cell lines. Vero cells showed an increase in AnHV-1 titer from 36 hpi and a maximum titer of $10^{5.5}$ $TCID_{50}$/ml observed at 84hpi and beyond the titer was reduced to 10^{3} $TCID_{50}$/ml at 120 hpi. Furthermore, no titer was observed till 48hpi and the titer of $10^{3.5}$ $TCID_{50}$/ml was recorded at 60 hpi, which continued till 120 hpi in MDCK cells. The virus titer was maximum at 60 hpi which is 10^{6} $TCID_{50}$/ml and maintained at $10^{6.3}$ $TCID_{50}$/ml till 84 hpi in the DF-1 cell line. In CEF, the maximum virus titer was recorded as early as 48 hpi which is $10^{5.5}$ $TCID_{50}$/ml and the maximum titer was recorded at 84 hpi which is $10^{7.5}$ $TCID_{50}$/ml. In the QT-35 cell line, a maximum virus titer of $10^{6.5}$ $TCID_{50}$/ml and $10^{6.3}$ $TCID_{50}$/ml was recorded at 84 hpi and 96 hpi. Comparison of virus titer indicated that the AnHV-1 titer was highest in the CEF cell line and significant titer was observed in Vero, DF-1, and QT-35 cell line. In contrast, the least viral titer was observed in the MDCK cell line (Figure 2.3)

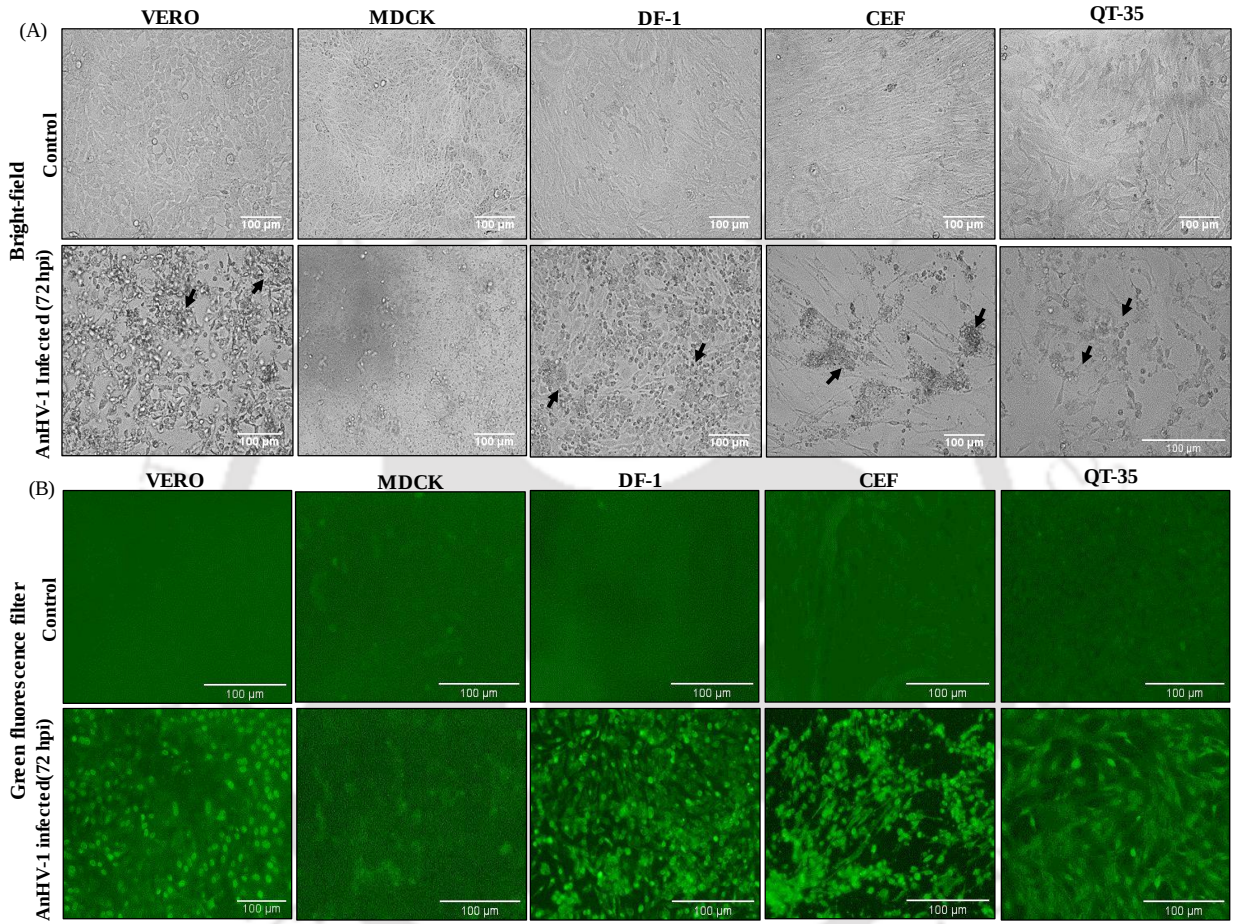

Figure 2.1. Bright-field images of mock uninfected and AnHV-1 infected Vero, MDCK, DF-1, CEF, and QT-35 cells showing cytopathic changes of bulging, aggregation, and clumping of rounded cells at 10th passage 72 hpi (20X) (A). Immunofluorescence staining. The Vero, MDCK, DF-1, CEF, and QT-35 cells were infected by AnHV-1 and analyzed for immunofluorescence using primary AnHV-1 polyclonal antibody and secondary fluorescein isothiocyanate (FITC)-conjugated rabbit anti-chicken IgG antibodies for the presence of AnHV-1 antigen 72 hpi, under fluorescence microscopy (green channel, 20X). Green fluorescence exhibits AnHV-1 specific antigen in Vero, DF-1, CEF, and QT-35 cells (B).

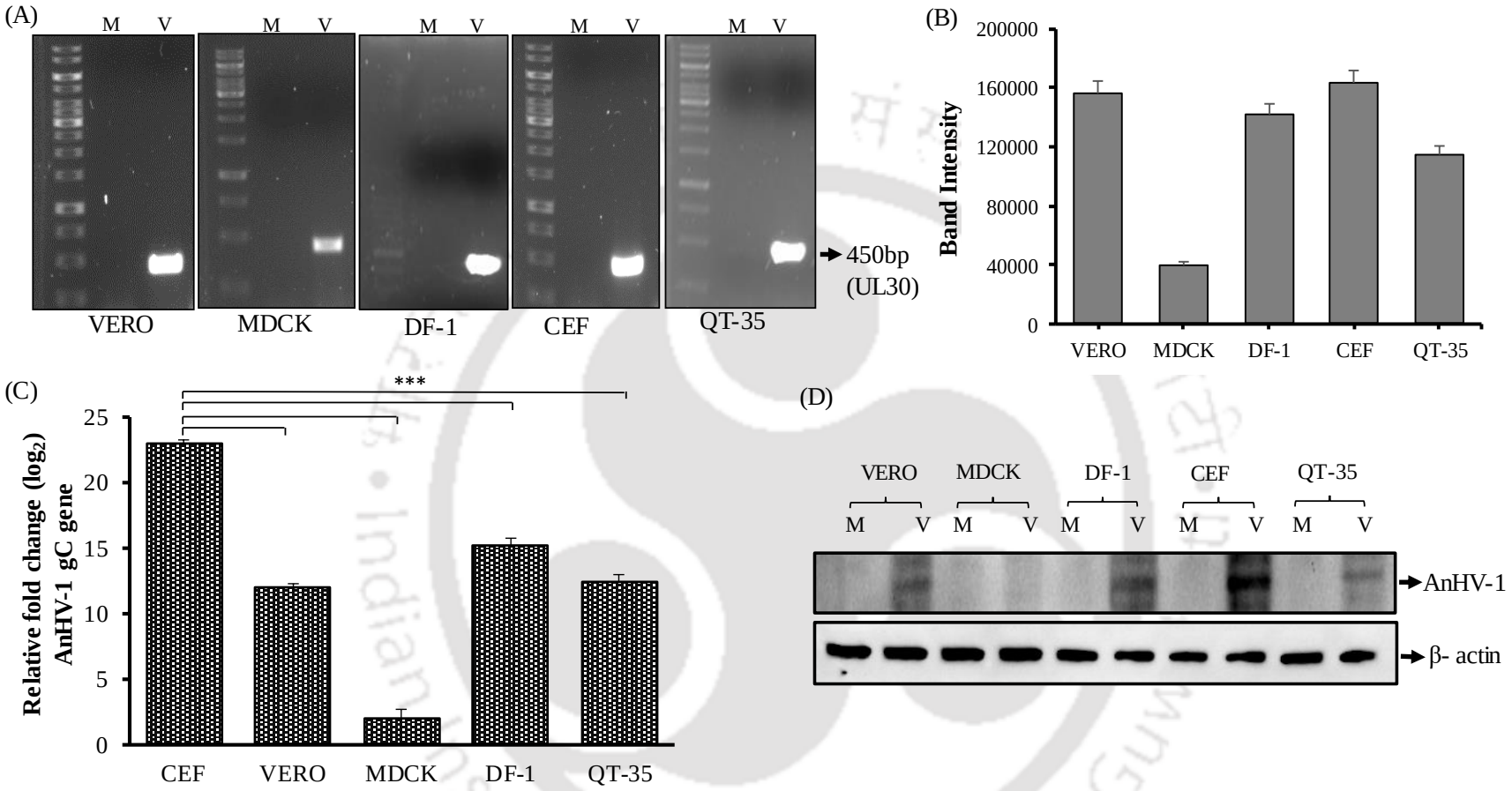

Figure 2.2. PCR confirmation of AnHV-1 infected cells. The Vero, MDCK, DF-1, CEF, and QT-35 cells were infected by AnHV-1 and viral DNA was extracted from mock uninfected and infected cells 72 hpi. PCR amplification of the UL30 gene was done. Lane M: mock uninfected control; Lane V: AnHV-1 infected cells (A). UL-30 amplification band intensity was analyzed using ImageJ software (B). Real-time expression analysis of the glycoprotein C gene of AnHV-1 in Vero, MDCK, DF-1, CEF, and QT-35 cells following its passage. The mRNA determinations were performed by qRT-PCR, and mRNA levels were normalized to GAPDH mRNA and represented as mean fold expression concerning control. The fold change in gene expression was calculated by $2^{-\Delta\Delta Ct}$. Statistical significance difference was determined by using one-way ANOVA (Dunnett's multiple comparisons test, GraphPad Prism 8). A p-value of 0.001 is flagged with three stars (***) (C). The cell lysate was prepared and analyzed for viral protein by immune blot assay. The β-actin was used as a loading control (D).

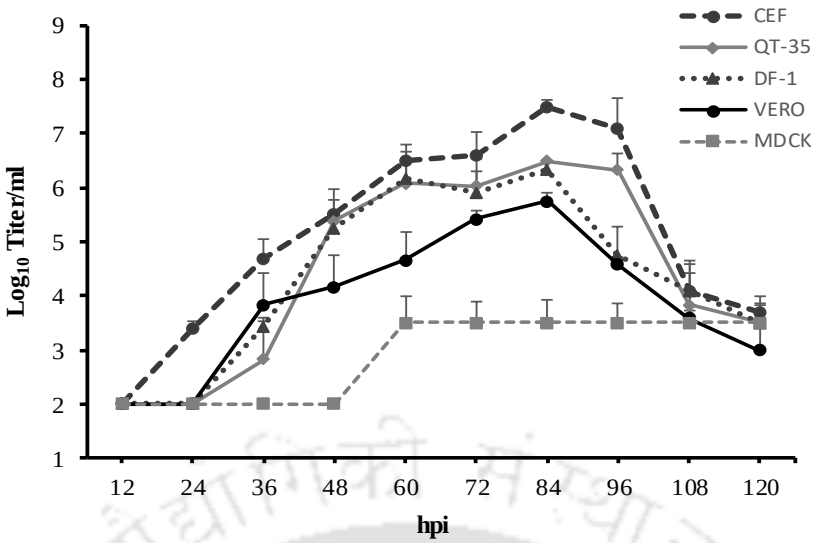

Figure 2.3. Multicycle growth kinetics of AnHV-1 in Vero, MDCK, DF-1, CEF, and QT-35 cells at various post-infection intervals 12h, 24h, 36, 48h, 60h, 72h, 84h, 96h, 108h, and 120 hpi was done using $TCID_{50}$.

2.5 Discussion

Primary duck embryo fibroblast (DEF) and primary Muscovy duck embryo fibroblasts (MDEF) has been reported to be used in AnHV-1 isolation. Besides, Muscovy duck embryo liver (MDEL) cells were thought to be even more sensitive for virus isolation (Wolf et al., 1976, Gough and Alexander, 1990). Primary virus isolation can also be done by inoculating the virus into the chorioallantoic membrane of 9-14 days old embryonated duck and chicken eggs (Campagnolo et al., 2001). However, embryonated eggs are less susceptible to infection with field strains of AnHV-1, and two to four serial blind passage of homogenized CAM is required before efficient virus isolation (Campagnolo et al., 2001). Primary cell lines retain the morphology and functional characteristics of their tissue of origin. However, this culture undergoes senescence and has a limited life span with the limited potential of self-renewal and its characteristics may change with each subsequent passage. By contrast, continuous cell lines have acquired the ability to proliferate indefinitely and expand over a long period with ease and have been used for the adaptation and attenuation of various viruses. Continuous cell lines are more robust and easier to work with than primary cells. AnHV-1 has been reported to

propagate in primary cell lines of avian origin (Tian et al., 2020) (Wolf et al., 1974, Mondal et al., 2010). The primary CEF has been reported to be utilized for the isolation of avian viruses (Johnson and Heneine, 2001). The finite life span, its prerequisites and tedious laboratory preparation makes the primary cells disadvantageous to explored as a cell to propagate AnHV-1.

The objective of this study was to explore a suitable cell substrate for the propagation of the AnHV-1 vaccine virus to optimum titer. We compared four continuous cell lines and CEF for this purpose. In this study, we observed prominent characteristic CPE of clumping and fused cells from 4-5 passage onwards. A similar CPE showing rounded cells produced in Vero, DF-1, and QT-35 cell lines, while no CPE was observed in the MDCK cell line at 96 hpi. IIFA results also supported the CPE results where AnHV-1 adapted and propagated in DF-1, Vero, and QT-35 cell lines along with CEF cells showed green fluorescence suggested the presence of viral antigen in the infected cells. DF-1 cells originated from line zero (endogenous-virus negative) embryos and do not contain any known endogenous virus (Himly et al., 1998, Kong et al., 2006). DF-1 is an immortalize CEF cell line which has been reported to support the growth of avian viruses such as avian sarcoma leukosis virus (Himly et al,. 1998, Schaefer-Klein et al., 1998), avian leukosis virus (Maas et al., 2006), Marek's disease virus (Levy et al., 2005), avian influenza virus (Lee et al., 2008, Moresco et al., 2010), and avian metapneumovirus (Kong et al., 2006, Tiwari et al., 2006). PCR based molecular diagnostic tools are more sensitive in virus diagnosis and quantification. The PCR and qRT-PCR methods have been reported to be used for AnHV-1 detection (Plummeret al., 1998, Hansen et al., 1999, Pritchard et al., 1999, Hansen et al,. 2000, Yang et al., 2005). The AnHV-1 infection in Vero, DF-1, and QT-35, and MDCK cell lines were also confirmed by PCR using UL30 of AnHV-1. The result suggests the highest rate of virus replication in CEF. Also, the rate of AnHV-1 replication was significant in DF-1, Vero, and QT-35 whereas the

lowest band intensity in MDCK suggests limited virus replication. Our result demonstrates that the expression of gC gene of AnHV-1 was greatly upregulated in CEF cells. Besides, the significant expression of gC in DF-1, Vero, and QT-35 suggests the susceptibility of these cells for replication of AnHV-1. Furthermore, detection of viral protein also revealed the AnHV-1 propagation in CEF, DF-1, Vero, and QT-35 cells. Continuous mammalian cell lines like Vero and MDCK have been successfully used for influenza vaccine preparation (Reisingeret al., 2009, Genzel et al., 2010). The MDCK derived influenza vaccine was shown to be comparable with the egg-derived trivalent inactivated vaccine (TIV) in terms of efficacy, immunogenicity, and safety (Groth et al., 2009, Reisinger et al., 2009, Szymczakiewicz-Multanowska et al,. 2009, Vesikari et al., 2012). Vero and QT-35 have been used for isolating field strains of avian pneumovirus (Chiang et al., 1998, Tiwari et al., 2006). Vero cells have also been used for many years for the production of live poliovirus vaccine (Vidor et al., 1997), rotavirus (Bernstein et al., 1999). Furthermore, QT-35 has been used for the propagation and titration of metapneumovirus (Sabara and Larence, 2002). In the present work, the virus yielded maximum titer in CEF. Moreover, optimal titer was observed in Vero, DF-1, and QT-35 continuous cell lines. In contrast, the least titer was seen in the MDCK cell line. The DF-1 cells are continuous cell line of chicken origin which can be used instead of primary CEF and QT-35 cells. Moreover, DF-1 is also derived from avian, which may be a better cell substrate for AnHV-1 propagation and isolation. The results of the present study suggest the utility of continuous Vero, MDCK, DF-1, and QT-35 cells for AnHV-1 propagation and titration. The study was carried out in a comparative manner using primary CEF since they are most widely used for AnHV-1 propagation and isolation. Our result shows that DF-1, Vero, and QT-35 cells are almost equally susceptible as CEF cells to support viral multiplication with the potential to be probable cell lines for developing continuous cell culture-based vaccine against AnHV-1 infection. Moreover, cell culture provides the advantage of availability, scalability, host

compatibility, and ease of manipulation for vaccine manufacturing. Viral culture also expedites the production of high titer of virus used in antibody testing and viral characterization.

Chapter 3.

The immune response of AnHV-1 immunization in ducks

Chapter 3

3.1 Abstract

To investigate the immune response of Khaki Campbell ducks to AnHV-1, an immunization experiment was performed in 2 weeks old duckling. We systemically explored the expression profile of innate immune cytokines in different organs and peripheral blood mononuclear cells (PBMC). Our results showed that AnHV-1 could replicate in several tissues with significant titer. Real-time quantitative PCR results showed that expression of several cytokines was up-regulated mainly in the brain and spleen of immunized ducks as well as in PBMC. This study indicates that the vaccine strain of AnHV-1 can productively replicates in PBMC and different organs. Modulation of innate immune-related genes upon immunization with vaccine strain will provide information regarding the protective efficacy of vaccination. Taken together, our result shows that cooperative induction of cytokine, IFN, and ISG in AnHV-1 infection.

3.2 Introduction

Commercial duck farming is based on breeds derived from Khaki Campbell, Indian runner, and Pekin breeds, and naturally occurring AnHV-1 infections have been reported in the domestic breeds (Banda A., 2019). In India, Khaki Campbell is among the egg-laying breeds, its egg-laying capacity ranges from 240-280 eggs/bird/year. Vaccination and disease-free stock are the only preventive measures against AnHV-1 infection. It is well recognized that innate immunity provides the first line of defense and plays a crucial role in the host immune response upon viral infection. It is activated through toll-like receptors (TLR) which are a class of pattern recognition receptors (PRRs) that induce inflammatory cytokine and production of type I IFN (Takeda and Akira, 2001, Takeuchi and Akira, 2010, Barbalat et al., 2011). In this study, we analyzed the viral distribution in different duckling organs inoculated with a vaccine strain of AnHV-1 and evaluated the immune response to the virus.

3.3 Materials and methods

3.3.1 Experimental animal and virus

The study was conducted in two weeks old Khaki Campbell duckling. The ducklings were maintained in an animal facility at the College of Veterinary Science, Khanapara, Guwahati, Assam. All experimental procedures were performed in compliance with the guidelines of institutional animal use and institutional biosafety committees. The ducklings were divided into two groups of 9 and housed separately. The animals from the first group received an intramuscular inoculation with 0.5ml of virus stock. A cell culture adapted AnHV-1 vaccine strain was used in the study. The viral suspension was made by diluting 0.1mg of lyophilized virus in 1ml PBS and it was subsequently, titrated in CEF. The AnHV-1 infected CEF cells were freeze-thawed, and its supernatant was used for further experiments. The AnHV-1 vaccine strain procured from the College of Veterinary Science, Khanapara, Guwahati, India, and characterized in our lab was used in the study (Makhija and Kumar 2017). The other group was set as a control group and were intramuscularly inoculated with 0.5ml PBS. On days 1, 3, and 5 post-immunization blood was collected into an EDTA-containing tube, and animals were sacrificed from each group to collect brain, bursa, lung, liver, and spleen. The organs were stored at -20^{o}C for RNA extraction.

3.3.2 PBMC isolation from whole blood

The whole blood was transferred to a 15 ml conical centrifuge tube and an equal volume of PBS was added. In a separate 15ml conical centrifuge tube 3ml of histopaque-1077 (Sigma-Aldrich, Cat. No.10771) at room temperature was added. The diluted whole blood was overlaying slowly over the histopaque-1077 without disturbing the two layers and centrifuged at 400xg for 30 min at room temperature. After centrifugation, the upper layer was aspirated carefully with a pipette to within 0.5 cm of the opaque interface between the histopaque-1077 and plasma containing mononuclear cells, the upper layer was discarded. The cells were re-

suspended in 5ml of PBS and centrifuged at 250xg for 10 min for washing. The washing was repeated twice to remove the remaining erythrocytes.

3.3.3 Viral and immune response genes expression analysis by qRT-PCR

The total RNA from PBMC and organs from the experimental animals were isolated and cDNA was synthesized as mentioned in section 2.3.5. The mRNA expression level of the immune-related genes IL-1β, IL-2, IL-6, IL-8, IFNs (IFN-α, IFN-β, IFN-γ) and ISG (viperin) and their relative level were quantified using the primers listed in Table 1. All data were statistically expressed as mean ± SD of three independent experiments and analyzed with one-way ANOVA (Dunnett's multiple comparisons test, GraphPad Prism 8).

Primer name	Sequence (5'-3')	
	Forward	Reverse
IL-1β	GCTGACCCGCTTCATCTTCTA	CGCCCACTTAGCTTGTAGGT
IL-2	GCCAAGAGCTGACCAACTTC	ATCGCCCACACTAAGAGCAT
IL-6	TTCGACGAGGAGAAATGCTT	CCTTATCGTCGTTGCCAGAT
IL-8	AAGTTCATCCACCCTAAATC	GCATCAGAATTGAGCTGAGC
IFN-α	TCCTCCAACACCTCTTCGAC	GGGCTGTAGGTGTGGTTCTG
IFN-β	CCTCAACCAGATCCAGCATT	GGATGAGGCTGTGAGAGGAG
IFN-γ	GCTGATGGCAATCCTGTTTT	GGATTTTCAAGCCAGTCAGC
Viperin	TGCCGAGATTATGCTGTTGC	AGCATCTTCCCCACTGTTCT
GAPDH	ATGTTCGTGATGGGTGTGAA	CTGTCTTCGTGTGTGGCTGT

Table 3.1. List of primers used in the study.

3.4. Results

3.4.1 Viral gene and cytokine expression in PBMC

In duck PBMC, viral gene (gC) expression was found to be elevated at 3 and 5 dpi. At 1 dpi no viral gene expression was noticed whereas, maximum expression was observed at 3 dpi followed by diminished expression of a viral gene on day 5 (Figure 3.1 A). Expression of cytokines namely IL-1β, IL-2, IL-6, IL-8, IFN-α, IFN-β, IFN-γ, and viperin was examined. As shown in (Figure 3.1 B) at 1 dpi significant expression of IL-1β only, no expression was

observed for another cytokine, IFN, and viperin. Significant upregulation of pro-inflammatory cytokine IL-1β, IL-2, IL-6, IL-8, and IFN from 3 dpi was seen and the highest was on 5 dpi along with the upregulation of viperin at 3 and 5 dpi. Among IFNs, maximum fold change was observed in IFN-γ at 5 dpi.

3.4.2 Viral gene expression in different organs

The viral gene expression was measured by real-time quantitative PCR. As shown in (Figure 3.2) no significant expression of the viral gene was observed in the bursa, lung, liver, and spleen whereas marginal expression was seen in the brain on 1 dpi. At 3 dpi, viral gene expression in various tissue was elevated. In the brain, the expression was elevated by 6.16 fold and 5.5 fold in the spleen, which represents the highest among all tissues, followed by bursa (2.7 fold), and least in lung and liver. At 5 dpi, the expression of the viral gene in the brain was declined by three-fold and by four-fold in the spleen, and a similar trend was observed in the bursa, lung, and liver. In qRT-PCR the gC mRNA levels were normalized to GAPDH mRNA and represented as mean fold expression with respect to the control group. The fold change in gene expression was calculated by $2^{-\Delta\Delta Ct}$.

3.4.3 Cytokine profiling in different organs

Activation of innate immunity is through PRRs, upon PRRs stimulation, several pro-inflammatory cytokines including IL-1β, IL-2, IL-6, IL-8 were induced. The expression of IL-1β was elevated at 3dpi in the brain, bursa, lung, liver, and spleen and scarcely increased at 5 dpi (Figure 3.3 A). The highest expression of IL-2 was recognized in the brain, lung, and spleen at 5dpi (Figure 3.3 B). The expression of IL-6 and IL-8 was up-regulated in the brain from day 1 and highest fold change at 3 dpi, while the expression change was relatively low in the spleen followed by a bursa, and no significant expression was noticed in the lung and liver. (Figure 3.3 C and 3.3 D). IFNs system gets initiated with the activation of PRRs leads to the induction

of ISGs. We examined the expression of IFNs (IFN-α, IFN-β, IFN-γ) and ISG (viperin) in all the organs. The expression of IFN-α, IFN-β, IFN-γ was observed from 1dpi and elevated from 3dpi till 5dpi. The highest expression of IFN-α was observed in the brain and marginal expression was seen in the lung and spleen (Figure 3.3 E) whereas the expression of IFN-β was significantly observed in the brain, bursa, lung, and spleen (Figure 3.3 F). The expression of IFN-γ was highest in the brain and no significant expression was observed in other organs (Figure 3.3 G). The expression of viperin was observed at 1, 3, and 5dpi in the brain, and also the expression was elevated at 5dpi in the lung and spleen (Figure 3.3 H).

.

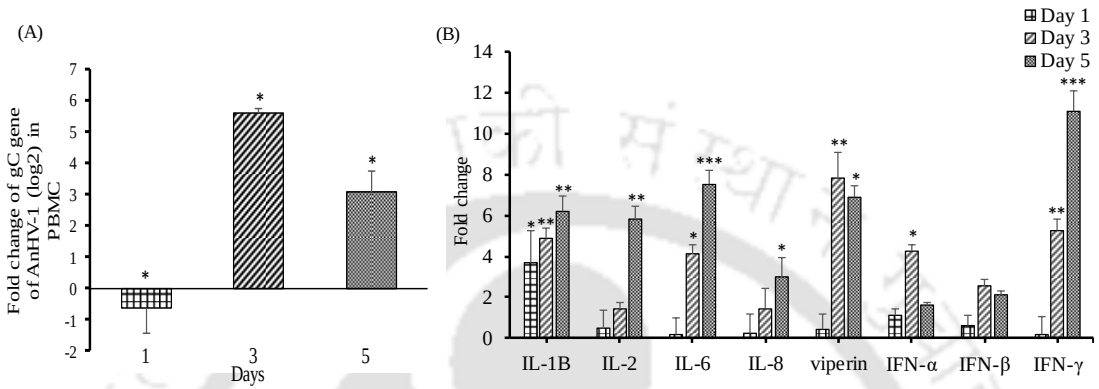

Figure 3.1. AnHV-1 gC gene expression in PBMC isolated from duck blood at 1, 3, and 5 dpi. The data were expressed as means ± standard deviation (A). Expression profiles of cytokines in PBMC of immunized ducks at 1, 3, and 5 dpi (B). Total RNA was extracted, and cDNA was prepared for detecting the cytokines. The expressions of cytokines tested in this study were measured using a $2^{-\Delta\Delta Ct}$ method by relative quantification. Data were expressed as mean fold change. Statistical significance difference was determined by using one-way ANOVA (Dunnett's multiple comparisons test, GraphPad Prism 8). An asterisk indicates a significant difference (*), (**), (***) of $P < 0.05$; $P < 0.01$; $P < 0.001$ respectively.

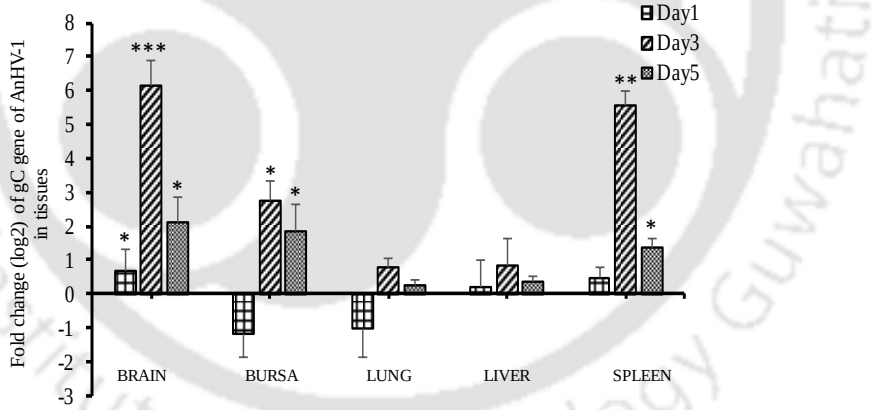

Figure 3.2. Expression of gC gene of AnHV-1 was determined by the qRT-PCR. Different organs were collected from duck at 1, 3, and 5dpi. and analyzed for their relative mRNA levels. The data were expressed as means ± standard deviation. The mRNA determinations were performed by qRT-PCR, and mRNA levels were normalized to GAPDH mRNA and represented as mean fold expression with respect to the control group. The fold change in gene expression was calculated by 2–ΔΔCt and the data were transformed in log base 2. The results were statistically analyzed using one-way ANOVA (Dunnett's multiple comparisons test, GraphPad Prism 8). An asterisk indicates a significant difference (*), (**), (***) of $P < 0.05$; $P < 0.01$; $P < 0.001$ respectively.

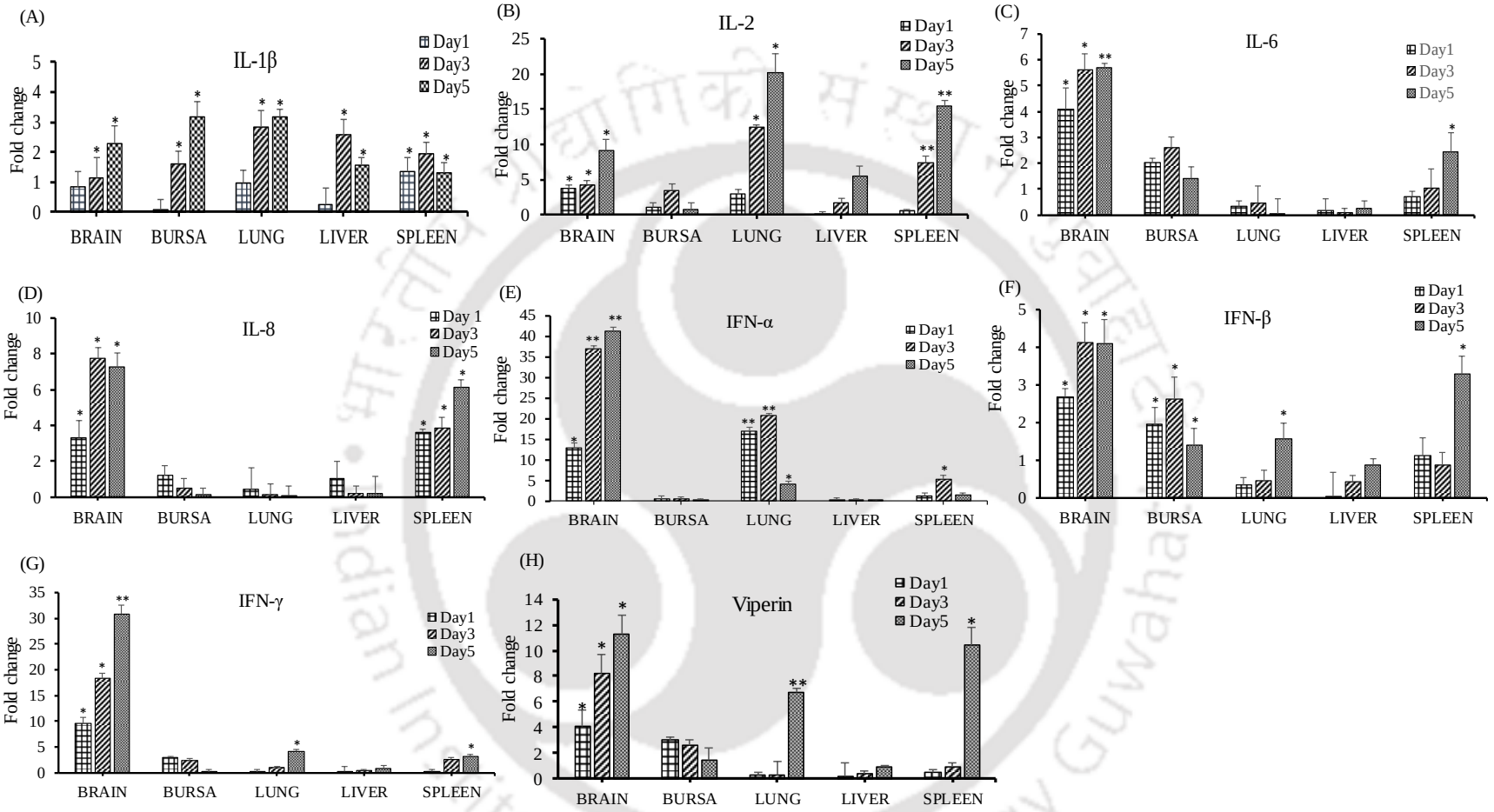

Figure 3.3 Expression profiles of different cytokines in different organs of immunized ducks at 1, 3, and 5 dpi (A-H). Total RNA was extracted and cDNA was prepared for detecting the cytokines. The expressions of cytokines tested in this study were measured using a $2^{-\Delta\Delta Ct}$ method by relative quantification and mRNA levels were normalized to GAPDH mRNA. Data were expressed as mean fold change. Statistical significance difference was determined by using one-way ANOVA (Dunnett's multiple comparisons test, GraphPad Prism 8). An asterisk indicates a significant difference (*), (**), (***) of $P < 0.05$; $P < 0.01$; $P < 0.001$ respectively.

3.5 Discussion

The present study investigated the change in expression of the pro-inflammatory cytokine, IFNs, and viperin in ducks immunized with a vaccine strain of AnHV-1. Expression analysis on PBMC suggests cooperative induction of cytokines, IFNs, and viperin at 5 dpi which explains the diminished viral gene expression at 5 dpi. AnHV-1 has been reported to show broad organ tropism (Liu et al., 2017).Our results suggested that AnHV-1 can enter and replicate in a variety of tissues, mainly in the brain, bursa, and spleen. The highest viral gene expression in the brain indicated that AnHV-1 can quickly replicate in the central nervous system and these findings agree with previous studies (Li et al., 2016). Pro-inflammatory cytokine's function is critical for the initiation of inflammatory response; however, its level may have peaked before the appearance of clinical signs and symptoms. Differential expression of IL-1β, IL-2, IL-6, IL-8 has been observed with the highest expression in the brain compared to other organs. This may suggest the neurotropic nature of AnHV-1. In previous studies, tissue-specific immune response has been discussed, earlier it has been reported that in HSV-1 brain is involved in the innate immunity (Marques et al., 2006). There is a significant correlation between the expression of IFNs and ISG (viperin) in the brain. These cytokines along with IFNs are known to promote both specific and non-specific immune response (Belardelli, 1995). A signalling molecule like cytokines is secreted from subsets of T_H immune cells that promote inflammation and plays an important role in mediating innate immune response. The evaluation of immune mediators is important to classify the host immune response during viral infection and may provide a better understanding of the immune efficiency of the host to the vaccination.

Chapter 4.

Understanding the role of viperin in AnHV-1 infection

Chapter 4

4.1 Abstract

AnHV-1 is a concern to the poultry industry. The prophylactic strategy should be explored that elicit immunity against the virus. Approaches that rely on the induction of host innate antiviral response has to be evaluated. In this study, we have studied the role of viperin in AnHV-1 infection. The modeling of the viperin protein was done using I-TASSER bioinformatics tool. We amplified and cloned chicken viperin which has 90% amino acid sequence identity with duck viperin in the eukaryotic expression system. We found that viperin overexpression in the DF-1 cell line significantly impairs AnHV-1 infection. Furthermore, the cellular localization of viperin was examined by immunofluorescence. The results showed its localization in lipid droplets. We have also evaluated if the cholesterol on the cellular membrane was altered by overexpression of viperin and it has been found that the inhibitory function of viperin was associated with reducing cholesterol in viperin overexpressed DF-1 cells. The recombinant NDV expressing viperin showed reduced replication of the virus upon its growth kinetics. Our results suggest a downregulation of AnHV-1 replication in the presence of viperin. The study will be important to elaborate our understanding of the poultry innate immune system which could help develop antiviral strategies against AnHV-1 infection.

4.2 Introduction

Viral entry, replication, and maturation are crucial for viral pathogenesis. To overcome viruses and restrict their replication and infectivity host antiviral defence mechanism comes in the form of PRRs which ultimately activate IFN response. Binding of IFN to their receptor results in the transcription of ISGs. ISGs encode for proteins that can interfere with the viruses at different stages which can interfere with viruses at different stages of the virus replication cycle, and act as antiviral protein (Sadler and Williams, 2008). Viperin is induced in various cells by type I/II IFNs, poly(I: C), dsRNA, viral DNA, lipopolysaccharides (LPS), and a broad range of viruses (Chin and Cresswell, 2001, Ishii et al., 2006, Rivieccioet al., 2006, Severa et al., 2006, Suh et

al., 2007). It is highly conserved across various species and involved in regulating host innate immune response (Chin and Cresswell, 2001, Jiang et al., 2008, Fitzgerald, 2011). Viperin localizes in the endoplasmic reticulum (ER) from ER it is transported to a lipid enriched compartment called lipid droplets (LDs) (Chan et al., Wang et al. 2013). The role of LDs in immunity has been studied and it has been shown that it acts as an assembly and replication platform for some viruses (Jiang and Chen, 2011, Saka and Valdivia, 2012). Viperin is known to bind and inhibit FPPS (Makins et al., 2016). Thus, cholesterol-rich rafts membranes that serve as sites for the recruitment of several viral proteins are consequently perturbed and impair virus release from the host membrane (Wang et al., 2007). AnHV-1 is an enveloped virus that may rely on cellular lipid for its replication and establish infection. This work intends to extend knowledge on host antiviral factors focusing on lipid structures that are of great importance for virus replication. It is critical to examine the role of ISGs in detail against viral for the development of novel therapeutics. In the present study, we have analyzed the modulation of AnHV-1 replication upon expression of viperin in DF-1 and shown the reduced cholesterol concentration in viperin overexpressed cells.

4.3 Materials and Methods

4.3.1 Three-dimensional protein structure prediction and phylogenetic analysis

The structure prediction and determination of physiological and biochemical properties of the protein was based on the amino acid sequence of viperin. A ProtParam tool from the ExPASy bioinformatics resource portal was used to compute the physical and chemical features such as molecular weight, amino acid composition, and molecular coefficient of the uncharacterized viperin protein (Hoogland C. 2005). I-TASSER, a computational server was used to predict and generate the 3-D structure of viperin (Yang et al., 2015). I-TASSER server initially retrieves a template from the PDB library using LOMETS, a meta-threading approach. The continuous fragments obtained from PDB prototypes were re-assembled into full-fledged

models by Monte-Carlo simulations. Of the obtained analysis, the lowest energy state proteins are picked using SPICKER (Zhang and Skolnick, 2004). The top five models were re-generated and guided by TM-align, an algorithm used to compare independent proteins with the help of their sequence-order (Zhang and Skolnick, 2005). As viperin is conserved over mammalian species (Goossens et al., 2015), the structure that was closely related to the viperin protein was chosen using a superimposition by pyMOL based on the RMSD value (DeLano, 2002). The available crystal structure of *Musmusculus* viperin (PDB id 5VSL) is used to superimpose the predicted viperin (Fenwick et al., 2017). The quality of the selected model was further validated using PROCHECK (Laskowski.,1993) a tool that generates a Ramachandran plot and discusses the stereochemical aspects of the viperin. VERIFY 3D (Eisenberg et al., 1997) tool was also used for the validation of the predicted model, and the ProSA server (Wiederstein and Sippl, 2007) was used to calculate the native conformation. Viperin sequence from 16 different species was obtained from the NCBI protein repository and realize the identity and the conserved region among the other species. Multiple sequence alignment by Clustal Omega was used to calculate the identity as well as the regions that are conserved among viperin protein among species. The phylogenetic tree was constructed using the phylogeny.fr platform (Dereeper et al., 2008, Dereeperet al., 2010).

4.3.2 Virus and cells

The DF-1 cells were obtained from ATCC (Manassas, VA, USA) and HEp-2 was procured from the NCCS, Pune, India, and maintained in DMEM supplemented with 10% FBS and 1% antibiotics-antimycotics at 37^0C in 5% CO_2. The vaccine strain of AnHV-1 mentioned in section 2.3.1 was used for the infection studies. Besides, the recombinant NDV (rNDV) and recombinant NDV expressing GFP (rNDV.GFP) available in the laboratory was used for the comparative studies of recombinant virus (Shah, et al., 2019).

4.3.3 Cloning and expression of viperin

The PBMCs were isolated from chicken whole blood as mentioned in section 3.3.2. Further, total RNA was extracted from PBMCs using TRIzol® reagent (Invitrogen, USA) according to the manufacturer's protocol. The cDNA was synthesized using a SuperScript™III RT enzyme (Invitrogen, USA) and the viperin gene was amplified by gene-specific primers (forward:5´-CTAGCTAGCATGGACTACAAAGACGATGACGACAAGATGCTGCTGGGCGTTC-3´and reverse: 5´- CGGAATTCTTACCAGTCCAGAATC - 3´). The amplified viperin gene product was cloned into a pcDNA3.1 mammalian expression vector (Invitrogen, USA). The positive clones containing the viperin gene were confirmed by restriction digestion, and further by nucleotide sequencing. The expression of viperin was confirmed using qRT-PCR, DF-1 cells were transfected with plasmid DNA expressing viperin using Lipofectamine reagent (Invitrogen, USA) following the manufacturer's instructions and RNA was isolated from the viperin transfected cells. The cDNA was synthesized by PrimeScript first-strand cDNA synthesis kit (TaKaRa, Japan). Viperin gene expression was quantified using real-time primer mentioned in table 3.1 and GAPDH as an internal control. Also, the transfected cell lysate was used to check the expression of the proteins by western blotting. The blots were developed using polyclonal anti-viperin (Thermo Fisher Scientific, USA.) and anti-β-actin mAb (Invitrogen, USA) with ECL reagent (Thermo Fisher Scientific, USA).

4.3.4 AnHV-1 infectivity studies upon overexpression of viperin

The DF-1 cells were transfected with plasmid DNA expressing viperin to deduce the effects of viperin on AnHV-1 replication. AnHV-1 with an MOI of 1 was used to infect the DF-1 at 24 h post viperin transfection. The expression of the viperin and UL-30 gene of AnHV-1 was checked by semi-quantitative PCR and GAPDH was used as an internal control. For qPCR RNA was isolated from the viperin transfected cells followed by AnHV-1 infection, gC gene

of AnHV-1 and viperin gene expression were quantified using GAPDH as an internal control. The relative fold gene expression was analyzed using the $2^{-\Delta\Delta Ct}$ method and the results were statistically expressed as the average of three independent experiments and were shown as the mean ± S.D. Besides, the infected cell lysate was used to check the expression of the proteins by western blotting. The blots were developed using anti-AnHV-1 polyclonal antibody, anti-β-actin mAb (Invitrogen, USA). AnHV-1 titer was also determined in viperin overexpressed cells by $TCID_{50}$ assay using the method mentioned in section 2.3.7.

4.3.5 Cellular localization study

The DF-1 cells were seeded on a coverslip and incubated overnight for attachment and growth. The next day the cells were transfected with pcDNA.viperin-FLAG and pcDNA 3.1. After 48h the cells were fixed by 4% paraformaldehyde, washed, and then permeabilized with 0.1% Triton-X 100, fixed cells were washed with PBS and incubated in 5% blocking buffer (5% BSA in PBS) for 1 h at 37^0C. For viperin detection, cells were incubated with 1/100 dilution of mouse monoclonal anti-FLAG (Invitrogen) for 1 h at 37^0C, followed by a secondary incubation with 1/100 dilution of Alexa 594 conjugated goat anti-mouse IgG antibody (Invitrogen) respectively. For lipid droplet staining cells were incubated with 2uM of BODIPY 493/503 (molecular probe) for 20 min, which allows fluorescent detection of LDs. After the final wash with PBS, cells were stained with 4′, 6-diamidino-2-phenylindole dihydrochloride (DAPI) and washed with PBS. After final washing slides were mounted and then examined under 63X objective using a Leica SP5 confocal microscope.

4.3.6 Cholesterol estimation upon overexpression of viperin

For cholesterol estimation, the cells were transfected with plasmid DNA expressing viperin, 48 hours post-transfection the cells were lysed in 1% (v/v) Triton X-100 in PBS and incubated on ice for 30 min to quantify the cholesterol. The cell lysate was centrifuged at 13,000 rpm for 10

min after incubation, and the supernatant was collected for cholesterol estimation. The amount of cholesterol in samples was determined by the Amplex red cholesterol assay kit (Cat no. A12216; Life Technologies, USA) following the manufacturer's instructions.

4.3.7 Construction and recovery of recombinant NDV expressing viperin

A reverse genetics approach is used to develop the recombinant NDV to express the viperin gene. A lentogenic strain of NDV has been used for constructing the recombinant NDV expressing viperin. The rNDV full-length expression plasmid (pNDV), available in the laboratory and reported earlier (Kumar, Kumar et al. 2019) was used to clone the viperin gene. The genomic sequence of NDV was flanked by the T7 promoter and the hepatitis delta virus (HDV) ribozyme sequence with the T7 terminator sequence. The restriction enzyme site of *AscI* (3236nt to 3243nt) was created by site-directed mutagenesis in pNDV which was utilized to insert the viperin gene in pNDV between the non-coding region of P and M gene of NDV. The ORF encoding the viperin gene was engineered to contain NDV gene start and gene end sequence of M gene of NDV. The primer used to have the *AscI* site, NDV gene end, gene start transcriptional signal and an intergenic sequence was used to amplify the viperin gene cassette (forward-5'-
AGGCGCGCCTTAAGAAAAAATACGGGTAGAAACCATGCTGCTGGGCGTTCTGG - 3') and (reverse-5'- AGGCGCGCCTTACCAGTCCAGAATCATGTCTG - 3'). PCR was performed using Ex Taq DNA polymerase (Takara, Japan) and PCR amplified fragment of the viperin gene was digested with *AscI* (NEB, USA) and cloned at *AscI* site of pNDV. The orientation of positive clones was confirmed by PCR and restriction digestion. Furthermore, the sequence integrity of the cassette was confirmed by sequencing. The rNDV full-length expression plasmid containing viperin was named pNDV.viperin.

The HEp-2 cells were grown overnight and were co-transfected with 3ug of pNDV.viperin together with 1ug of each three accessory plasmid bearing N, P, and L gene of

NDV (available in the laboratory) using 6ul of Lipofectamine 2000 reagent following manufacturer's instructions (Invitrogen, USA). Before transfection, the HEp-2 cells were infected with one focus forming unit of recombinant vaccinia virus strain Ankara expressing T7 polymerase (MVA/T7) (a Kind gift from Dr. Bernard Moss, NIH, USA) for efficient expression of T7 polymerase. After 6h post-transfection, the media was replaced with DMEM containing 2%FBS and 10% freshly collected allantoic fluid. The HEp-2 cells were scraped, freeze and thawed 96h post-transfection and centrifuged to collect the supernatant. 100ul of clarified supernatant was inoculated in the allantoic cavity of a 9-day-old SPF chicken embryonated egg. The inoculated eggs were monitored by candling and the allantoic fluid was harvested 96h post-inoculation and check for virus by haemagglutination assay (HA). The presence of rNDV.viperin in the allantoic fluid was confirmed by RT-PCR. The DF-1 cells were infected with recovered rNDV.viperin at MOI of 0.01. The cells lysate was harvested 48 hpi and western blot assay was performed using a monoclonal antibody against HN protein of NDV (a kind gift of Dr. R. Iorio, University of Massachusetts, USA), a polyclonal antibody against viperin (Thermo Scientific, USA), and β-actin was as an internal control (Invitrogen, USA). The recovered rNDV.viperin was further amplified and passaged ten times in 9-day-old SPF chicken embryonated egg and RT-PCR and nucleotide sequencing was performed from genomic RNA of rescued rNDV.viperin to check the integrity of the viperin gene.

4.3.8 Characterization of rNDV expressing viperin

The OIE recommended pathogenicity tests for NDV, MDT, and ICPI were performed. The MDT test is conducted on 9-day-old SPF chicken embryonated egg inoculated with a serial dilution of the virus. MDT is the meantime in hours for the minimal lethal dose to kill an embryo. The MDT < 60 hours for velogenic, 60-90 hours for mesogenic, and >90 hours for the lentogenic strain of NDV. A series of 10-fold serial dilution of the virus was made in sterile 1X PBS and 100ul of dilution was inoculated in the allantoic cavity of 9-day-old SPF chicken

embryonated egg. The inoculated eggs were incubated at 37°C and monitored by candling for 7 days and the time point of embryo death was recorded. Intracerebral pathogenicity index (ICPI) was performed in 1-day-old SPF chicks. A virus dilution was injected intra-cerebrally into 1-day-old SPF chicks. The birds are observed daily for eight days and scored 0 if normal, 1 if sick and 2 if dead. Index values of 0 (no clinical signs seen in birds during the 8 days) for lentogenic and 2 (birds dead within 24 hours) for velogenic strains of NDV. The growth kinetics of rNDV.viperin was performed by infecting DF-1 cell line with rNDV.viperin at different time points. The DF-1 cells were infected with rNDV, rNDV.GFP (available in the laboratory) and rNDV.viperin at an MOI of 0.01. The virus released was calculated by $TCID_{50}$ titer from the collected cell culture supernatant every 12 hpi.

4.4 Results

4.4.1 Physiological properties and protein structure prediction of viperin

The molecular weight of the viperin was predicted around 40kDa with an isoelectric point (pI) of 6.69. Bioinformatics analysis showed the presence of 50% positively charged, 49% negatively charged, and the rest non-polar amino acids in viperin. Additionally, leucine was found to be the most abundant amino acid in viperin. The molar extinction coefficient of viperin was 1.265 when all cysteine residues form cystine while the value of 1.250 was calculated when all cysteine is reduced. The three-dimensional structure of viperin was obtained using I-TASSER and validated by the PROCHECK server through the Ramachandran plot (Figure 4.1 A). Based on TM-align, the structure closest to viperin of *Mus musculus* had a confidence score of -1.38 and the TM-align score of both viperin was 0.73. Any TM-score in the range of (0.5, 1) is considered to be very similar in nature (structurally). The RMSD value was found to be 0.45. The best model showed the presence of 213 residues (67.8%) in the most favourable regions, 67 residues (21.3%) in additionally allowed regions, 23 residues (7.3%) in generously

allowed regions, and 11 residues (3.5%) in disallowed regions (Figure 4.1B). The amino acid sequence of viperin from 16 different species was analyzed to compare the sequence identity and to determine the conserved regions using multiple sequence alignment by clustal omega. The sequence identity of viperin with other species has been shown in (Table 4.1), and a phylogenic tree was constructed. The phylogenic tree showed close clustering of viperin with duck viperin gene with high bootstrap value (Figure 4.1C).

Accession No.	Organism	Percentage similarity
ALM30210.1	Branchiostoma japonicum	62.72
XP_002197540.1	Taeniopygia guttata	84.97
AJG06248.1	Anas platyrhynchos	89.27
XP_003204532.1	Meleagris gallopavo	96.05
AAL50054.1	Mus musculus	76.01
NP_620236.1	Rattus norvegicus	76.30
XP_851276.1	Canis lupus familiaris	77.10
NP_001129006.1	Pongo abelii	77.97
AAL50053.1	Homo sapiens	78.26
AFO10959.1	Pan troglodytes	77.68
AFO10974.1	Aotus trivirgatus	75.94
AFO10975.1	Plecturocebus moloch	75.94
AAI05456.1	Bos taurus	78.16
NP_998982.1	Sus scrofa	77.17
ABJ97316.1	Danio rerio	73.31
ABO48457.1	Siniperca undulata	69.71

Table 4.1. Percentage similarity between amino acids. Different viperin and chicken viperin sequences were collected from the NCBI protein repository to realize the similarity. Clustal Omega was used to calculate the similarity as well as the regions that are conserved among viperin protein of various species.

4.4.2 The viperin expression is upregulated in DF-1 cells by AnHV-1 infection

The expression of viperin was investigated in DF-1 cells following AnHV-1 infection. The viperin mRNA expression was continued to increase up to 84 h following viral infection (Figure 4.2 A). Similarly, AnHV-1 infection showed upregulation of its gene expression (gC gene) from 24 h till 72 hpi. The expression of the viral gene was reduced marginally from 72h till 96 hpi (Figure 4.2 B).

4.4.3 Construction and expression of viperin in the eukaryotic expression system

The viperin was successfully amplified from isolated PBMC and cloned into the pcDNA3.1 expression vector (pcDNA.viperin). The positive clone of pcDNA.viperin showed a release of the 1065bp band upon digestion with *Nhe*I and *EcoR*I (Figure 4.3A). The sequence analysis of pcDNA.viperin confirmed the absence of any inadvertent mutation and right orientation of the viperin into a eukaryotic expression system. The expression of pcDNA.viperin was confirmed by qRT-PCR, viperin expression was 18 fold high in pcDNA.viperin transfected cells compared to untransfected cells (Figure 4.3 B). The pcDNA.viperin showed expression of viperin protein following its transfection in DF-1cells. β-actin was used as an internal control to check the expression of the cellular protein. In addition, western blot analysis with a polyclonal antibody against the viperin protein (Thermo Scientific, USA) detected a band of the molecular mass of ~40kDa in cell lysate transfected with pcDNA.viperin (Figure 4.3 C).

4.4.4 Inhibition of AnHV-1 upon viperin expression in DF-1 cells

The role of viperin in inhibiting AnHV-1 infection was determined by transfecting DF-1 cells with pcDNA.viperin followed by AnHV-1 infection. Gene expression of AnHV-1 'UL30' gene and viperin was quantified by semi-quantitative PCR considering GAPDH as an internal control (Figure 4.4 A). Transfection of pcDNA.viperin showed a reduction in AnHV-1 gC gene expression by 3.7-fold (log_2 scale) as compared to mock-infected control in the qRT-PCR analysis (Figure 4.4 B). The finding of AnHV-1 reduction was further validated by western blot analysis using polyclonal AnHV-1 antibody which displayed a very faint AnHV-1 protein band upon viperin expression (Figure 4.4 C). In addition, the viral titer showed a significant reduction of AnHV-1 following viperin expression in DF-1 cells (Figure 4.4 D).

4.4.5 Cellular localization study and cholesterol estimation

The viperin was examined for its association with LDs by immunofluorescence assay. Transfection study of viperin showed its co-localization with the LDs (Fig. 4.5 A). Transfection

of viperin in DF-1 cells was followed by the staining with anti-viperin antibody showed red and lipid droplets stained with BODIPY dye as green fluorescence whereas no expression of viperin was detected in plain vector and cell control. The orange spots in the merged panel correspond to the overlap region showing the localization of viperin in LDs. The cell nuclei were stained with DAPI showed blue color. Upon cholesterol estimation, we observed cholesterol levels were reduced to 65% in DF-1 cells transfected with pcDNA.viperin as compared to un-transfected cell control (Figure 4.5 B).

4.4.6 Construction and recovery of recombinant NDVs expressing viperin

The viperin gene was inserted into pNDV vector. The ORF of the gene was flanked by gene start and gene end sequence of M gene of NDV. The transcriptional cassette of viperin was cloned into the unique AscI site created between the P and M gene in the pNDV backbone to generate pNDV.viperin plasmid. A schematic representation of pNDV.viperin was shown (Figure 4.6 A). The pNDV.viperin was confirmed by *AscI* digestion, which led to the release of 1065bp gene fragment (Figure 4.6 B). Additionally, the PCR amplification and nucleotide sequencing of the viperin gene showed its correct orientation in the pNDV construct. The rNDV.viperin was successfully recovered in HEp-2 cells following transfection of recombinant plasmid pNDV.viperin. The recovered rNDV.viperin showed a titer of 2^3 HA units in the second passage, which increased to 2^7 HA units following subsequent passage in the embryonated chicken egg. Confirmation of recovered recombinant virus was done by PCR using forward primer of pNDV vector and reverse primers of viperin as well as with gene-specific primers (Figure 4.6 C). Recovery of recombinant virus and expression of viperin was further confirmed by western blot in DF-1 cells infected with rNDV and rNDV.viperin using NDV-HN specific monoclonal antibody and viperin specific polyclonal antibody. The NDV-HN specific monoclonal antibody showed a band of ~74kDa corresponding to the HN protein

of rNDV and rNDV.viperin. Parallel blots developed with anti-viperin antibody showed a band of ~40kDa. (Figure 4.6 D).

4.4.7 Characterization of the recombinant NDV expressing viperin

MDT and ICPI are tested to determine the virulence of rNDVs whether, it belongs to lentogenic, mesogenic or velogenic strain. The MDT values for rNDV, rNDV.viperin, and rNDV.GFP was found >120h. The ICPI values for rNDV, rNDV.viperin, and rNDV.GFP was recorded zero. To investigate the role of viperin in the viral life cycle, replication analysis of rNDV and rNDV.viperin was performed in the DF-1 cell line. The genomic RNA analysis of N gene of NDV of rNDV.viperin showed two-fold reductions as compared to the rNDV at 72 hpi (Figure 4.7 A). The N gene mRNA levels were normalized to GAPDH mRNA and represented as mean fold expression with respect to control. The fold change in gene expression was calculated by $2^{-\Delta\Delta Ct}$. Similar findings were observed in their protein analysis where rNDV.viperin showed lower protein concentration as compared to the rNDV (Figure 4.7 B). The multi-cycle growth kinetics were performed in DF-1 cells. Moreover, the rNDV.viperin showed a decrease in titer of more than one $\log_{10}$ as compared to parental rNDV and rNDV.GFP in all the time points in the growth kinetics study (Figure 4.7 C).

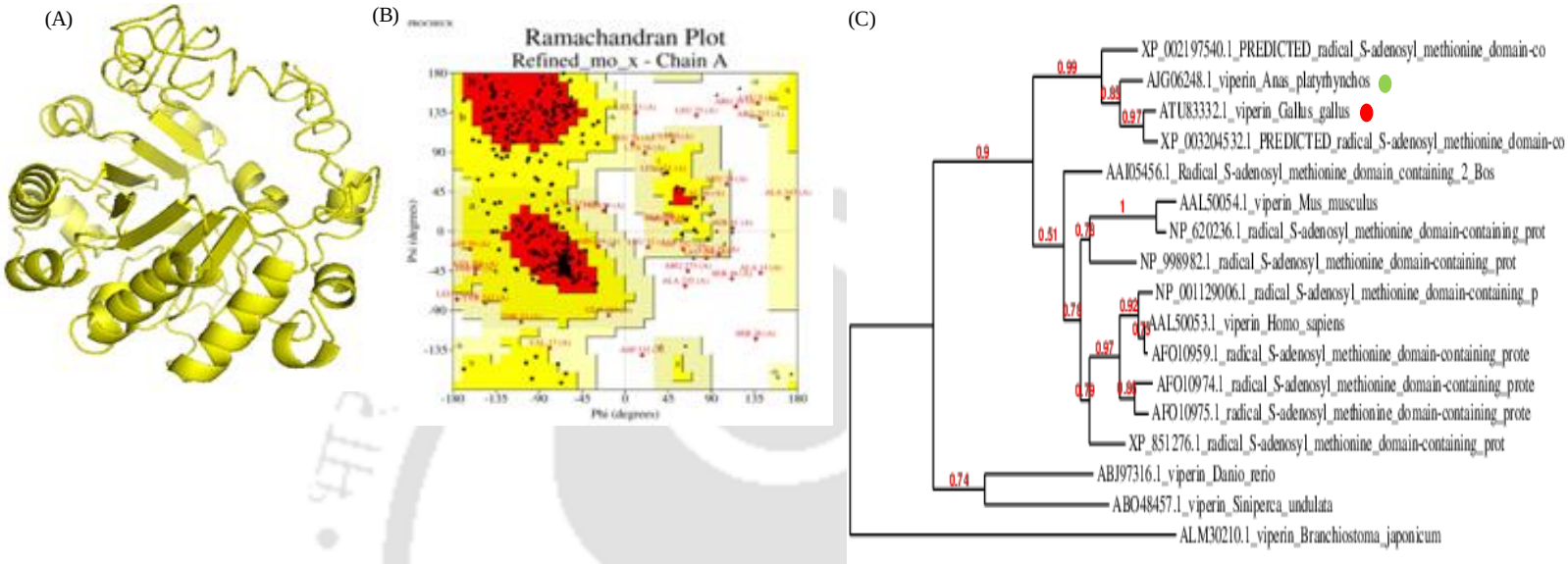

Figure 4.1 The predicted protein structure of viperin by I-TASSER (A) with its analyzed Ramachandran plot (B). Phylogenic analysis of viperin. The chicken viperin protein was analyzed with 16 different viperin sequence. The phylogenic tree was constructed using phylogeny.fr (www.phylogeny.fr) (C).

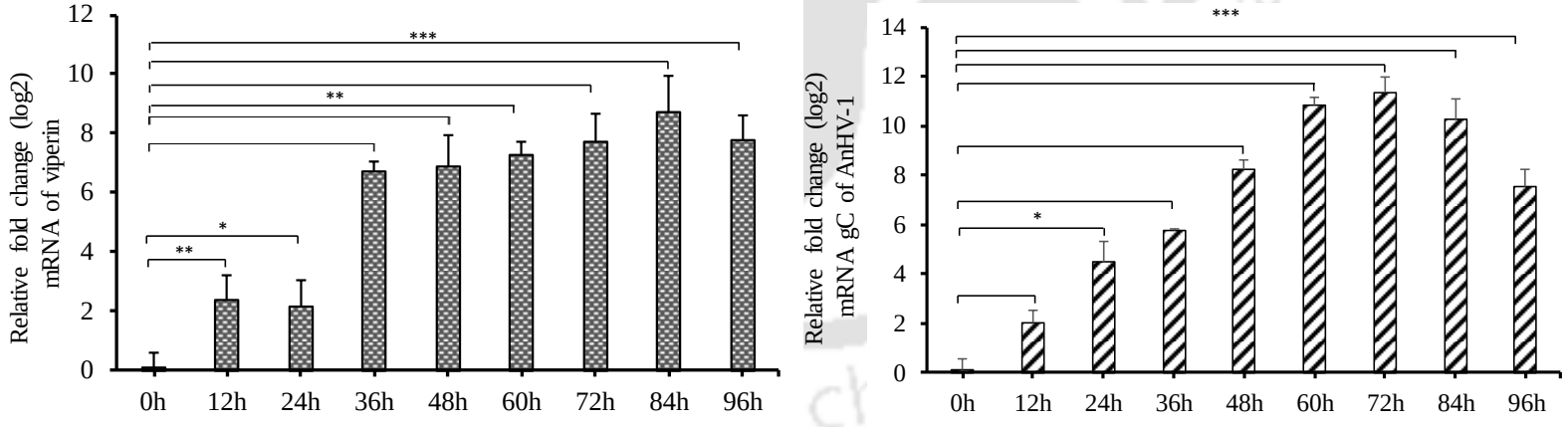

Figure 4.2 Expression of viperin upon AnHV-1 infection was analyzed by qRT-PCR, and mRNA levels were normalized to GAPDH mRNA and represented as mean fold expression with respect to control. (A) Expression of gC gene of AnHV-1 was determined by the qRT-PCR. The DF-1 cells infected with AnHV-1 were collected after 0, 12,

24, 36, 48, 60,72, 84, and 96 h post infections and analyzed for their relative mRNA levels (B). The data presented are the average of three independent experiments and was shown as the mean ± S.D. The fold change in gene expression was calculated by $2^{-\Delta\Delta Ct}$ and the data were transformed in log base 2. The results were statistically analyzed using one-way ANOVA (Dunnett's multiple comparisons test, GraphPad Prism 8). An asterisk indicates a significant difference (*), (**), (***) of $P < 0.05$; $P < 0.01$; $P < 0.001$ respectively.

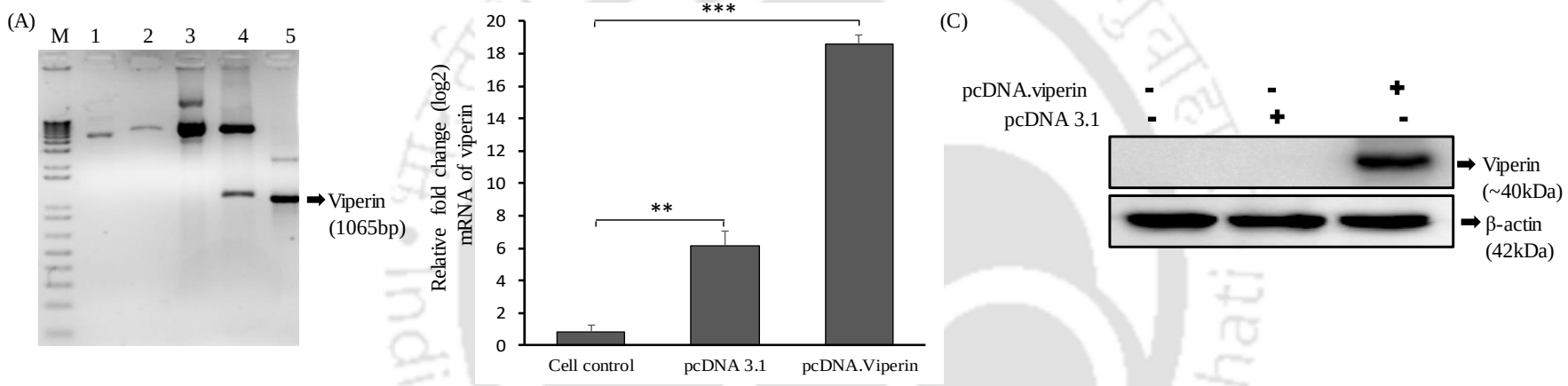

Figure 4.3 The molecular cloning of viperin from Gallus gallus. Lane M: DNA ladder 1kb; lane 1: undigested pcDNA3.1; lane 2: linearized pcDNA3.1; lane 3: undigested pcDNA.viperin; lane 4: double digested pcDNA.viperin using NheI and EcoRI; lane 5: PCR confirmation of viperin gene by gene-specific primers. (A). The expression of viperin was checked using qRT-PCR in DF-1 cells transfected with pcDNA 3.1 and pcDNA.viperin and compared with un-transfected control). The data presented are the average of three independent experiments and were shown as the mean ± S.D. The fold change in gene expression was calculated by $2^{-\Delta\Delta Ct}$ and the data were transformed in log base 2. The results were statistically analyzed using one-way ANOVA (Dunnett's multiple comparisons test, GraphPad Prism 8). An asterisk indicates a significant difference (*), (**), (***) of $P < 0.05$; $P < 0.01$; $P < 0.001$ respectively. (B). The cell lysates were prepared at 48 h post-transfection and analyzed for viperin protein by an immune blot. The β-actin was used as a loading control (C).

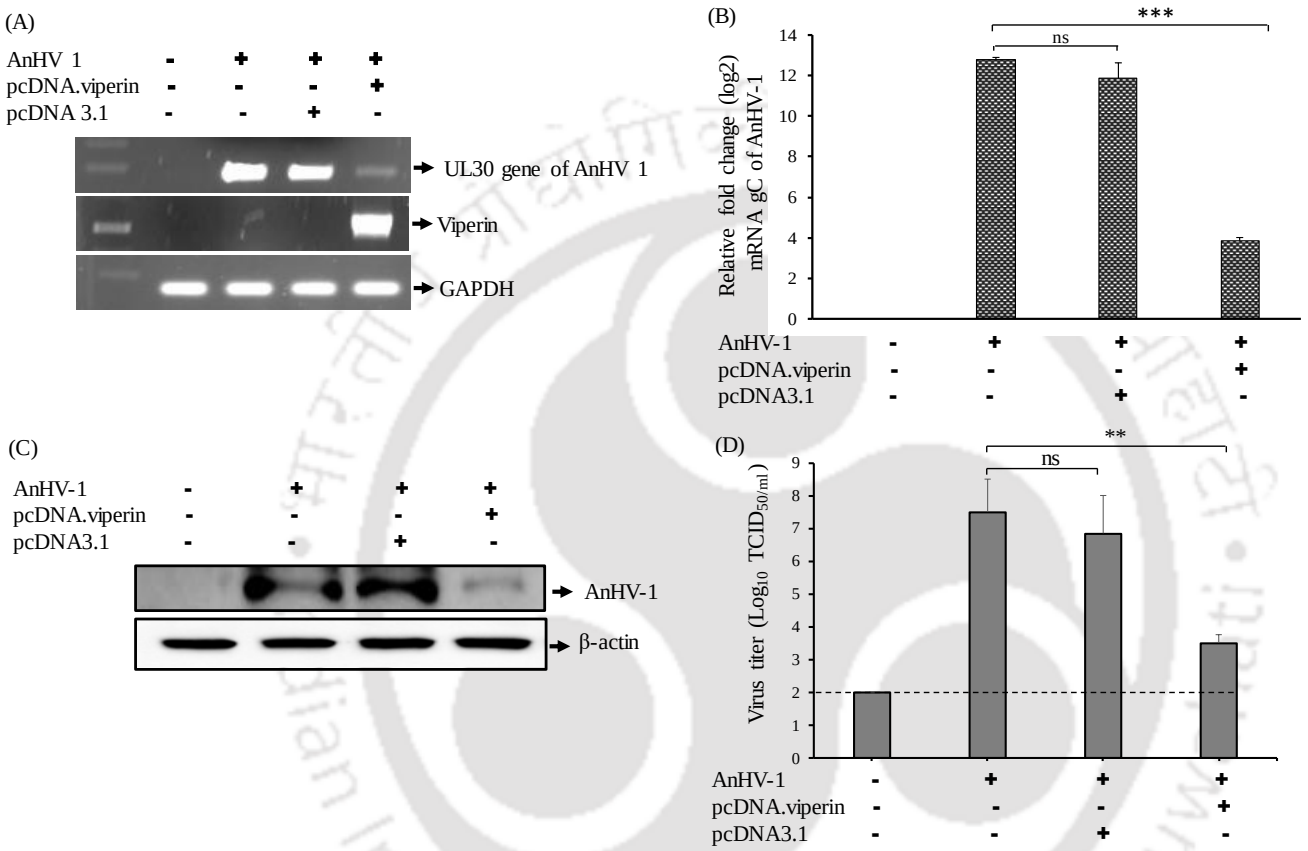

Figure 4.4. The expression of the AnHV-1, UL30 gene was analyzed by the semi-quantitative PCR in DF-1 cells transfected with pcDNA3.1 and pcDNA.viperin (A) The mRNA expression of gC gene of AnHV-1 was analyzed by the qRT-PCR, and mRNA levels were normalized to GAPDH mRNA and represented as mean fold expression with respect to control. The fold change in gene expression was calculated by $2^{-\Delta\Delta Ct}$ and the data were transformed in log base 2. The results were statistically analyzed using one-way ANOVA (Dunnett's multiple comparisons test, GraphPad Prism 8). (B). The DF-1cells were transfected with pcDNA3.1 and pcDNA.viperin, and cell lysates were analyzed for AnHV-1 protein by western blot at 72 hpi. The β-actin was used as a loading control. (C). The pcDNA3.1 and pcDNA.viperin transfected cells were infected with AnHV-1, and virus yield was calculated by $TCID_{50}$. (D). The data represent the mean ± standard deviation of three independent experiments. Statistical significance difference was determined by using one-way ANOVA (Dunnett's multiple comparisons test, GraphPad Prism 8). An asterisk indicates a significant difference (*), (**), (***) of $P < 0.05$; $P < 0.01$; $P < 0.001$ respectively.

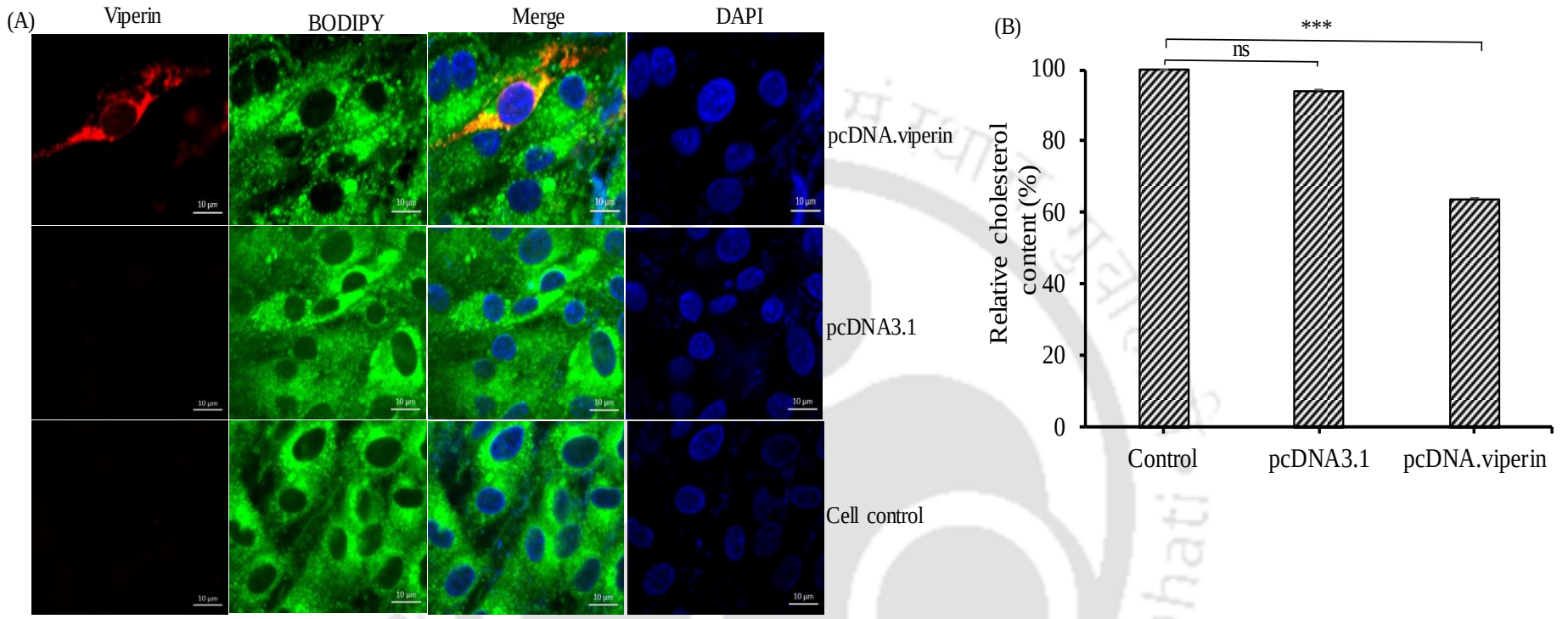

Figure 4.5 Cellular localization of viperin and lipid droplets. The DF-1 cells were seeded over coverslip, and the cells have been transiently transfected with viperin. The cells were analyzed by immunofluorescence for localization to lipid droplets using BODIPY lipid droplet marker and mouse anti-FLAG antibody for viperin expression after 48 h post-transfection. Representative images represent DF-1 cells stained with anti-viperin (red channel) and lipid droplets (green channel). The merged panel shows the co-localization of viperin and lipid droplets. Cell nuclei were stained with DAPI (blue channel). Samples were visualized under confocal microscopy with a magnification of 63X. (A). DF-1 cells were transfected with pcDNA3.1 and pcDNA.viperin, and the amount of cholesterol was determined in comparison to untreated cells using an Amplex red cholesterol assay kit. Statistical significance difference was determined by using one-way ANOVA (Dunnett's multiple comparisons test, GraphPad Prism 8) A p-value of less than 0.001 is flagged with three stars (***) and p-valve of more than 0.05 is labeled as non-significant (ns) (B).

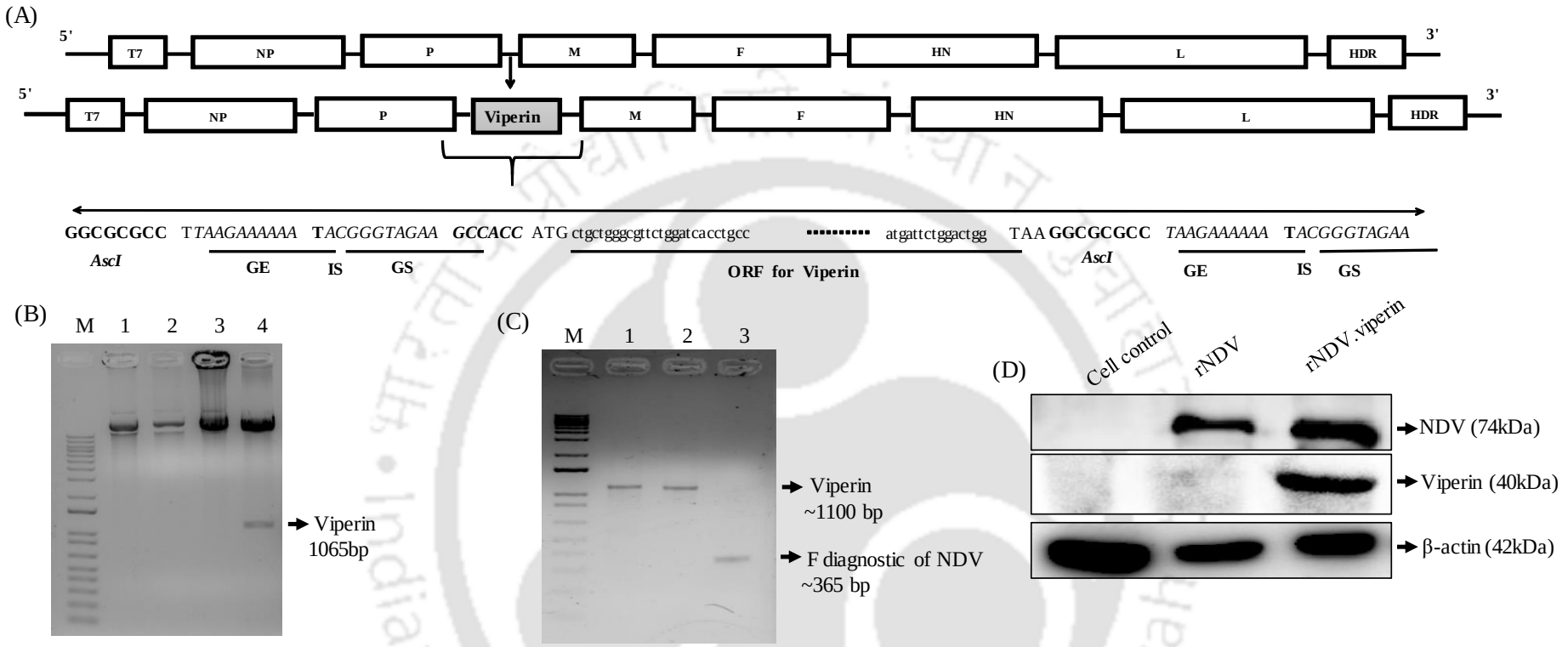

Figure 4.6. Construction of recombinant plasmid pNDV.viperin (A). The upper strand represents pNDV (T7 promoter, NP- nucleoprotein, P- phosphoprotein, M- matrix protein, F-fusion glycoprotein, HN-hemagglutinin-neuraminidase protein, L-large polymerase protein, and HDR- hepatitis delta ribozyme) and the lower strand represents pNDV.viperin. The viperin cloned at AscI site between the P and M genes of the NDV antigenomic cDNA. The ORF of viperin has a flanking sequence of NDV gene end (GE), an intergenic T nucleotide, and a gene start (GS). The confirmation of pNDV.viperin full-length clone (B). Lane M: DNA ladder; lane 1: undigested pNDV; lane 2: AscI digested pNDV; lane 3: undigested pNDV.viperin; lane 4: AscI digested pNDV.viperin showing the release of a 1065 bp gene. The PCR confirmation of rNDV.viperin (C). Lane M: DNA ladder; lane 1: amplification by the forward primer of pNDV vector and reverse primer of the viperin gene; lane 2: amplification by viperin gene-specific primer; lane 3: amplification by pNDV specific primers. The western blot analysis for the confirmation of NDV and viperin protein expressions by rNDV.viperin using the monoclonal antibody of HN and polyclonal antibody of viperin, respectively (D).

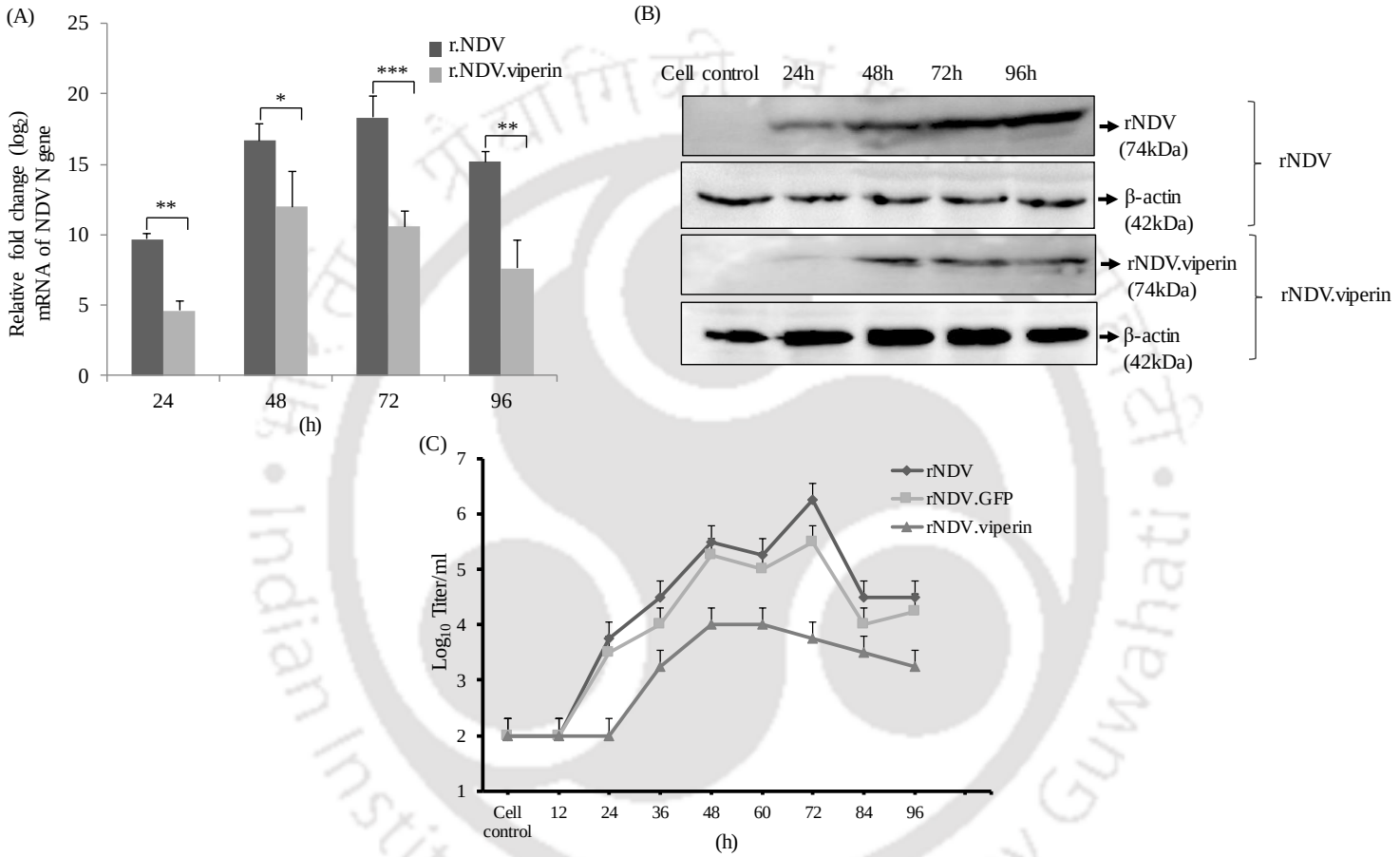

Figure 4.7 Reduced replication of rNDV.viperin as compared to rNDV and rNDV.GFP at different time points post-infection in DF-1 cells. The expression of the N gene was analysed by the qRT-PCR in DF-1 cells infected with rNDV and rNDV.viperin. PCR and mRNA levels were normalized to GAPDH mRNA and represented as mean fold expression with respect to control. The qRT-PCR data were transformed in log base 2 (A). The western blot analysis is showing the reduction in the HN protein levels of rNDV.viperin as compared to rNDV (B). The growth kinetics of rNDV.viperin as compared to rNDV and rNDV.GFP is showing reduced viral titers (C). The q-PCR was performed three times and statistically analysed using the one-way ANOVA. An asterisk indicates a significant difference (*), (**), (***) of $P < 0.05$; $P < 0.01$; $P < 0.001$ respectively.

4.5 Discussion

AnHV- 1 causes highly virulent disease of poultry and has a severe impact on the economy of agriculture-based countries. The innate immune system is an evolutionarily conserved system of defence against pathogens (Kawai and Akira, 2005). The IFNs are important cytokines released by the host immune system in response to diverse poultry pathogens (Zhou et al., 2014). Upon infection, the host reacts by producing IFN-α/β which ultimately triggers several ISG. Recently type III IFNs have been recognized as antiviral cytokines and inducer of ISGs. Receptors of type I IFN is ubiquitous, whereas receptors of type III IFN are confined to the mucosal epithelium (Domanski et al., 1995, Sommereyns et al., 2008). The antiviral role of type III IFN has been shown against the Porcine epidemic diarrhoea virus (PEDV) (Zhang et al., 2018). Currently, limited data is available with respect to avian ISGs, and their antiviral functions need to be explored which can be efficaciously supplemented to control AnHV-1 and other poultry viral infections. Type I, II and III IFN inducible ISG has been identified in chicken fibroblast cells (Santhakumar et al., 2019). Recently, in a systematic study in chicken has determined 205 type I, 299 type II, and 421 type III ISGs (Dai et al., 2020). Viperin is also recognized as one such ISGs that are highly conserved. Furthermore, an ISG known as cholesterol 25-hydroxylase (CH25H) has been identified in chicken showing enhanced expression upon induction by chicken IFN α (Xie et al.,2019). The phylogenic study suggested that chicken viperin showed identity with viperin from other species inferring its conserved nature. However, the effect of viperin on AnHV-1 replication has not been reported. Our results reveal that the infection of DF-1 by AnHV-1 led to the induction of viperin. The overexpression of viperin significantly reduced the viral protein level. Our result demonstrates that the viperin effectively suppresses AnHV-1 proliferation both in the viral mRNA and protein level. Reduced virus titer in viperin overexpressed cells also suggests the reduced propagation of

AnHV-1. It has been reported that the viperin localizes to the cytoplasmic face of the ER and LDs (Hinson and Cresswell, 2009).

A comparison between chicken viperin and mouse viperin has shown 88% total amino acid similarity. The radical SAM enzyme hallmark CxxxCxxC conserved motif was found in the viperin of both organisms (Goossens et al., 2015). The predicted structure of viperin using bioinformatics tools showed a high confidence score. The study could have been more accurate provided the presence of more related proteins of the radical SAM family in I-TASSER's dataset. The small yet sufficient dataset yielded four proteins out of which the best was picked and refined. In our study, the changes in the conformation of a few amino acids were made using 3D refine server without altering their native conformation as reported during the modeling of other proteins (Bhattacharya et al., 2016). This could have changed the amino acid residues into their favourable state without reducing their number in disallowed regions. To understand the native structure, ProSA analysis was done and the z-score turned out to be in the range of native conformations reassured to use the structure for further analysis. The z-score of -7.57 obtained from the ProSA server suggests the native conformation of viperin as reported for other proteins (Wiederstein and Sippl, 2007). In previous studies, it has been shown that human viperin is composed of three distinct domains, an N-terminal domain, with variable length and sequence among different species (Seo et al., 2011). Amphipathic α helix present in the N-terminal is responsible for its association with the cytosolic face of the ER and lipid droplets (Hinson and Cresswell, 2009). The central domain contains three cysteine residues organized in CxxxCxxC motif, responsible for binding with iron-sulfur clusters tan (Duschene and Broderick, 2010, Shaveta et al., 2010), and the C-terminal domain a highly conserved between the species might perform a role in protein-protein interaction (Seo et al., 2011). Our results showed localization of viperin to LDs as reported earlier (Wang et al., 2013). As LDs are derived from ER where the synthesis of cholesterol occurs, it is possible that viperin

could affect the type and content of lipid in LDs (Hinson and Cresswell, 2009). In the present study, viperin has been shown to be induced by AnHV-1 infection and inhibits its replication in vitro. The localization of viperin to LDs may reflect the mechanism that viperin deploys to inhibits AnHV-1 replication. The diverse anti-viral mechanisms of viperin have been studied for various viruses. Viperin is the first reported molecule to affect rabies virus replication by reducing cholesterol and sphingomyelin of the host cell membrane (Tanget al., 2016). The anti-viral activity of viperin by inhibiting virus release was shown in the case of influenza and HIV-1 (Wang et al., 2007, Nasr et al., 2012, Tan et al., 2012). Our results of cholesterol estimation suggest that viperin may reduce cholesterol concentration in the cellular membrane and may alter the infectivity of AnHV-1.

Reverse genetics of NDV has been explored to understand its pathogenicity, vaccine, and anticancer activities. In this study, viperin was cloned, and the rNDV expressing viperin was recovered to interrogate the effect of viperin. The recovered rNDV.viperin showed no enhancement in its pathogenicity as analyzed by the MDT and ICPI tests suggesting the virus to be avirulent. The reduced viral titer of rNDV.viperin was observed as compared to parental NDV in the growth kinetics study which indicates that virus expressing viperin gets attenuated and its replication rate is diminished. The rNDV.GFP used as a control showed a minimal difference in the replication kinetics of NDV suggesting that the effect is not because of the addition of the foreign protein. Furthermore, the effect was also evident in both RNA and protein levels.

Chapter 5.

Role of cholesterol in AnHV-1 infection

Chapter 5

5.1 Abstract

Cholesterol is one of the major constituents of the plasma membrane and plays an important role in stabilizing cellular membrane structure. For several viruses, virus entry is cholesterol dependent. In this study, we demonstrated the effect of cholesterol depletion in both host cell membrane and viral envelope on the infectivity of AnHV-1. Cholesterol depletion from DF-1 cells by methyl-B-cyclodextrin (MβCD) inhibited the infectivity of AnHV-1. This inhibitory effect was moderately reversed by the exogenous replenishment of cholesterol in the cells. Furthermore, the inhibition of endogenous cholesterol synthesis by a statin drug also inhibited the infectivity of AnHV-1. Cholesterol depletion of the viral envelope reduced AnHV-1 infectivity might be by disrupting the viral envelope. Loss of infectivity of the virus might be due to MβCD mediated cholesterol depletion from the cell membrane. The results implicate that the cell membrane cholesterol is vital for the infectivity of AnHV-1 in DF-1 cells, and its depletion from virion curtails the infectivity by destabilizing the envelope.

5.2 Introduction

AnHV-1 is an enveloped alphaherpesvirus causing DVE in free-living, domestic duck, geese, and swans (Sandhu, 1997). The disease is widespread and frequent in captive waterfowl. Cholesterol is crucial for cell proliferation, provides the rigidity, and maintains the order of the host cell membrane (Singer and Nicolson, 1972, Mukherjee et al., 1998, Goluszko and Nowicki, 2005, Ikonen, 2008) and more than 90% of its total cellular content resides in the plasma membrane. As the crucial constituent of the plasma membrane, cholesterol affects the function and properties of membrane proteins such as receptors and enzymes (Gimpl, et al., 1997). Apart from its role in maintaining normal homeostasis, cholesterol has been shown to modulate various viral infections. The first step in viral infection is binding and entry of the virus into the host cells. Cholesterol present in lipid rafts is a critical component required by

microorganisms to enter or exit the intracellular compartments (Takahashi, 2009). In enveloped viruses, the fusion of viral membrane and host cellular membrane is a critical step for entry into the host cell in order to deliver the viral capsid into the cell cytosol. Many studies have demonstrated the entry of the enveloped virus into the host cell in a cholesterol-dependent manner including coronavirus, poxvirus, paramyxovirus, and herpesvirus (Bender, et al., 2003, Choi et al., 2005, Chung et al., 2005, Martinet al., 2012). The use of compounds like MβCD results in depletion of cholesterol from plasma membrane followed by dissociation of proteins from rafts (Simons and Toomre, 2000). Treatment of cells with inhibitors of cholesterol biosynthesis such as statin drugs is also another approach for manipulating lipid raft constituents. MβCD has been used to show the effect of cholesterol/lipid rafts for the entry of several viruses (Marjomaki et al., 2002, Danthi and Chow, 2004, Imhoff et al., 2007, Ren et al., 2008).

In the present study, we examined the role of cholesterol on AnHV-1 infection in DF-1 cells by altering cellular membrane and viral envelope cholesterol. We observed that intact cell membrane cholesterol was critical for the virus infection and the viral envelope cholesterol was also imperative for the viral infectivity in avian fibroblast cells.

5.3 Material and Methods

5.3.1 Cells culture and virus

The DF-1 cells were obtained from ATCC (Manassas, VA, USA) and maintained in DMEM supplemented with 10% FBS and 1% antibiotics-antimycotics at 37^0C in 5% CO_2. The vaccine strain of AnHV-1 procured from the College of Veterinary Sciences, Guwahati, India, and characterized in our laboratory was used for the study (Makhija and Kumar, 2017). The cells infected with virus stock with a series of 10-fold dilution were fixed with methanol and stained

with crystal violet 96h post-infection and titrated (Reed and Muench, 1938). All virus stocks were adapted in DF-1 cells, titrated, and stored at -80 °C for further use.

5.3.2 Chemicals and their cytotoxicity assays

The cytotoxicity of cholesterol (Cat no. C3045, Sigma Aldrich, USA) and MβCD (Cat no. TC227; Sigma Aldrich, USA) and lovastatin (Cat no. 1370600; Sigma USA) on DF-1 cells was analyzed by using MTT reagent as per manufacturer's instruction. Briefly, DF-1 cells were seeded in 96 well plates and treated with different concentrations of the compound. 10µl of MTT reagent (Cat no. 33611; SRL, India) was added into the culture medium after incubation at 37 ºC for 48h and then 100µl of dimethyl sulfoxide (DMSO) was added to dissolve the formazan crystals. The cell viability was determined as compared with the control. The optical density at 570 nm was measured by using a spectrophotometer (Multiskan Go, Thermo Scientific, USA).

5.3.3 Cholesterol depletion and replenishment assay

The DF-1 cells were treated with MβCD at concentrations 5, 10, 15, 20 mM, or lovastatin (4 µM) for 1h at 37 ºC in a serum-free medium to deplete the cholesterol. Lovastatin is a competitive inhibitor of the rate-limiting enzyme HMG-CoA reductase in cholesterol biosynthesis (Sinensky, Beck et al. 1990). MβCD or lovastatin was removed by washing the cells thrice with PBS and infected by AnHV-1 with a multiplicity of infection (MOI) of 1. For cholesterol replenishment, the DF-1 cells in 6 well plate were pre-treated with 20 mM MβCD or lovastatin (4 µM) for 1h at 37 ºC, the cells were washed with PBS, and further, the cells were incubated with 200 µg/ml of cholesterol in DMEM for another 1h at 37 ºC. The cells were subjected to AnHV-1 infection after washing with PBS and lysates for qRT-PCR were collected 60 hpi. The cells were lysed in 1% (v/v) Triton X-100 in PBS and incubated on ice for 30 min to quantify the cholesterol. The cell lysate was centrifuged at 13,000 rpm for 10 min

after incubation, and the supernatant was collected for cholesterol estimation. The amount of cholesterol in samples was determined by the Amplex red cholesterol assay kit (Cat no. A12216; Life Technologies, USA) following the manufacturer's instructions. Filipin is a polyene macrolide compound that binds to sterol molecule and has been the molecule of choice for sterol visualization using fluorescence microscopy (Loura, Castanho et al. 2001) Cells treated with various concentrations of MβCD/cholesterol were fixed with 4% formaldehyde and labelled with 50 µg/ml filipin (Cat no. F9765; Sigma Aldrich, USA) (25 mg/ml in DMSO stock) in PBS for 45 min. The cells were washed with PBS, and the image was taken after 60 h of incubation on a fluorescence microscope at 20X objective using UV excitation.

5.3.4 Viral gene expression analysis by qRT-PCR

The DF-1 cells were infected with AnHV-1 (MOI of 1) pre-treated with the different compounds, as mentioned earlier, and the total RNA was extracted using RNAiso Plus reagent (TaKaRa, Japan) 60 hpi and transcribed using reverse transcriptase (Invitrogen, USA) for cDNA synthesis. The qRT-PCR was performed using AnHV-1 glycoprotein C (gC) primers as mentioned in section 2.3.5. The transcript level of the target gene was relatively quantified using the $2^{-\Delta\Delta Ct}$ method. The relative amount of viral gene mRNA was normalized to that of GAPDH mRNA in the same sample, which was used as an internal reference.

5.3.5 Virion preparation

DF-1 cells were grown to 90% confluency and infected with AnHV-1 at MOI of 1. The media was harvested 96 hpi after showing cytopathic effect and centrifuged at 8,000 rpm for 10min to remove cell debris. The clarified supernatant was collected and centrifuged at 80,000g (~21,000 rpm) for 1h at 4ºC to pellet AnHV-1 virion. Pellet was re-suspended in 2 ml (PBS, pH 7.4) and loaded on 15-20% (w/v) sucrose density gradient, and sedimented at 80,000g for 1h. The gradient solution above the virus band was removed, and the pellet was re-suspended

in PBS to a total volume of 10 ml. Virion particles were pelleted again at 80,000g for 1h and resuspended in PBS for transmission electron microscopy sample preparation (Dai and Zhou, 2014).

5.3.6 Transmission electron microscopy

Transmission electron microscopy (TEM) was carried out to examine the change in morphology of AnHV-1 before and after MβCD treatment. The virus was purified to ensure the preparation was free from cell debris and other membrane contaminants. Purified AnHV-1 in PBS was diluted 100 times and incubated with MβCD for 1h at 37 ºC and was adsorbed on copper grids (300 mesh) (Electron Microscopy Sciences, USA) for 30 min. Grids were negatively stained with 0.5% uranyl acetate and examined by JEOL JEM-2100F transmission electron microscope (JEOL Ltd. Tokyo, Japan) and photographed at a magnification of 60,000 X. Further, AnHV-1 suspension was incubated with 20 mM of MβCD for 1h at 37 ºC. The drug was then removed from viral suspension by passing the viral suspension through the PD-10 column (GE life sciences, USA). The untreated AnHV-1 suspension was also passed through the PD-10 column as control, and infectivity was determined.

5.3.7 Statistical analysis

The data presented in the results are the average of three independent experiments and were shown as the mean $\pm$ S.D. Statistical significance difference was determined by using one-way ANOVA (Dunnett's multiple comparisons test, GraphPad Prism 8). A p-value of less than 0.05 is flagged with one star (*), less than 0.01 with two stars (**), less than 0.001 with three stars (***). The p-value of more than 0.05 is labelled as non-significant (ns), respectively.

5.4 Result

5.4.1 Cellular cholesterol is required for AnHV-1 infectivity

DF-1 cells were pre-treated with mentioned concentrations of MβCD, and the cell viability was monitored to elucidate the involvement of cellular cholesterol in the AnHV-1 infectivity. The purpose of the cholesterol depletion assay was to remove a significant amount of cholesterol while keeping the cells viable. The result showed that MβCD of up to 20 mM was non-toxic to DF-1 cells, and more than 80% cellular viability was observed in all the tested concentrations of MβCD (Figure 5.1 A). Therefore, all the further experiments were conducted with a 20 mM concentration of MβCD treated DF-1 cells. The depletion in cholesterol content was estimated in MβCD treated DF-1 cells using a cholesterol assay kit. The result showed MβCD concentration-dependent reduction in the cellular cholesterol concentration after 1h incubation (Figure 5.1 B). Subsequently, the reduction of cholesterol content in MβCD treated DF-1 cells was also evident by filipin labelling (Figure 5.1 C). To further investigate, if cholesterol depletion affects AnHV-1 infectivity, cells were pre-treated with increasing concentration of MβCD followed by infection with AnHV-1. Significantly lower 2.83 fold AnHV-1 gene expression levels (gC gene were observed in MβCD treated cells as compared with mock-infected control (Figure 5.1 D). Furthermore, the AnHV-1 titer was 2.7 times lower than the mock-infected control cells pre-treated with MβCD (Figure 5.1 E).

5.4.2 Cholesterol replenishment partially reversed the effect of MβCD in AnHV-1 infectivity

The importance of cholesterol in AnHV-1 infection was explored by investigating the effect of replenishment of exogenous cholesterol in MβCD treated DF-1 cells. To determine the cytotoxicity of cholesterol, DF-1 cells were treated with different concentrations of exogenous cholesterol. The result showed that exogenous cholesterol of less than and 400 µg/ml was not toxic to the DF-1 cells (Figure 5.2 A). The cholesterol replenishment assay was performed by adding exogenous cholesterol at a final concentration of 200 µg/ml in MβCD treated cells. The result demonstrated that the cholesterol levels are recovered in MβCD pre-treated cells (Figure

5.2 B). Based on this observation, replenishment in cholesterol content was also confirmed by filipin labeling. An increase in fluorescence was observed upon exogenous addition of cholesterol in MβCD pre-treated cells (Figure 5.2 C). To confirm that the inhibitory effect was due to the cholesterol depletion, cell membrane cholesterol was replenished with exogenous cholesterol in MβCD pre-treated cells, followed by AnHV-1 infection. Correspondingly, AnHV-1 infection was restored upon exogenous cholesterol replenishment, the expression of the viral gene was significantly increased by the addition of exogenous cholesterol as compared with the infected cells pre-treated with only MβCD (Figure 5.2 D). The reduction in viral titer was also observed following the MβCD treatment. Cholesterol replenishment of MβCD treated cells partially restored AnHV-1 titers in DF-1 cells (Figure 5.2 E). Upon the MβCD mediated cholesterol depletion, the AnHV-1 infection was remarkably repressed, which was partially restored by cholesterol replenishment, suggesting the requirement of cellular cholesterol in AnHV-1 infectivity.

5.4.3 Statin reduces AnHV-1 infectivity in DF-1 cells

The DF-1 cells were treated with lovastatin to determine the effect of statin drugs followed by AnHV-1 infection. Lovastatin act by inhibiting the biosynthesis of cholesterol inside the cells. The lovastatin above 6 µM concentration was toxic to the DF-1 cells, whereas more than 80% of cell viability was observed at 4 µm concentration (Figure 5.3 A). Furthermore, around 42% reduction in the cholesterol content was observed upon lovastatin treatment (Figure 5.3 B). The DF-1 cells pre-treated with 4 µm of lovastatin followed by AnHV-1 infection showed 1.6 fold lower viral gene expression as compared to the mock-treated cells (Figure 5.3 C). A similar finding was observed in a viral titration where lovastatin treated cells showed lower AnHV-1 titer as compared with the mock-treated cells (Figure 5.3 D).

5.4.4 Viral envelope cholesterol is required for AnHV-1 infectivity

The role of viral cholesterol on AnHV-1 infectivity was determined by depleting cholesterol from the viral envelope. Disruption of the viral envelope was observed in MβCD treated virion while the envelope of untreated virion was intact (Figure 5.4 A). The DF-1 cells were infected with MβCD treated and untreated AnHV-1 suspension. The expression of the viral gene in MβCD treated AnHV-1 suspension is marginally less as compared to untreated one (Figure 5.4 B). Also, the DF-1 cells infected with cholesterol depleted virus showed lower AnHV-1 titer as compared to cells infected with an untreated virus (Figure 5.4 C).

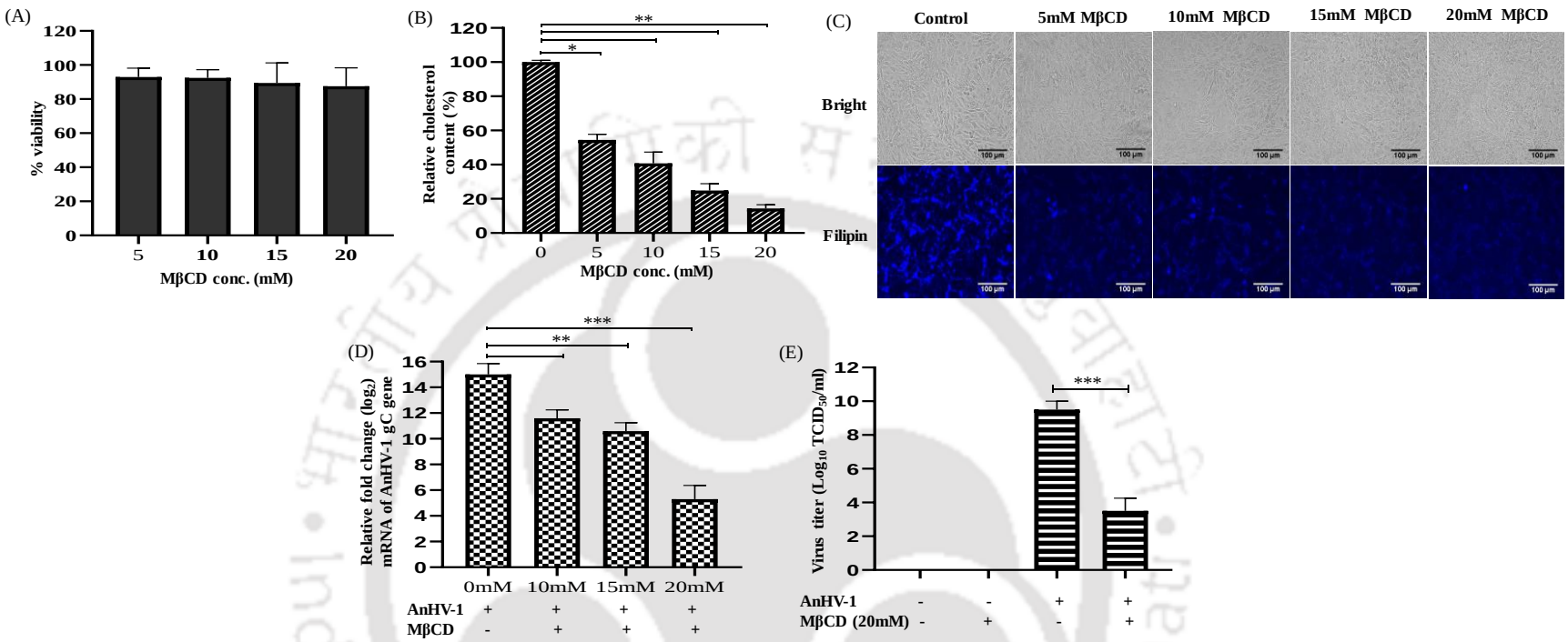

Figure 5.1 The depletion of cellular cholesterol with MβCD inhibits AnHV-1 infection. Cell viability was determined using MTT assay in DF-1 cells following MβCD treatment. DF-1 cells were pre-treated with indicated concentrations of MβCD for 1h and cultured for 48h, and the percentage of cell viability was calculated. The data represent the mean ± standard deviation of three independent experiments (A). DF-1 cells were treated with mentioned concentrations of MβCD, and the amount of cholesterol was determined in comparison to untreated cells using an Amplex red cholesterol assay kit. Statistical significance difference was determined by using one-way ANOVA (Dunnett's multiple comparisons test, GraphPad Prism 8). A p-value of less than 0.05 is flagged with one star (*) and less than 0.01 with two stars (**) (B). Bright-field and filipin labeled images of DF-1 cells treated with different concentrations of MβCD (C). Real-time analysis of viral mRNA using gC gene-specific amplification. The DF-1 cells were treated with varying concentrations of MβCD, followed by AnHV-1 infection and analyzed for their relative mRNA levels. The mRNA determinations were performed by qRT-PCR, and mRNA levels were normalized to GAPDH mRNA and represented as mean fold expression concerning control. The fold change in gene expression was calculated by $2^{-\Delta\Delta Ct}$. Statistical significance difference was determined by using one-way ANOVA (Dunnett's multiple comparisons test, GraphPad Prism 8). A p-value of less than 0.01 is flagged with two stars (**), and less than 0.001 is flagged with three stars (***) (D). The MβCD treated cells were infected with AnHV-1, and virus yield was calculated by $TCID_{50}$. The data represent the mean ± standard deviation of three independent experiments. Statistical significance difference was determined by using one-way ANOVA (Dunnett's multiple comparisons test, GraphPad Prism 8). A p-value of less than 0.001 is flagged with three stars (***) (E).

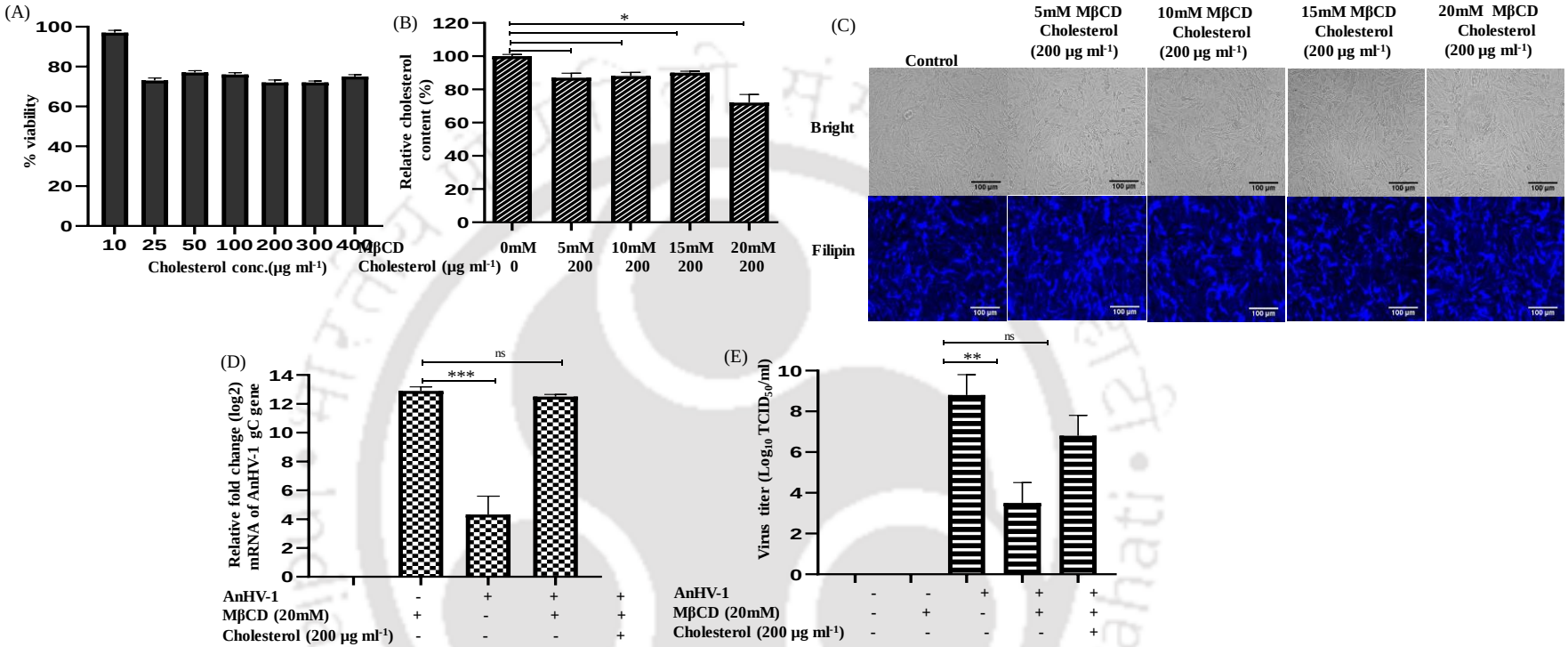

Figure 5.2 Replenishment of exogenous cholesterol in MβCD-treated cells restores AnHV-1 infection in DF-1 cells. Cell viability was determined using MTT assay after the addition of exogenous cholesterol to DF-1 cells. The data represent the mean ± standard deviation of three independent experiments. (A). DF-1 cells were treated with different concentrations of MβCD for 1h and incubated with exogenous cholesterol for 1h. The amount of cellular cholesterol was determined using the Amplex red cholesterol assay kit. Statistical significance difference was determined by using one-way ANOVA (Dunnett's multiple comparisons test, GraphPad Prism 8). A p-value of less than 0.05 is flagged with one star (*) (B). Bright-field and filipin labelled images of DF-1 cells treated with different concentrations of MβCD, followed by exogenous cholesterol replenishment (C). Real-time analysis of viral mRNA using gC gene-specific amplification. The DF-1 cells were treated with varying concentrations of MβCD and replenished with cholesterol, followed by AnHV-1 infection and analyzed for their relative mRNA levels. The data presented are the average of three independent experiments and were shown as the mean ± S.D. The mRNA determinations were performed by qRT-PCR, and mRNA levels were normalized to GAPDH mRNA and represented as mean fold expression concerning control. Statistical significance difference was determined by using one-way ANOVA (Dunnett's multiple comparisons test, GraphPad Prism 8). A p-value of less than 0.001 is flagged with three stars (***), and a p-value of more than 0.05 is labelled as non-significant (ns) (D). Viral titer was determined after the replenishment of cholesterol by $TCID_{50}$. The data represent the mean ± standard deviation of three independent experiments. Statistical significance difference was determined by using one-way ANOVA (Dunnett's multiple comparisons test, GraphPad Prism 8). A p-value of less than 0.01 is flagged with two stars (**) and a p-value more than 0.05 is labelled as non-significant (ns) (E).

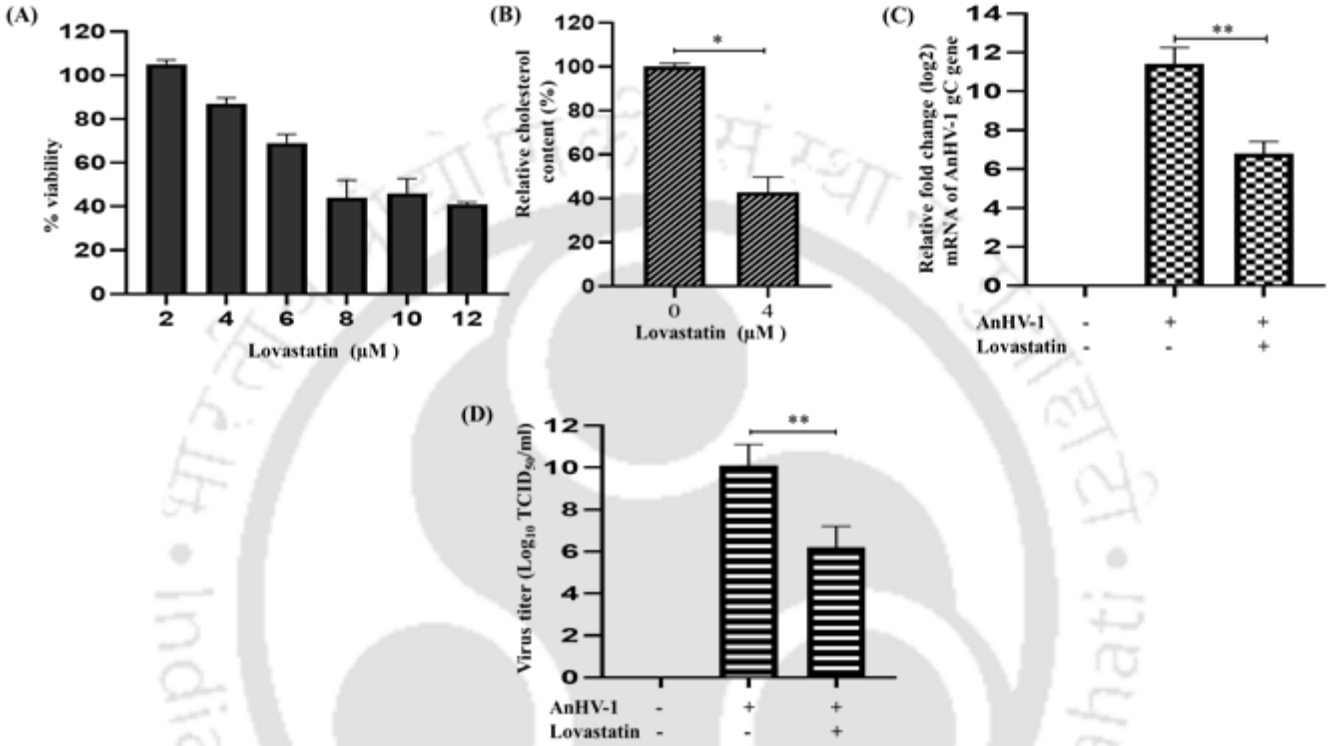

Figure 5.3 Lovastatin blocks AnHV-1 infection by inhibiting cholesterol biosynthesis. Cytotoxicity analyses of lovastatin using MTT assay in DF-1 cells after 48 h. The data represent the mean ± standard deviation of three independent experiments (A). DF-1 cells were treated with 4µM of lovastatin, and the cholesterol content was measured. Statistical significance difference was determined by using one-way ANOVA (Dunnett's multiple comparisons test, GraphPad Prism 8). A p-value of less than 0.05 is flagged with one star (*) (B). The expression of a viral gene (gC) of AnHV-1 was determined by the qRT-PCR and normalized to GAPDH mRNA and represented as mean fold expression concerning control. Statistical significance difference was determined by using one-way ANOVA (Dunnett's multiple comparisons test, GraphPad Prism 8). A p-value of less than 0.01 is flagged with two stars (**) (C). AnHV-1 infectivity post lovastatin treatment was determined with virus titration in DF-1 cells. The data represent the mean ± standard deviation of three independent experiments. Statistical significance difference was determined by using one-way ANOVA (Dunnett's multiple comparisons test, GraphPad Prism 8). A p-value of less than 0.01 is flagged with two stars (**) (D)

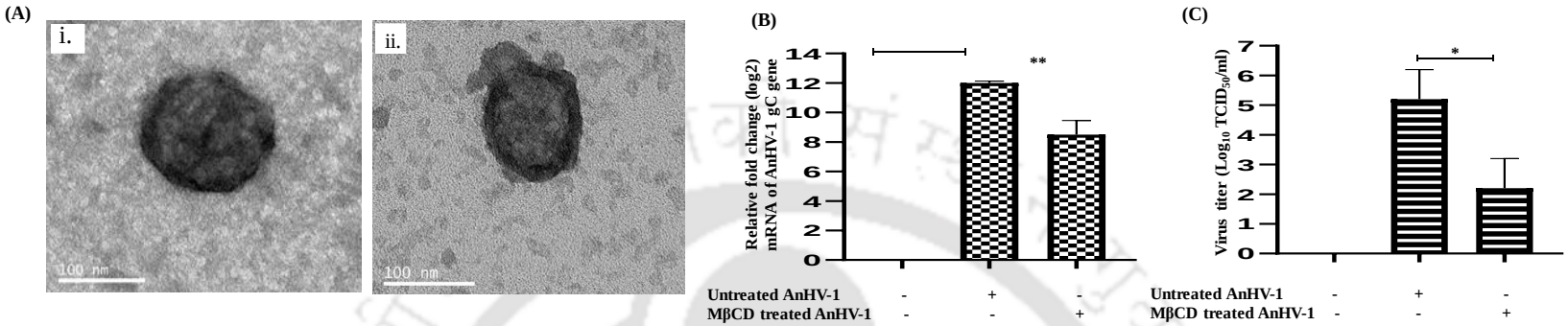

Figure 5.4 Removal of viral envelope cholesterol affects virus infection. The purified virions were treated with 20 mM MβCD and compared with untreated virion (A). The image shows a single virion comprising of an intact viral envelope (i), and disruption of the viral envelope was observed in MβCD treated virion as indicated by an arrow Samples were visualized under a transmission electron microscopy with a magnification of X 60,000. Virus suspension treated with MβCD was used to infect DF-1 cells, and mRNA expression of viral gC gene was determined by qRT-PCR, and mRNA levels were normalized to GAPDH mRNA and represented as mean fold expression concerning control. Statistical significance difference was determined by using one-way ANOVA (Dunnett's multiple comparisons test, GraphPad Prism 8). A p-value of less than 0.01 is flagged with two stars (**) (B). DF- 1 cell were infected with viral suspension treated with MβCD and untreated control, and virus titer was measured. The data represent the mean ± standard deviation of three independent experiments. Statistical significance difference was determined by using one-way ANOVA (Dunnett's multiple comparisons test, GraphPad Prism 8). A p-value of less than 0.05 is flagged with one star (*) (C).

5.5 Discussion

In this study, we investigated the role of cholesterol in AnHV-1 infection. The significance of cholesterol in either host cell membranes or viral envelopes has been determined for several viruses, and cholesterol is known to modulate the infectivity of enveloped viruses. The binding of viral glycoprotein to the host cell receptor induces membrane fusion. Infectivity of influenza and canine distemper viruses are inhibited upon cholesterol depletion from the viral membrane (Sun and Whittaker, 2003, Imhoff et al., 2007). Also, the variation of cholesterol in both the viral and cellular membrane decrease the infectivity of HIV (Liao et al., 2001, Graham et al., 2003, Liaoet al., 2003), HSV (Rahn et al., 2011) and bovine herpesvirus type 1 (BoHV-1) (Zhu et al., 2010). Furthermore, cell membrane cholesterol is required for the entry of VZV and PRV (Hambleton et al., 2007, Desplanques et al., 2008). In the case of ecotropic murine leukemia virus, membrane fusion is affected by cellular cholesterol depletion from the target cells (Lu et al,. 2002). In the present study, we demonstrated that cholesterol depletion from the viral and cell membrane is associated with the impairment of AnHV-1 infection. The MβCD has been widely used in studying the importance of cholesterol. The results showed the cholesterol content of chicken cell membranes was reduced with the increasing concentration of MβCD, as also reported in other cells (Yu et al., 2019). Furthermore, cholesterol depletion by MβCD was supported by filipin labelling, which is used for visualizing the depletion of cholesterol in the cells. Filipin binds to the cholesterol accumulated in cells and is used for the screening of compounds that might reduce cholesterol (Pipalia et al., 2006, Maxfield and Wustner, 2012). Since sterol is a crucial compound of lipid rafts, filipin fluorescence can be used to detect the presence of cholesterol in the lipid rafts. In the plasma membrane, most of the cholesterol is preferentially localized in lipid rafts. Lipid rafts have been implicated in the assembly and release of the virus. In a recent study role of lipid rafts has been observed in influenza A virus (IAV) entry by endocytosis (Verma et al., 2018). Furthermore, lipid rafts play an important

role in several cell physiological function such as, signal transduction, receptor activation, formation of extracellular vesicles and lipid and protein trafficking in the cells (Koyama-Honda et al., 2020, Shi and Ruan, 2020, Skryabin et al., 2020, Ouweneel et al., 2020). As a result of its involvement in various cellular process, lipid rafts contribute to immune response and host pathogen interaction (Varshney et al., 2016, Bukrinsky et al., 2020). Our result showed restoration of AnHV-1 infection by replenishing cellular cholesterol level, suggesting the effect on virus infectivity would be due to the removal of cholesterol. The results presented in this study contribute to the role of sterol rich lipid rafts in virus infection. Interestingly the ISG such as Viperin and ZAP, have been shown to inhibit virus budding by disrupting the lipid rafts in the cell membrane (Gao et al., 2002, Wang et al., 2007). Recently, in HCV infection, cholesterol and its derivatives have emerged as immune modulators that induce an innate immune response and may favour the clearance of viruses naturally or induced by treatment. The WNV has been shown to directly manipulate host cell pathways involved in cholesterol biosynthesis to promote virus replication and viral evasion from host cellular antiviral response (Mackenzie et al., 2007). Understanding a synergy between lipid pathway and innate immune response may provide novel host therapeutic targets before and after treatment with direct antiviral drugs. In the case of animals may be a diet composed of additional components that have been related to inhibiting AnHV-1 replication could be considered as a curative alternative.

Statin drugs are a reversible inhibitor of 3-hydroxy-3-methylglutaryl-CoA (HMG-CoA) reductase an enzyme involved in the biosynthesis of cholesterol (Moghadasian, 1999). HMG-CoA analogues compete for the binding sites of the enzyme and have been reported to show antiviral activity against hepatitis C, dengue, and influenza viruses (Andrus and East, 2010, Martinez-Gutierrez et al,. 2011, Mehrbod et al., 2014, Mehrbod, et al., 2014). Here, we report similar evidence with AnHV-1, where treatment of cells with lovastatin lowers its

infectivity in DF-1 cells. Although the AnHV-1 infectivity in lovastatin treated cells was not as low as MβCD treated cells, it could be inferred that inhibition of endogenous cholesterol biosynthesis curtails AnHV-1 infectivity. This result implies that AnHV-1 infectivity is hampered to a greater extent upon depletion of cholesterol from the host cell.

The cholesterol present in the viral envelope can sustain the integrity of the virion. The results suggested that cholesterol depletion from the AnHV-1 virions reduced its infectivity. The MβCD treated AnHV-1 was filtered to avoid any contamination of cholesterol back into the virion. Our results corroborate with the earlier report, where the MβCD mediated removal of viral envelope cholesterol reduces the infectivity of bovine herpesvirus (Zhu et al., 2010). Presumably, the cholesterol depletion from the AnHV-1 envelope might be disintegrating the virus particle by disturbing its envelope integrity resulting in its reduced infectivity. These observations suggest that cholesterol influences the early stages of AnHV-1 replication. Furthermore, the cholesterol sequestering drug inhibited AnHV-1 infection reveals the underlying requirement of cholesterol in both host and viral membranes to establish a successful infection. Besides, lipid rafts could be a potential target to prevent AnHV-1 infection.

Chapter 6.

Future Prospects

We have characterized and propagated AnHV-1, CEF adapted vaccine strain in different continuous cell lines. We comparatively studied the permissive spectrum of Vero, DF-1, QT-35, and MDCK for vaccine strain of AnHV-1 and observed an enhanced replication in Vero, DF-1, QT-35 cell lines. Little is known regarding the interaction of AnHV-1 surface proteins with host factors and different cell-surface receptors. Bioinformatics, docking studies, and a monoclonal antibody directed against viral protein approach can be done in the future to explore which viral proteins are involved in the interaction with host cell-surface receptors. It can provide a great insight into the molecular interaction between virus proteins and host cell adhesion molecules, which are the major viral receptors identified. Characterized cell lines can further be validated for the production of continuous cell culture adapted vaccine candidate for AnHV-1. Exploring cell substrates for the propagation of AnHV-1 in high titer should provide an excellent system to investigate the cellular events of AnHV-1 infection, which subsequently could be used for viral detection, isolation, and attenuation of virus for vaccine production.

We studied the role of viperin in AnHV-1 infection. We have shown that overexpression of viperin significantly impairs AnHV-1 infectivity. In vitro protein interaction study between viperin and viral protein remains for future studies, which may help in understanding the underlying mechanism of viperin in inhibiting AnHV-1 replication. Using reverse genetics approach recombinant virus expressing viperin was constructed and recovered using Newcastle disease virus vector to interrogate its function in viral infection and another therapeutic potential. Under field conditions vaccine alone cannot provide complete protection against the poultry pathogens; therefore, understanding the role of potent host immunostimulants can help in reducing the risk of infection and developing prophylactic. Recombinant virus expressing viperin can be explored how it impacts immune response, which could explain future strategies to protect against both viruses and cancer. It can be used as a tool in cancer immunotherapy.

Bibliography

Ahamed, M., Hossain, MT., Rahman, M., Nazir, KHMNH., Khan, MFR., Parvej, MS., Ansari, WK., Noor, MN., Chiste, AA., Amin, KB, et al., (2015). "Molecular characterization of Duck Plague virus isolated from Bangladesh." J Adv Vet Anim Res **2(3)**: 296–303.

Abu-Farha M, Thanaraj TA, Qaddoumi MG, Hashem A, Abubaker J, Al-Mulla F (2020). "The Role of Lipid Metabolism in COVID-19 Virus Infection and as a Drug Target". Int J Mol Sci. **21**(10):3544.

Ali N, Allam H, Bader T, May R, Basalingappa KM, Berry WL, Chandrakesan P, Qu D, Weygant N, Bronze MS, Umar S, Janknecht R, Sureban SM, Huycke M, Houchen CW (2013). "Fluvastatin interferes with hepatitis C virus replication via microtubule bundling and a doublecortin-like kinase-mediated mechanism". PLoS One. **19**;8(11)

Aloia, R. C., H. Tian and F. C. Jensen (1993). "Lipid composition and fluidity of the human immunodeficiency virus envelope and host cell plasma membranes." Proc Natl Acad Sci U S A **90**(11): 5181-5185.

Andrus, M. R. and J. East (2010). "Use of statins in patients with chronic hepatitis C." South Med J **103**(10): 1018-1022; quiz 1023.

Aravind, S., N. M. Kamble, S. S. Gaikwad, S. K. Shukla, S. Dey and C. M. Mohan (2015). "Adaptation and growth kinetics study of an Indian isolate of virulent duck enteritis virus in Vero cells." Microb Pathog **78**: 14-19.

Armstrong, A. J., A. K. Gebre, J. S. Parks and C. C. Hedrick (2010). "ATP-binding cassette transporter G1 negatively regulates thymocyte and peripheral lymphocyte proliferation." J Immunol **184**(1): 173-183.

Banda A. (2019). Duck Viral Enteritis (Duck plague, Anatid herpes, Eendenpest, Entenpest, Peste du canard) USA, Mississippi State University.

Barbalat, R., S. E. Ewald, M. L. Mouchess and G. M. Barton (2011). "Nucleic acid recognition by the innate immune system." Annu Rev Immunol **29**: 185-214.

Barr, B. C., D. A. Jessup, D. E. Docherty and L. J. Lowenstine (1992). "Epithelial intracytoplasmic herpes viral inclusions associated with an outbreak of duck virus enteritis." Avian Dis **36**(1): 164-168.

Baudet, A. E. R. F. (1923). "Mortality in ducks in the Netherlands caused by a filtrable virus (fowl plague)." Tijdschrift voor Diergeneeskunde **50**: 455–459.

Belardelli, F. (1995). "Role of interferons and other cytokines in the regulation of the immune response." APMIS **103**(3): 161-179.

Bender, F. C., J. C. Whitbeck, M. Ponce de Leon, H. Lou, R. J. Eisenberg and G. H. Cohen (2003). "Specific association of glycoprotein B with lipid rafts during herpes simplex virus entry." J Virol **77**(17): 9542-9552.

Bensinger, S. J., M. N. Bradley, S. B. Joseph, N. Zelcer, E. M. Janssen, M. A. Hausner, R. Shih, J. S. Parks, P. A. Edwards, B. D. Jamieson and P. Tontonoz (2008). "LXR signaling couples sterol metabolism to proliferation in the acquired immune response." Cell **134**(1): 97-111.

Bernstein, D. I., D. A. Sack, E. Rothstein, K. Reisinger, V. E. Smith, D. O'Sullivan, D. R. Spriggs and R. L. Ward (1999). "Efficacy of live, attenuated, human rotavirus vaccine 89-12 in infants: a randomised placebo-controlled trial." Lancet **354**(9175): 287-290.

Bhattacharya, D., J. Nowotny, R. Cao and J. Cheng (2016). "3Drefine: an interactive web server for efficient protein structure refinement." Nucleic Acids Res **44**(W1): W406-409.

Boudinot, P., S. Riffault, S. Salhi, C. Carrat, C. Sedlik, N. Mahmoudi, B. Charley and A. Benmansour (2000). "Vesicular stomatitis virus and pseudorabies virus induce a vig1/cig5 homologue in mouse dendritic cells via different pathways." J Gen Virol **81**(Pt 11): 2675-2682.
Brand, C. J. and D. E. Docherty (1984). "A survey of North American migratory waterfowl for duck plague (duck virus enteritis) virus." J Wildl Dis **20**(4): 261-266.
Briggs, D. J. (2007). Rabies, Academic Press.
Brown, D. A. and E. London (2000). "Structure and function of sphingolipid- and cholesterol-rich membrane rafts." J Biol Chem **275**(23): 17221-17224.
Bukrinsky MI, Mukhamedova N, Sviridov D (2020). "Lipid rafts and pathogens: the art of deception and exploitation". J Lipid Res. **61**(5):601-610.
Bu, X., M. Li, Y. Zhao, S. Liu, M. Wang, J. Ge, Z. Bu and Y. Yan (2016). "Genetically engineered Newcastle disease virus expressing human interferon-lambda1 induces apoptosis in gastric adenocarcinoma cells and modulates the Th1/Th2 immune response." Oncol Rep **36**(3): 1393-1402.
Bulbule, V. (1982). "Some common diseases of ducks, their prevention and control." Poult. Adv. **26**: 37–40.
Burgess, E. and T. Yuill (1983). "The influence of seven environmental and physiological factors on duck plague virus shedding by carrier mallards." J Wildl Dis **19**(2): 77-81.
Burgess, E. C., J. Ossa and T. M. Yuill (1979). "Duck plague: a carrier state in waterfowl." Avian Dis **23**(4): 940-949.
Burgess, E. C. and T. M. Yuill (1981). "Vertical transmission of duck plague virus (DPV) by apparently healthy DPV carrier waterfowl." Avian Dis **25**(4): 795-800.
Burgess, E. C. and T. M. Yuill (1983). "The influence of seven environmental and physiological factors on duck plague virus shedding by carrier mallards." J Wildl Dis **19**(2): 77-81.
Byrne, K. M., D. W. Horohov and K. G. Kousoulas (1995). "Glycoprotein B of bovine herpesvirus-1 binds heparin." Virology **209**(1): 230-235.
Campagnolo, E. R., M. Banerjee, B. Panigrahy and R. L. Jones (2001). "An outbreak of duck viral enteritis (duck plague) in domestic Muscovy ducks (Cairina moschata domesticus) in Illinois." Avian Dis **45**(2): 522-528.
Chambal, K., Upadhyaya, T. N., Goswami, S., and Dutta, B. (2009). "Studies on the incidence and pathology of naturally occurring duck plague in Assam." Indian Journal of Veterinary Pathology **33**: 213-215.
Chan, S. Y., C. J. Empig, F. J. Welte, R. F. Speck, A. Schmaljohn, J. F. Kreisberg and M. A. Goldsmith (2001). "Folate receptor-alpha is a cofactor for cellular entry by Marburg and Ebola viruses." Cell **106**(1): 117-126.
Chiang, S. J., A. Dar, S. M. Goyal, K. V. Nagaraja, D. Halvorson and V. Kapur (1998). "Isolation of avian pneumovirus in QT-35 cells." Vet Rec **143**(21): 596.
Chin, K. C. and P. Cresswell (2001). "Viperin (cig5), an IFN-inducible antiviral protein directly induced by human cytomegalovirus." Proc Natl Acad Sci U S A **98**(26): 15125-15130.
Choi, K. S., H. Aizaki and M. M. Lai (2005). "Murine coronavirus requires lipid rafts for virus entry and cell-cell fusion but not for virus release." J Virol **79**(15): 9862-9871.
Chung, C. S., C. Y. Huang and W. Chang (2005). "Vaccinia virus penetration requires cholesterol and results in specific viral envelope proteins associated with lipid rafts." J Virol **79**(3): 1623-1634.
Converse, K. A. and G. A. Kidd (2001). "Duck plague epizootics in the United States, 1967-1995." J Wildl Dis **37**(2): 347-357.

Daffis, S., K. J. Szretter, J. Schriewer, J. Li, S. Youn, J. Errett, T. Y. Lin, S. Schneller, R. Zust, H. Dong, V. Thiel, G. C. Sen, V. Fensterl, W. B. Klimstra, T. C. Pierson, R. M. Buller, M. Gale, Jr., P. Y. Shi and M. S. Diamond (2010). "2'-O methylation of the viral mRNA cap evades host restriction by IFIT family members." Nature **468**(7322): 452-456.
Danthi, P. and M. Chow (2004). "Cholesterol removal by methyl-beta-cyclodextrin inhibits poliovirus entry." J Virol **78**(1): 33-41.
Dardiri, A. H. (1975). "Duck viral enteritis (duck plague) characteristics and immune response of the host." Am J Vet Res **36**(4 Pt 2): 535-538.
Dardiri, A. H. and P. Gailunas (1969). "Response to Pekin and mallard ducks and Canada geese to experimental infection with duck plague virus." Wildl Dis **5**(3): 235-247.
Dardiri, A. H. and W. R. Hess (1967). "The incidence of neutralizing antibodies to duck plague virus in serums from domestic ducks and wild waterfowl in the United States of America." Proc Annu Meet U S Anim Health Assoc **71**: 225-237.
Dai M, Xie T, Liao M, Zhang X, Feng M (2020). "Systematic identification of chicken type I, II and III interferon-stimulated genes". Vet Res. **24**;51(1):70.
Davison, S., K. A. Converse, A. N. Hamir and R. J. Eckroade (1993). "Duck viral enteritis in domestic muscovy ducks in Pennsylvania." Avian Dis **37**(4): 1142-1146.
De Veer, M. J., M. Holko, M. Frevel, E. Walker, S. Der, J. M. Paranjape, R. H. Silverman and B. R. Williams (2001). "Functional classification of interferon-stimulated genes identified using microarrays." J Leukoc Biol **69**(6): 912-920.
DeLano W. L. (2002). The PyMOL Molecular Graphics System. Palo Alto, CA, USA, DeLano Scientific.
Dereeper, A., S. Audic, J. M. Claverie and G. Blanc (2010). "BLAST-EXPLORER helps you building datasets for phylogenetic analysis." BMC Evol Biol **10**: 8.
Dereeper, A., V. Guignon, G. Blanc, S. Audic, S. Buffet, F. Chevenet, J. F. Dufayard, S. Guindon, V. Lefort, M. Lescot, J. M. Claverie and O. Gascuel (2008). "Phylogeny.fr: robust phylogenetic analysis for the non-specialist." Nucleic Acids Res **36**(Web Server issue): W465-469.
Desplanques, A. S., H. J. Nauwynck, D. Vercauteren, T. Geens and H. W. Favoreel (2008). "Plasma membrane cholesterol is required for efficient pseudorabies virus entry." Virology **376**(2): 339-345.
Diamond, D. L., A. J. Syder, J. M. Jacobs, C. M. Sorensen, K. A. Walters, S. C. Proll, J. E. McDermott, M. A. Gritsenko, Q. Zhang, R. Zhao, T. O. Metz, D. G. Camp, 2nd, K. M. Waters, R. D. Smith, C. M. Rice and M. G. Katze (2010). "Temporal proteome and lipidome profiles reveal hepatitis C virus-associated reprogramming of hepatocellular metabolism and bioenergetics." PLoS Pathog **6**(1): e1000719.
DiNapoli, J. M., A. Kotelkin, L. Yang, S. Elankumaran, B. R. Murphy, S. K. Samal, P. L. Collins and A. Bukreyev (2007). "Newcastle disease virus, a host range-restricted virus, as a vaccine vector for intranasal immunization against emerging pathogens." Proc Natl Acad Sci U S A **104**(23): 9788-9793.
Domanski, P., M. Witte, M. Kellum, M. Rubinstein, R. Hackett, P. Pitha and O. R. Colamonici (1995). "Cloning and expression of a long form of the beta subunit of the interferon alpha beta receptor that is required for signaling." J Biol Chem **270**(37): 21606-21611.
Duschene, K. S. and J. B. Broderick (2010). "The antiviral protein viperin is a radical SAM enzyme." FEBS Lett **584**(6): 1263-1267.
Eagle, H. and K. Habel (1956). "The nutritional requirements for the propagation of poliomyelitis virus by the HeLa cell." J Exp Med **104**(2): 271-287.

Eich, C., C. Manzo, S. de Keijzer, G. J. Bakker, I. Reinieren-Beeren, M. F. Garcia-Parajo and A. Cambi (2016). "Changes in membrane sphingolipid composition modulate dynamics and adhesion of integrin nanoclusters." Sci Rep **6**: 20693.
Eisenberg, D., R. Luthy and J. U. Bowie (1997). "VERIFY3D: assessment of protein models with three-dimensional profiles." Methods Enzymol **277**: 396-404.
El-Tholoth, M., M. F. Hamed, A. A. Matter and K. I. Abou El-Azm (2019). "Molecular and pathological characterization of duck enteritis virus in Egypt." Transbound Emerg Dis **66**(1): 217-224.
Everett, R. D. (2000). "ICP0, a regulator of herpes simplex virus during lytic and latent infection." Bioessays **22**(8): 761-770.
Fan, X., H. Lu, Y. Cui, X. Hou, C. Huang and G. Liu (2018). "Overexpression of p53 delivered using recombinant NDV induces apoptosis in glioma cells by regulating the apoptotic signaling pathway." Exp Ther Med **15**(5): 4522-4530.
Fenner, F., Gibbs, EPJ., Murphy, FA., Rott, R., Studdert, MJ., White, DO, (1993). Veterinary virology, Academic Press.
Fenwick, M. K., Y. Li, P. Cresswell, Y. Modis and S. E. Ealick (2017). "Structural studies of viperin, an antiviral radical SAM enzyme." Proc Natl Acad Sci U S A **114**(26): 6806-6811.
Fitzgerald, K. A. (2011). "The interferon inducible gene: Viperin." J Interferon Cytokine Res **31**(1): 131-135.
Flemington, E. K. (2001). "Herpesvirus lytic replication and the cell cycle: arresting new developments." J Virol **75**(10): 4475-4481.
Flynn, S. J. and P. Ryan (1996). "The receptor-binding domain of pseudorabies virus glycoprotein gC is composed of multiple discrete units that are functionally redundant." J Virol **70**(3): 1355-1364.
Fontaine, K. A., R. Camarda and M. Lagunoff (2014). "Vaccinia virus requires glutamine but not glucose for efficient replication." J Virol **88**(8): 4366-4374.
Fontaine, K. A., E. L. Sanchez, R. Camarda and M. Lagunoff (2015). "Dengue virus induces and requires glycolysis for optimal replication." J Virol **89**(4): 2358-2366.
Freed, E. O. (2002). "Virology. Rafting with Ebola." Science **296**(5566): 279.
Friend, M. (1999). Duck plague. In Field Manual of Wildlife Diseases: General Field Procedures and Diseases of Birds. U.S. Geological Survey, National Wildlife Health Center, Madison,Wisconsin**:** 141–151.
Fukuchi, K., M. Sudo, Y. S. Lee, A. Tanaka and M. Nonoyama (1984). "Structure of Marek's disease virus DNA: detailed restriction enzyme map." J Virol **51**(1): 102-109.
Fuller, A. O. and P. G. Spear (1987). "Anti-glycoprotein D antibodies that permit adsorption but block infection by herpes simplex virus 1 prevent virion-cell fusion at the cell surface." Proc Natl Acad Sci U S A **84**(15): 5454-5458.
Gao, G., X. Guo and S. P. Goff (2002). "Inhibition of retroviral RNA production by ZAP, a CCCH-type zinc finger protein." Science **297**(5587): 1703-1706.
Gardner, R., J. Wilkerson and J. C. Johnson (1993). "Molecular characterization of the DNA of Anatid herpesvirus 1." Intervirology **36**(2): 99-112.
Ge, J., G. Deng, Z. Wen, G. Tian, Y. Wang, J. Shi, X. Wang, Y. Li, S. Hu, Y. Jiang, C. Yang, K. Yu, Z. Bu and H. Chen (2007). "Newcastle disease virus-based live attenuated vaccine completely protects chickens and mice from lethal challenge of homologous and heterologous H5N1 avian influenza viruses." J Virol **81**(1): 150-158.

Genzel, Y., C. Dietzsch, E. Rapp, J. Schwarzer and U. Reichl (2010). "MDCK and Vero cells for influenza virus vaccine production: a one-to-one comparison up to lab-scale bioreactor cultivation." Appl Microbiol Biotechnol **88**(2): 461-475.
Gimpl, G., K. Burger and F. Fahrenholz (1997). "Cholesterol as modulator of receptor function." Biochemistry **36**(36): 10959-10974.
Goldman, A. (2006). "Isolation of fibroblasts from chicken embryos." CSH Protoc **2006**(2).
Goluszko, P. and B. Nowicki (2005). "Membrane cholesterol: a crucial molecule affecting interactions of microbial pathogens with mammalian cells." Infect Immun **73**(12): 7791-7796.
Goossens, K. E., A. J. Karpala, A. Rohringer, A. Ward and A. G. Bean (2015). "Characterisation of chicken viperin." Mol Immunol **63**(2): 373-380.
Gough, R. (2008). Duck virus enteritis. In : Poultry diseases, Saunders Elsevier.
Gough, R. E. and D. J. Alexander (1990). "Duck virus enteritis in Great Britain, 1980 to 1989." Vet Rec **126**(24): 595-597.
Graham, D. R., E. Chertova, J. M. Hilburn, L. O. Arthur and J. E. Hildreth (2003). "Cholesterol depletion of human immunodeficiency virus type 1 and simian immunodeficiency virus with beta-cyclodextrin inactivates and permeabilizes the virions: evidence for virion-associated lipid rafts." J Virol **77**(15): 8237-8248.
Groth, N., E. Montomoli, C. Gentile, I. Manini, R. Bugarini and A. Podda (2009). "Safety, tolerability and immunogenicity of a mammalian cell-culture-derived influenza vaccine: a sequential Phase I and Phase II clinical trial." Vaccine **27**(5): 786-791.
Grunewald, K., P. Desai, D. C. Winkler, J. B. Heymann, D. M. Belnap, W. Baumeister and A. C. Steven (2003). "Three-dimensional structure of herpes simplex virus from cryo-electron tomography." Science **302**(5649): 1396-1398.
Hall, S. A. and J. R. Simmons (1972). "Duck plague (duck virus enteritis) in Britain." Vet Rec **90**(24): 691.
Haller, O., S. Stertz and G. Kochs (2007). "The Mx GTPase family of interferon-induced antiviral proteins." Microbes Infect **9**(14-15): 1636-1643.
Hambleton, S., S. P. Steinberg, M. D. Gershon and A. A. Gershon (2007). "Cholesterol dependence of varicella-zoster virion entry into target cells." J Virol **81**(14): 7548-7558.
Hansen, W. R., S. E. Brown, S. W. Nashold and D. L. Knudson (1999). "Identification of duck plague virus by polymerase chain reaction." Avian Dis **43**(1): 106-115.
Hansen, W. R., S. W. Nashold, D. E. Docherty, S. E. Brown and D. L. Knudson (2000). "Diagnosis of duck plague in waterfowl by polymerase chain reaction." Avian Dis **44**(2): 266-274.
Hanson, J. A. and N. G. Willis (1976). "An outbreak of duck virus enteritis (duck plague) in Alberta." J Wildl Dis **12**(2): 258-262.
Hayakawa, S., S. Shiratori, H. Yamato, T. Kameyama, C. Kitatsuji, F. Kashigi, S. Goto, S. Kameoka, D. Fujikura, T. Yamada, T. Mizutani, M. Kazumata, M. Sato, J. Tanaka, M. Asaka, Y. Ohba, T. Miyazaki, M. Imamura and A. Takaoka (2011). "ZAPS is a potent stimulator of signaling mediated by the RNA helicase RIG-I during antiviral responses." Nat Immunol **12**(1): 37-44.
Hegedus, A., M. Kavanagh Williamson and H. Huthoff (2014). "HIV-1 pathogenicity and virion production are dependent on the metabolic phenotype of activated CD4+ T cells." Retrovirology **11**: 98.
Hess, W. R. and A. H. Dardiri (1968). "Some properties of the virus od duck plague." Arch Gesamte Virusforsch **24**(1): 148-153.

Highlander, S. L., S. L. Sutherland, P. J. Gage, D. C. Johnson, M. Levine and J. C. Glorioso (1987). "Neutralizing monoclonal antibodies specific for herpes simplex virus glycoprotein D inhibit virus penetration." J Virol **61**(11): 3356-3364.
Himly, M., D. N. Foster, I. Bottoli, J. S. Iacovoni and P. K. Vogt (1998). "The DF-1 chicken fibroblast cell line: transformation induced by diverse oncogenes and cell death resulting from infection by avian leukosis viruses." Virology **248**(2): 295-304.
Hinson, E. R. and P. Cresswell (2009). "The antiviral protein, viperin, localizes to lipid droplets via its N-terminal amphipathic alpha-helix." Proc Natl Acad Sci U S A **106**(48): 20452-20457.
Hinson, E. R. and P. Cresswell (2009). "The N-terminal amphipathic alpha-helix of viperin mediates localization to the cytosolic face of the endoplasmic reticulum and inhibits protein secretion." J Biol Chem **284**(7): 4705-4712.
Hoogland C., G. E., Gattiker A., Duvaud S., Wilkins M.R., Appel R. D., Bairoch A., (2005). The Proteomics Protocols Handbook, Humana Press.
Huang, H., Y. Li, T. Sadaoka, H. Tang, T. Yamamoto, K. Yamanishi and Y. Mori (2006). "Human herpesvirus 6 envelope cholesterol is required for virus entry." J Gen Virol **87**(Pt 2): 277-285.
Hwang, J., E. T. Mallinson and R. E. Yoxheimer (1975). "Occurrence of duck virus enteritis (duck plague) in Pennsylvania, 1968-74." Avian Dis **19**(2): 382-384.
Ikonen, E. (2008). "Cellular cholesterol trafficking and compartmentalization." Nat Rev Mol Cell Biol **9**(2): 125-138.
Imhoff, H., V. von Messling, G. Herrler and L. Haas (2007). "Canine distemper virus infection requires cholesterol in the viral envelope." J Virol **81**(8): 4158-4165.
Irie, T., K. Fukunaga and J. Pitha (1992). "Hydroxypropylcyclodextrins in parenteral use. I: Lipid dissolution and effects on lipid transfers in vitro." J Pharm Sci **81**(6): 521-523.
Isaacs, A. and J. Lindenmann (1957). "Virus interference. I. The interferon." Proc R Soc Lond B Biol Sci **147**(927): 258-267.
Isaacs, A. and J. Lindenmann (1987). "Virus interference. I. The interferon. By A. Isaacs and J. Lindenmann, 1957." J Interferon Res **7**(5): 429-438.
Ishii, K. J., C. Coban, H. Kato, K. Takahashi, Y. Torii, F. Takeshita, H. Ludwig, G. Sutter, K. Suzuki, H. Hemmi, S. Sato, M. Yamamoto, S. Uematsu, T. Kawai, O. Takeuchi and S. Akira (2006). "A Toll-like receptor-independent antiviral response induced by double-stranded B-form DNA." Nat Immunol **7**(1): 40-48.
Islam, M. R. and M. A. Khan (1995). "An immunocytochemical study on the sequential tissue distribution of duck plague virus." Avian Pathol **24**(1): 189-194.
Jana, C., Mukhopadhayay, S. K., Bhowmik, M. K., Mandal, P. S., Biswas, S., and Mondal. B., (2014). "Pathological and molecular diagnosis of duck enteritis virus in Khaki Campbell ducks in a field outbreak." Indian Journal of Veterinary Pathology **38**.
Janke, M., B. Peeters, O. de Leeuw, R. Moorman, A. Arnold, P. Fournier and V. Schirrmacher (2007). "Recombinant Newcastle disease virus (NDV) with inserted gene coding for GM-CSF as a new vector for cancer immunogene therapy." Gene Ther **14**(23): 1639-1649.
Jansen, J. (1968). "Duck plague." J Am Vet Med Assoc **152**(7): 1009-1016.
Jansen, J., and Kunst. H., (1964). "The reported incidence of duck plague in Europe and Asia." Tijdschrift voor Diergeneeskunde **89**: 765–769.
Jia, R., A. Cheng, M. Wang, X. Qi, D. Zhu, H. Ge, Q. Luo, F. Liu, Y. Guo and X. Chen (2009). "Development and evaluation of an antigen-capture ELISA for detection of the UL24 antigen of the duck enteritis virus, based on a polyclonal antibody against the UL24 expression protein." J Virol Methods **161**(1): 38-43.

Jiang, D., H. Guo, C. Xu, J. Chang, B. Gu, L. Wang, T. M. Block and J. T. Guo (2008). "Identification of three interferon-inducible cellular enzymes that inhibit the replication of hepatitis C virus." J Virol **82**(4): 1665-1678.
Jiang, D., J. M. Weidner, M. Qing, X. B. Pan, H. Guo, C. Xu, X. Zhang, A. Birk, J. Chang, P. Y. Shi, T. M. Block and J. T. Guo (2010). "Identification of five interferon-induced cellular proteins that inhibit west nile virus and dengue virus infections." J Virol **84**(16): 8332-8341.
Jiang, X. and Z. J. Chen (2011). "Viperin links lipid bodies to immune defense." Immunity **34**(3): 285-287.
Johnson, D. C., R. L. Burke and T. Gregory (1990). "Soluble forms of herpes simplex virus glycoprotein D bind to a limited number of cell surface receptors and inhibit virus entry into cells." J Virol **64**(6): 2569-2576.
Johnson, J. A. and W. Heneine (2001). "Characterization of endogenous avian leukosis viruses in chicken embryonic fibroblast substrates used in production of measles and mumps vaccines." J Virol **75**(8): 3605-3612.
Kaleta, E. F., A. Kuczka, A. Kuhnhold, C. Bunzenthal, B. M. Bonner, K. Hanka, T. Redmann and A. Yilmaz (2007). "Outbreak of duck plague (duck herpesvirus enteritis) in numerous species of captive ducks and geese in temporal conjunction with enforced biosecurity (in-house keeping) due to the threat of avian influenza A virus of the subtype Asia H5N1." Dtsch Tierarztl Wochenschr **114**(1): 3-11.
Kaur, G. and J. M. Dufour (2012). "Cell lines: Valuable tools or useless artifacts." Spermatogenesis **2**(1): 1-5.
Kawai, T. and S. Akira (2005). "Pathogen recognition with Toll-like receptors." Curr Opin Immunol **17**(4): 338-344.
Khattar, S. K., S. Samal, A. L. Devico, P. L. Collins and S. K. Samal (2011). "Newcastle disease virus expressing human immunodeficiency virus type 1 envelope glycoprotein induces strong mucosal and serum antibody responses in Guinea pigs." J Virol **85**(20): 10529-10541.
Kim, S. H. and S. K. Samal (2016). "Newcastle Disease Virus as a Vaccine Vector for Development of Human and Veterinary Vaccines." Viruses **8**(7).
Kocan, R. M. (1976). "Duck plague virus replication in muscovy duck fibroblast cells." Avian Dis **20**(3): 574-580.
Konch, C., Upadhyaya, TN., Goswami, S. , Dutta, B., (2009). "Studies on the incidence and pathology of naturally occurring duck plague in Assam." Indian J. Vet. Pathol. **33**: 213–215.
Kong, B. W., L. K. Foster and D. N. Foster (2006). "Comparison of avian cell substrates for propagating subtype C avian metapneumovirus." Virus Res **116**(1-2): 58-68.
Krishnamurthy, S. and S. K. Samal (1998). "Nucleotide sequences of the trailer, nucleocapsid protein gene and intergenic regions of Newcastle disease virus strain Beaudette C and completion of the entire genome sequence." J Gen Virol **79 (Pt 10)**: 2419-2424.
Kulkarni, D. D., P. C. James and S. Sulochana (1998). "Assessment of the immune response to duck plague vaccinations." Res Vet Sci **64**(3): 199-204.
Kumar, R., V. Kumar, P. Kekungu, N. N. Barman and S. Kumar (2019). "Evaluation of surface glycoproteins of classical swine fever virus as immunogens and reagents for serological diagnosis of infections in pigs: a recombinant Newcastle disease virus approach." Arch Virol **164**(12): 3007-3017.
Laliberte, J. P., L. W. McGinnes, M. E. Peeples and T. G. Morrison (2006). "Integrity of membrane lipid rafts is necessary for the ordered assembly and release of infectious Newcastle disease virus particles." J Virol **80**(21): 10652-10662.

Laskowski R.A., M. M. W., Moss D.S.,Thornton J.M., (1993). "PROCHECK: a program to check the stereochemical quality of protein structures." J. Appl. Crystallogr. **26 (2)** 283–291.
Lee, C. W., K. Jung, S. J. Jadhao and D. L. Suarez (2008). "Evaluation of chicken-origin (DF-1) and quail-origin (QT-6) fibroblast cell lines for replication of avian influenza viruses." J Virol Methods **153**(1): 22-28.
Leibovitz, L. and J. Hwang (1968). "Duck plague on the American continent." Avian Dis **12**(2): 361-378.
Leland, D. S. and C. C. Ginocchio (2007). "Role of cell culture for virus detection in the age of technology." Clin Microbiol Rev **20**(1): 49-78.
Levy, A. M., O. Gilad, L. Xia, Y. Izumiya, J. Choi, A. Tsalenko, Z. Yakhini, R. Witter, L. Lee, C. J. Cardona and H. J. Kung (2005). "Marek's disease virus Meq transforms chicken cells via the v-Jun transcriptional cascade: a converging transforming pathway for avian oncoviruses." Proc Natl Acad Sci U S A **102**(41): 14831-14836.
Li, N., T. Hong, R. Li, M. Guo, Y. Wang, J. Zhang, J. Liu, Y. Cai, S. Liu, T. Chai and L. Wei (2016). "Pathogenicity of duck plague and innate immune responses of the Cherry Valley ducks to duck plague virus." Sci Rep **6**: 32183.
Li, Y., B. Huang, X. Ma, J. Wu, F. Li, W. Ai, M. Song and H. Yang (2009). "Molecular characterization of the genome of duck enteritis virus." Virology **391**(2): 151-161.
Li, Y., S. van Drunen Littel-van den Hurk, L. A. Babiuk and X. Liang (1995). "Characterization of cell-binding properties of bovine herpesvirus 1 glycoproteins B, C, and D: identification of a dual cell-binding function of gB." J Virol **69**(8): 4758-4768.
Li, Y., S. van Drunen Littel-van den Hurk, X. Liang and L. A. Babiuk (1997). "Functional analysis of the transmembrane anchor region of bovine herpesvirus 1 glycoprotein gB." Virology **228**(1): 39-54.
Lian, B., C. Xu, A. Cheng, M. Wang, D. Zhu, Q. Luo, R. Jia, F. Bi, Z. Chen, Y. Zhou, Z. Yang and X. Chen (2010). "Identification and characterization of duck plague virus glycoprotein C gene and gene product." Virol J **7**: 349.
Liao, Z., L. M. Cimakasky, R. Hampton, D. H. Nguyen and J. E. Hildreth (2001). "Lipid rafts and HIV pathogenesis: host membrane cholesterol is required for infection by HIV type 1." AIDS Res Hum Retroviruses **17**(11): 1009-1019.
Liao, Z., D. R. Graham and J. E. Hildreth (2003). "Lipid rafts and HIV pathogenesis: virion-associated cholesterol is required for fusion and infection of susceptible cells." AIDS Res Hum Retroviruses **19**(8): 675-687.
Lin, W., K. M. Lam and W. E. Clark (1984). "Isolation of an apathogenic immunogenic strain of duck enteritis virus from waterfowl in California." Avian Dis **28**(3): 641-650.
Liu, C., A. Cheng, M. Wang, S. Chen, R. Jia, D. Zhu, M. Liu, K. Sun, Q. Yang and X. Chen (2015). "Duck enteritis virus UL54 is an IE protein primarily located in the nucleus." Virol J **12**: 198.
Liu, J., P. Chen, Y. Jiang, L. Wu, X. Zeng, G. Tian, J. Ge, Y. Kawaoka, Z. Bu and H. Chen (2011). "A duck enteritis virus-vectored bivalent live vaccine provides fast and complete protection against H5N1 avian influenza virus infection in ducks." J Virol **85**(21): 10989-10998.
Liu T, Wang M, Cheng A, Jia R, Yang Q, Wu Y, Liu M, Zhao X, Chen S, Zhang S, Zhu D, Tian B, Rehman MU, Liu Y, Yu Y, Zhang L, Pan L, Chen X (2020). "Duck plague virus gE serves essential functions during the virion final envelopment through influence capsids budding into the cytoplasmic vesicles". Sci Rep.**10**(1):5658.
Liu T, Wang M, Cheng A, Jia R, Wu Y, Yang Q, Zhu D, Chen S, Liu M, Zhao X, Zhang S, Huang J, Mao S, Ou X, Gao Q, Wen X, Sun D, Liu Y, Yu Y, Zhang L, Tian B, Pan L, Chen X (2020). Research

Note: "Duck plague virus glycoprotein I influences cell-cell spread and final envelope acquisition". Poult Sci.(12):6647-6652
Liu T, Cheng A, Wang M, Jia R, Yang Q, Wu Y, Sun K, Zhu D, Chen S, Liu M, Zhao X, Chen X (2017). "RNA-seq comparative analysis of Peking ducks spleen gene expression 24 h post-infected with duck plague virulent or attenuated virus". Vet Res. **13**;48(1):47.
Loura, L. M., M. A. Castanho, A. Fedorov and M. Prieto (2001). "A photophysical study of the polyene antibiotic filipin. Self-aggregation and filipin--ergosterol interaction." Biochim Biophys Acta **1510**(1-2): 125-135.
Lu, X., Y. Xiong and J. Silver (2002). "Asymmetric requirement for cholesterol in receptor-bearing but not envelope-bearing membranes for fusion mediated by ecotropic murine leukemia virus." J Virol **76**(13): 6701-6709.
Luan, P., L. Yang and M. Glaser (1995). "Formation of membrane domains created during the budding of vesicular stomatitis virus. A model for selective lipid and protein sorting in biological membranes." Biochemistry **34**(31): 9874-9883.
Maas, R., D. van Zoelen, H. Oei and I. Claassen (2006). "Replacement of primary chicken embryonic fibroblasts (CEF) by the DF-1 cell line for detection of avian leucosis viruses." Biologicals **34**(3): 177-181.
MacDonald, C. (1990). "Development of new cell lines for animal cell biotechnology." Crit Rev Biotechnol **10**(2): 155-178.
Mackenzie, J. M., A. A. Khromykh and R. G. Parton (2007). "Cholesterol manipulation by West Nile virus perturbs the cellular immune response." Cell Host Microbe **2**(4): 229-239.
Makhija, A. and S. Kumar (2017). "Characterization of duck plague virus stability at extreme conditions of temperature, pH and salt concentration." Biologicals **45**: 102-105.
Makins, C., S. Ghosh, G. D. Roman-Melendez, P. A. Malec, R. T. Kennedy and E. N. Marsh (2016). "Does Viperin Function as a Radical S-Adenosyl-l-methionine-dependent Enzyme in Regulating Farnesylpyrophosphate Synthase Expression and Activity?" J Biol Chem **291**(52): 26806-26815.
Marques CP, Hu S, Sheng W, Lokensgard JR (2006). "Microglial cells initiate vigorous yet non-protective immune responses during HSV-1 brain infection". Virus Res. **121**(1):1-10.
Mardberg, K., E. Trybala, J. C. Glorioso and T. Bergstrom (2001). "Mutational analysis of the major heparan sulfate-binding domain of herpes simplex virus type 1 glycoprotein C." J Gen Virol **82**(Pt 8): 1941-1950.
Marjomaki, V., V. Pietiainen, H. Matilainen, P. Upla, J. Ivaska, L. Nissinen, H. Reunanen, P. Huttunen, T. Hyypia and J. Heino (2002). "Internalization of echovirus 1 in caveolae." J Virol **76**(4): 1856-1865.
Martin-Acebes, M. A., M. Gonzalez-Magaldi, K. Sandvig, F. Sobrino and R. Armas-Portela (2007). "Productive entry of type C foot-and-mouth disease virus into susceptible cultured cells requires clathrin and is dependent on the presence of plasma membrane cholesterol." Virology **369**(1): 105-118.
Martin, J. J., J. Holguera, L. Sanchez-Felipe, E. Villar and I. Munoz-Barroso (2012). "Cholesterol dependence of Newcastle Disease Virus entry." Biochim Biophys Acta **1818**(3): 753-761.
Martinez-Gutierrez, M., J. E. Castellanos and J. C. Gallego-Gomez (2011). "Statins reduce dengue virus production via decreased virion assembly." Intervirology **54**(4): 202-216.
Maxfield, F. R. and D. Wustner (2012). "Analysis of cholesterol trafficking with fluorescent probes." Methods Cell Biol **108**: 367-393.

Mehrbod, P., M. Hair-Bejo, T. A. Tengku Ibrahim, A. R. Omar, M. El Zowalaty, Z. Ajdari and A. Ideris (2014). "Simvastatin modulates cellular components in influenza A virus-infected cells." Int J Mol Med **34**(1): 61-73.
Mehrbod, P., A. R. Omar, M. Hair-Bejo, A. Haghani and A. Ideris (2014). "Mechanisms of action and efficacy of statins against influenza." Biomed Res Int **2014**: 872370.
Moghadasian, M. H. (1999). "Clinical pharmacology of 3-hydroxy-3-methylglutaryl coenzyme A reductase inhibitors." Life Sci **65**(13): 1329-1337.
Mondal, B., T. J. Rasool, H. Ram and S. Mallanna (2010). "Propagation of vaccine strain of duck enteritis virus in a cell line of duck origin as an alternative production system to propagation in embryonated egg." Biologicals **38**(3): 401-406.
Montgomery, R. D., G. Stein, Jr., M. N. Novilla, S. S. Hurley and R. J. Fink (1981). "An outbreak of duck virus enteritis (duck plague) in a captive flock of mixed waterfowl." Avian Dis **25**(1): 207-213.
Moresco, K. A., D. E. Stallknecht and D. E. Swayne (2010). "Evaluation and attempted optimization of avian embryos and cell culture methods for efficient isolation and propagation of low pathogenicity avian influenza viruses." Avian Dis **54**(1 Suppl): 622-626.
Mukerji, A., M. S. Das, B. B. Ghosh and J. L. Ganguly (1965). "Duck plague in West Bengal." Indian Vet J **42**(11): 811-815.
Mukherjee, S., X. Zha, I. Tabas and F. R. Maxfield (1998). "Cholesterol distribution in living cells: fluorescence imaging using dehydroergosterol as a fluorescent cholesterol analog." Biophys J **75**(4): 1915-1925.
Nasr, N., S. Maddocks, S. G. Turville, A. N. Harman, N. Woolger, K. J. Helbig, J. Wilkinson, C. R. Bye, T. K. Wright, D. Rambukwelle, H. Donaghy, M. R. Beard and A. L. Cunningham (2012). "HIV-1 infection of human macrophages directly induces viperin which inhibits viral production." Blood **120**(4): 778-788.
Niu Y, Liu B, Sun C, Zhao L, Chen H (2020). "Construction of the recombinant duck enteritis virus delivering capsid protein VP0 of the duck hepatitis A virus". Vet Microbiol. **249**:108837.
Ohtani, Y., T. Irie, K. Uekama, K. Fukunaga and J. Pitha (1989). "Differential effects of alpha-, beta- and gamma-cyclodextrins on human erythrocytes." Eur J Biochem **186**(1-2): 17-22.
Ohvo, H. and J. P. Slotte (1996). "Cyclodextrin-mediated removal of sterols from monolayers: effects of sterol structure and phospholipids on desorption rate." Biochemistry **35**(24): 8018-8024.
OIE (2012). Manual of diagnostic tests and vaccines for terrestrial animals. Duck virus enteritis. France**:** 555–556.
Pan, H., R. Cao, L. Liu, H. Sun, X. Ji, Y. Chen and P. Chen (2008). "Prokaryotic expression of N-terminal antigenic domain of duck plague virus gB protein and the establishment of putative indirect ELISA assay." Wei Sheng Wu Xue Bao **48**(1): 98-102.
Pazhanivel, N., J. Rajeswar, R. Ramprabhu, S. Manoharan, M. A. Bala, C. Balachandran, K. Kumanan, S. Prathaban and R. Saahithya (2019). "Duck plague outbreak in a Chara-Chemballi duck farm." Iran J Vet Res **20**(4): 308-312.
Peeters, B. P., O. S. de Leeuw, G. Koch and A. L. Gielkens (1999). "Rescue of Newcastle disease virus from cloned cDNA: evidence that cleavability of the fusion protein is a major determinant for virulence." J Virol **73**(6): 5001-5009.
Pessin, J. E. and M. Glaser (1980). "Budding of Rous sarcoma virus and vesicular stomatitis virus from localized lipid regions in the plasma membrane of chicken embryo fibroblasts." J Biol Chem **255**(19): 9044-9050.

Peterson, E. M., B. L. Hughes, S. L. Aarnaes and L. M. de la Maza (1988). "Comparison of primary rabbit kidney and MRC-5 cells and two stain procedures for herpes simplex virus detection by a shell vial centrifugation method." J Clin Microbiol **26**(2): 222-224.
Pichlmair, A., C. Lassnig, C. A. Eberle, M. W. Gorna, C. L. Baumann, T. R. Burkard, T. Burckstummer, A. Stefanovic, S. Krieger, K. L. Bennett, T. Rulicke, F. Weber, J. Colinge, M. Muller and G. Superti-Furga (2011). "IFIT1 is an antiviral protein that recognizes 5'-triphosphate RNA." Nat Immunol **12**(7): 624-630.
Pike, L. J. (2006). "Rafts defined: a report on the Keystone Symposium on Lipid Rafts and Cell Function." J Lipid Res **47**(7): 1597-1598.
Pipalia, N. H., A. Huang, H. Ralph, M. Rujoi and F. R. Maxfield (2006). "Automated microscopy screening for compounds that partially revert cholesterol accumulation in Niemann-Pick C cells." J Lipid Res **47**(2): 284-301.
Plummer, P. J., T. Alefantis, S. Kaplan, P. O'Connell, S. Shawky and K. A. Schat (1998). "Detection of duck enteritis virus by polymerase chain reaction." Avian Dis **42**(3): 554-564.
Pornillos, O., J. E. Garrus and W. I. Sundquist (2002). "Mechanisms of enveloped RNA virus budding." Trends Cell Biol **12**(12): 569-579.
Prip, M., B. Jylling, J. Flensburg and B. Bloch (1983). "An outbreak of duck virus enteritis among ducks and geese in Denmark." Nord Vet Med **35**(11): 385-396.
Pritchard, L. I., C. Morrissy, K. Van Phuc, P. W. Daniels and H. A. Westbury (1999). "Development of a polymerase chain reaction to detect Vietnamese isolates of duck virus enteritis." Vet Microbiol **68**(1-2): 149-156.
Qi, X., X. Yang, A. Cheng, M. Wang, Y. Guo and R. Jia (2009). "Replication kinetics of duck virus enteritis vaccine virus in ducklings immunized by the mucosal or systemic route using real-time quantitative PCR." Res Vet Sci **86**(1): 63-67.
Rahn, E., P. Petermann, M. J. Hsu, F. J. Rixon and D. Knebel-Morsdorf (2011). "Entry pathways of herpes simplex virus type 1 into human keratinocytes are dynamin- and cholesterol-dependent." PLoS One **6**(10): e25464.
Radenkovic D, Chawla S, Pirro M, Sahebkar A, Banach M (2020). "Cholesterol in Relation to COVID-19: Should We Care about It?". J Clin Med.**18**;9(6):1909.
Randall, R. E. and S. Goodbourn (2008). "Interferons and viruses: an interplay between induction, signalling, antiviral responses and virus countermeasures." J Gen Virol **89**(Pt 1): 1-47.
Reed, L. J., Muench, H., (1938). "A simple method of estimating fifty percent endpoints." Am. J. Hygiene **27**: 493–497.
Reichard, K. W., R. M. Lorence, C. J. Cascino, M. E. Peeples, R. J. Walter, M. B. Fernando, H. M. Reyes and J. A. Greager (1992). "Newcastle disease virus selectively kills human tumor cells." J Surg Res **52**(5): 448-453.
Reisinger, K. S., S. L. Block, A. Izu, N. Groth and S. J. Holmes (2009). "Subunit influenza vaccines produced from cell culture or in embryonated chicken eggs: comparison of safety, reactogenicity, and immunogenicity." J Infect Dis **200**(6): 849-857.
Rekha, K., C. Sivasubramanian, I. M. Chung and M. Thiruvengadam (2014). "Growth and replication of infectious bursal disease virus in the DF-1 cell line and chicken embryo fibroblasts." Biomed Res Int **2014**: 494835.
Ren, X., J. Glende, J. Yin, C. Schwegmann-Wessels and G. Herrler (2008). "Importance of cholesterol for infection of cells by transmissible gastroenteritis virus." Virus Res **137**(2): 220-224.

Richter, J., Horzinek, MC. (1993). Duck plague. Virus infections of birds. Amsterdam, Elsevier Science Publishers;.
Rivieccio, M. A., H. S. Suh, Y. Zhao, M. L. Zhao, K. C. Chin, S. C. Lee and C. F. Brosnan (2006). "TLR3 ligation activates an antiviral response in human fetal astrocytes: a role for viperin/cig5." J Immunol **177**(7): 4735-4741.
Rivera-Serrano EE, Gizzi AS, Arnold JJ, Grove TL, Almo SC, Cameron CE (2020). "Viperin Reveals Its True Function". Annu Rev Virol. **29**;7(1):421-446.
Roberts, A. and J. K. Rose (1998). "Recovery of negative-strand RNA viruses from plasmid DNAs: a positive approach revitalizes a negative field." Virology **247**(1): 1-6.
Roizmann, B., R. C. Desrosiers, B. Fleckenstein, C. Lopez, A. C. Minson and M. J. Studdert (1992). "The family Herpesviridae: an update. The Herpesvirus Study Group of the International Committee on Taxonomy of Viruses." Arch Virol **123**(3-4): 425-449.
Rue, C. A. and P. Ryan (2002). "Characterization of pseudorabies virus glycoprotein C attachment to heparan sulfate proteoglycans." J Gen Virol **83**(Pt 2): 301-309.
Santhakumar D, Rohaim MA, Munir M (2019). "Genome-Wide Classification of Type I, Type II and Type III Interferon-Stimulated Genes in Chicken Fibroblasts". Vaccines (Basel). **25**;7(4):160.
Sabara, M. I. and J. E. Larence (2002). "Evaluation of a Japanese quail fibrosarcoma cell line (QT-35) for use in the propagation and detection of metapneumovirus." J Virol Methods **102**(1-2): 73-81.
Sadler, A. J. and B. R. Williams (2007). "Structure and function of the protein kinase R." Curr Top Microbiol Immunol **316**: 253-292.
Sadler, A. J. and B. R. Williams (2008). "Interferon-inducible antiviral effectors." Nat Rev Immunol **8**(7): 559-568.
Saka, H. A. and R. Valdivia (2012). "Emerging roles for lipid droplets in immunity and host-pathogen interactions." Annu Rev Cell Dev Biol **28**: 411-437.
Sandhu, T., Metwally, SA. (2008). Duck virus enteritis (duck plague) In: Diseases of poultry, Blackwell Publishing.
Sandhu, T., Shawky, SA. (2003). Duck virus enteritis (duck plague) Diseases of poultry. Ames (IA), Iowa State University Press.
Sandhu, T. S., and Leibovitz,L. (1997). Duck virus enteritis (duck plague). Ames, Iowa, Diseases of Poultry. Iowa State University Press.
Schaefer-Klein, J., I. Givol, E. V. Barsov, J. M. Whitcomb, M. VanBrocklin, D. N. Foster, M. J. Federspiel and S. H. Hughes (1998). "The EV-O-derived cell line DF-1 supports the efficient replication of avian leukosis-sarcoma viruses and vectors." Virology **248**(2): 305-311.
Schirrmacher, V. and P. Fournier (2009). "Newcastle disease virus: a promising vector for viral therapy, immune therapy, and gene therapy of cancer." Methods Mol Biol **542**: 565-605.
Sekellick, M. J., A. F. Ferrandino, D. A. Hopkins and P. I. Marcus (1994). "Chicken interferon gene: cloning, expression, and analysis." J Interferon Res **14**(2): 71-79.
Sen, G. C. and S. N. Sarkar (2007). "The interferon-stimulated genes: targets of direct signaling by interferons, double-stranded RNA, and viruses." Curr Top Microbiol Immunol **316**: 233-250.
Seo, J. Y., R. Yaneva and P. Cresswell (2011). "Viperin: a multifunctional, interferon-inducible protein that regulates virus replication." Cell Host Microbe **10**(6): 534-539.
Severa, M., E. M. Coccia and K. A. Fitzgerald (2006). "Toll-like receptor-dependent and -independent viperin gene expression and counter-regulation by PRDI-binding factor-1/BLIMP1." J Biol Chem **281**(36): 26188-26195.

Shah, M., M. S. K. Bharadwaj, A. Gupta, R. Kumar and S. Kumar (2019). "Chicken viperin inhibits Newcastle disease virus infection in vitro: A possible interaction with the viral matrix protein." Cytokine **120**: 28-40.
Shah, M. and S. Kumar (2020). "Role of cholesterol in anatid herpesvirus 1 infections in vitro." Virus Res **290**: 198174.
Shaveta, G., J. Shi, V. T. Chow and J. Song (2010). "Structural characterization reveals that viperin is a radical S-adenosyl-L-methionine (SAM) enzyme." Biochem Biophys Res Commun **391**(3): 1390-1395.
Shawky, S. and K. A. Schat (2002). "Latency sites and reactivation of duck enteritis virus." Avian Dis **46**(2): 308-313.
Shawky, S. A. and T. S. Sandhu (1997). "Inactivated vaccine for protection against duck virus enteritis." Avian Dis **41**(2): 461-468.
She, R. C., G. Crist, E. Billetdeaux, J. Langer and C. A. Petti (2006). "Comparison of multiple shell vial cell lines for isolation of enteroviruses: a national perspective." J Clin Virol **37**(3): 151-155.
Simons, K. and D. Toomre (2000). "Lipid rafts and signal transduction." Nat Rev Mol Cell Biol **1**(1): 31-39.
Sinensky, M., L. A. Beck, S. Leonard and R. Evans (1990). "Differential inhibitory effects of lovastatin on protein isoprenylation and sterol synthesis." J Biol Chem **265**(32): 19937-19941.
Singer, S. J. and G. L. Nicolson (1972). "The fluid mosaic model of the structure of cell membranes." Science **175**(4023): 720-731.
Sommereyns, C., S. Paul, P. Staeheli and T. Michiels (2008). "IFN-lambda (IFN-lambda) is expressed in a tissue-dependent fashion and primarily acts on epithelial cells in vivo." PLoS Pathog **4**(3): e1000017.
Spear, P. G., R. J. Eisenberg and G. H. Cohen (2000). "Three classes of cell surface receptors for alphaherpesvirus entry." Virology **275**(1): 1-8.
Spieker, J. O., T. M. Yuill and E. C. Burgess (1996). "Virulence of six strains of duck plague virus in eight waterfowl species." J Wildl Dis **32**(3): 453-460.
Stirnweiss, A., A. Ksienzyk, K. Klages, U. Rand, M. Grashoff, H. Hauser and A. Kroger (2010). "IFN regulatory factor-1 bypasses IFN-mediated antiviral effects through viperin gene induction." J Immunol **184**(9): 5179-5185.
Suh, H. S., M. L. Zhao, M. Rivieccio, S. Choi, E. Connolly, Y. Zhao, O. Takikawa, C. F. Brosnan and S. C. Lee (2007). "Astrocyte indoleamine 2,3-dioxygenase is induced by the TLR3 ligand poly(I:C): mechanism of induction and role in antiviral response." J Virol **81**(18): 9838-9850.
Sun, X. and G. R. Whittaker (2003). "Role for influenza virus envelope cholesterol in virus entry and infection." J Virol **77**(23): 12543-12551.
Surls, J., C. Nazarov-Stoica, M. Kehl, C. Olsen, S. Casares and T. D. Brumeanu (2012). "Increased membrane cholesterol in lymphocytes diverts T-cells toward an inflammatory response." PLoS One **7**(6): e38733.
Swayne D, G. J., McDougald LR, Nolan LK, Suarez DL, Nair VL (2013). Viral infections of waterfowl. Ames (IA), Wiley-Blackwell.
Szymczakiewicz-Multanowska, A., N. Groth, R. Bugarini, M. Lattanzi, D. Casula, A. Hilbert, T. Tsai and A. Podda (2009). "Safety and immunogenicity of a novel influenza subunit vaccine produced in mammalian cell culture." J Infect Dis **200**(6): 841-848.
Tag-El-Din-Hassan, H. T., N. Sasaki, K. Moritoh, D. Torigoe, A. Maeda and T. Agui (2012). "The chicken 2'-5' oligoadenylate synthetase A inhibits the replication of West Nile virus." Jpn J Vet Res **60**(2-3): 95-103.

Takahashi, T. and T. Suzuki (2011). "Function of membrane rafts in viral lifecycles and host cellular response." Biochem Res Int **2011**: 245090.
Takahashi, T., Suzuki, T., (2009). "Role of membrane rafts in viral infection." Open Dermatol. J. **3**: 178–194.
Takeda, K. and S. Akira (2001). "Roles of Toll-like receptors in innate immune responses." Genes Cells **6**(9): 733-742.
Takeuchi, O. and S. Akira (2010). "Pattern recognition receptors and inflammation." Cell **140**(6): 805-820.
Tal-Singer, R., C. Peng, M. Ponce De Leon, W. R. Abrams, B. W. Banfield, F. Tufaro, G. H. Cohen and R. J. Eisenberg (1995). "Interaction of herpes simplex virus glycoprotein gC with mammalian cell surface molecules." J Virol **69**(7): 4471-4483.
Tall, A. R. and L. Yvan-Charvet (2015). "Cholesterol, inflammation and innate immunity." Nat Rev Immunol **15**(2): 104-116.
Tan, K. S., F. Olfat, M. C. Phoon, J. P. Hsu, J. L. C. Howe, J. E. Seet, K. C. Chin and V. T. K. Chow (2012). "In vivo and in vitro studies on the antiviral activities of viperin against influenza H1N1 virus infection." J Gen Virol **93**(Pt 6): 1269-1277.
Tang, H. B., Z. L. Lu, X. K. Wei, T. Z. Zhong, Y. Z. Zhong, L. X. Ouyang, Y. Luo, X. W. Xing, F. Liao, K. K. Peng, C. Q. Deng, N. Minamoto and T. R. Luo (2016). "Viperin inhibits rabies virus replication via reduced cholesterol and sphingomyelin and is regulated upstream by TLR4." Sci Rep **6**: 30529.
Tantaswasdi, U., W. Wattanavijarn, S. Methiyapun, T. Kumagai and M. Tajima (1988). "Light, immunofluorescent and electron microscopy of duck virus enteritis (duck plague)." Nihon Juigaku Zasshi **50**(6): 1150-1160.
Tiwari, A., D. P. Patnayak, Y. Chander and S. M. Goyal (2006). "Permissibility of different cell types for the growth of avian metapneumovirus." J Virol Methods **138**(1-2): 80-84.
Tian B, Cai D, He T, Deng L, Wu L, Wang M, Jia R, Zhu D, Liu M, Yang Q, Wu Y, Zhao X, Chen S, Zhang S, Huang J, Ou X, Mao S, Yu Y, Zhang L, Liu Y, Cheng A (2020). "Isolation and Selection of Duck Primary Cells as Pathogenic and Innate Immunologic Cell Models for Duck Plague Virus". Front Immunol. **28**;10:3131.
Trybala, E., T. Bergstrom, D. Spillmann, B. Svennerholm, S. J. Flynn and P. Ryan (1998). "Interaction between pseudorabies virus and heparin/heparan sulfate. Pseudorabies virus mutants differ in their interaction with heparin/heparan sulfate when altered for specific glycoprotein C heparin-binding domain." J Biol Chem **273**(9): 5047-5052.
Van Dorssen, C., Kunst, H. (1955). "Susceptibility of ducks and various other waterfowl to duck plague virus " Tijdschr Diergeneeskd **80**: 1286–1295.
Vastag, L., E. Koyuncu, S. L. Grady, T. E. Shenk and J. D. Rabinowitz (2011). "Divergent effects of human cytomegalovirus and herpes simplex virus-1 on cellular metabolism." PLoS Pathog **7**(7): e1002124.
Varshney P, Yadav V, Saini N (2016). "Lipid rafts in immune signalling: current progress and future perspective". Immunology. **149**(1):13-24.
Vesikari, T., A. Forsten, K. H. Herbinger, G. D. Cioppa, J. Beygo, A. Borkowski, N. Groth, M. Bennati and F. von Sonnenburg (2012). "Safety and immunogenicity of an MF59((R))-adjuvanted A/H5N1 pre-pandemic influenza vaccine in adults and the elderly." Vaccine **30**(7): 1388-1396.
Viard, M., I. Parolini, M. Sargiacomo, K. Fecchi, C. Ramoni, S. Ablan, F. W. Ruscetti, J. M. Wang and R. Blumenthal (2002). "Role of cholesterol in human immunodeficiency virus type 1 envelope protein-mediated fusion with host cells." J Virol **76**(22): 11584-11595.

Vidor, E., C. Meschievitz and S. Plotkin (1997). "Fifteen years of experience with Vero-produced enhanced potency inactivated poliovirus vaccine." Pediatr Infect Dis J **16**(3): 312-322.
Vigil, A., O. Martinez, M. A. Chua and A. Garcia-Sastre (2008). "Recombinant Newcastle disease virus as a vaccine vector for cancer therapy." Mol Ther **16**(11): 1883-1890.
Vigil, A., M. S. Park, O. Martinez, M. A. Chua, S. Xiao, J. F. Cros, L. Martinez-Sobrido, S. L. Woo and A. Garcia-Sastre (2007). "Use of reverse genetics to enhance the oncolytic properties of Newcastle disease virus." Cancer Res **67**(17): 8285-8292.
Walker, J. W., C. J. Pfow, S. S. Newcomb, W. D. Urban, H. E. Nadler and L. N. Locke (1969). "Status of duck virus enteritis (duck plague) in the United States." Proc Annu Meet U S Anim Health Assoc **73**: 254-279.
Walker PJ, Siddell SG, Lefkowitz EJ, Mushegian AR, Adriaenssens EM, Dempsey DM, Dutilh BE, Harrach B, Harrison RL, Hendrickson RC, Junglen S, Knowles NJ, Kropinski AM, Krupovic M, Kuhn JH, Nibert M, Orton RJ, Rubino L, Sabanadzovic S, Simmonds P, Smith DB, Varsani A, Zerbini FM, Davison AJ (2020). "Changes to virus taxonomy and the Statutes ratified by the International Committee on Taxonomy of Viruses" . Arch Virol. 2020 Nov;165(11):2737-2748.
Wang, G., Y. Qu, F. Wang, D. Hu, L. Liu, N. Li, R. Yue, C. Li and S. Liu (2013). "The comprehensive diagnosis and prevention of duck plague in northwest Shandong province of China." Poult Sci **92**(11): 2892-2898.
Wang, H., A. D. Quiroga and R. Lehner (2013). "Analysis of lipid droplets in hepatocytes." Methods Cell Biol **116**: 107-127.
Wang J, Osterrieder N (2011). "Generation of an infectious clone of duck enteritis virus (DEV) and of a vectored DEV expressing hemagglutinin of H5N1 avian influenza virus". Virus Res. **159**(1):23-31.
Wang, X., E. R. Hinson and P. Cresswell (2007). "The interferon-inducible protein viperin inhibits influenza virus release by perturbing lipid rafts." Cell Host Microbe **2**(2): 96-105.
Wen, Y., A. Cheng, M. Wang, H. Ge, C. Shen, S. Liu, J. Xiang, R. Jia, D. Zhu, X. Chen, B. Lian, H. Chang and Y. Zhou (2010). "A Thymidine Kinase recombinant protein-based ELISA for detecting antibodies to Duck Plague Virus." Virol J **7**: 77.
Wiederstein, M. and M. J. Sippl (2007). "ProSA-web: interactive web service for the recognition of errors in three-dimensional structures of proteins." Nucleic Acids Res **35**(Web Server issue): W407-410.
Wobeser, G. (1987). "Experimental duck plague in blue-winged teal and Canada geese." J Wildl Dis **23**(3): 368-375.
Wolf, K., C. N. Burke and M. C. Quimby (1974). "Duck viral enteritis: microtiter plate isolation and neutralization test using the duck embryo fibroblast cell line." Avian Dis **18**(3): 427-434.
Wolf, K., C. N. Burke and M. C. Quimby (1976). "Duck viral enteritis: a comparison of replication by CCL-141 and primary cultures of duck embryo fibroblasts." Avian Dis **20**(3): 447-454.
Wong, S. S. and R. J. Webby (2013). "Traditional and new influenza vaccines." Clin Microbiol Rev **26**(3): 476-492.
Wozniakowski, G. and E. Samorek-Salamonowicz (2014). "First survey of the occurrence of duck enteritis virus (DEV) in free-ranging Polish water birds." Arch Virol **159**(6): 1439-1444.
Wu, Y., A. Cheng, M. Wang, Q. Yang, D. Zhu, R. Jia, S. Chen, Y. Zhou, X. Wang and X. Chen (2012). "Complete genomic sequence of Chinese virulent duck enteritis virus." J Virol **86**(10): 5965.

Wu, Y., A. Cheng, M. Wang, S. Zhang, D. Zhu, A. B. Jia, B. Q. Luo, Z. Chen and X. Chen (2011). "Serologic detection of duck enteritis virus using an indirect ELISA based on recombinant UL55 protein." Avian Dis **55**(4): 626-632.
Wu, Y., A. Cheng, M. Wang, S. Zhang, D. Zhu, R. Jia, Q. Luo, Z. Chen and X. Chen (2011). "Establishment of real-time quantitative reverse transcription polymerase chain reaction assay for transcriptional analysis of duck enteritis virus UL55 gene." Virol J **8**: 266.
Wu, Y., A. Cheng, M. Wang, D. Zhu, R. Jia, S. Chen, Y. Zhou and X. Chen (2012). "Comparative genomic analysis of duck enteritis virus strains." J Virol **86**(24): 13841-13842.
Wu, Y., J. He, Y. An, X. Wang, Y. Liu, S. Yan, X. Ye, J. Qi, S. Zhu, Q. Yu, J. Yin, D. Li and W. Wang (2016). "Recombinant Newcastle disease virus (NDV/Anh-IL-2) expressing human IL-2 as a potential candidate for suppresses growth of hepatoma therapy." J Pharmacol Sci **132**(1): 24-30.
Wu, Y., J. He, J. Geng, Y. An, X. Ye, S. Yan, Q. Yu, J. Yin, Z. Zhang and D. Li (2017). "Recombinant Newcastle disease virus expressing human TRAIL as a potential candidate for hepatoma therapy." Eur J Pharmacol **802**: 85-92.
Xie L, Xie Z, Huang L, Wang S, Huang J, Zhang Y, Zeng T, Luo S (2017). "A polymerase chain reaction assay for detection of virulent and attenuated strains of duck plague virus". J Virol Methods.**249**:66-68.
Xie T, Feng M, Dai M, Mo G, Ruan Z, Wang G, Shi M, Zhang X (2019). "Cholesterol-25-hydroxylase Is a Chicken ISG That Restricts ALV-J Infection by Producing 25-hydroxycholesterol". Viruses. **30**;11(6):498.
Xu, X., Q. Sun, X. Yu and L. Zhao (2017). "Rescue of nonlytic Newcastle Disease Virus (NDV) expressing IL-15 for cancer immunotherapy." Virus Res **233**: 35-41.
Xuefeng, Q., Y. Xiaoyan, C. Anchun, W. Mingshu, Z. Dekang and J. Renyong (2008). "The pathogenesis of duck virus enteritis in experimentally infected ducks: a quantitative time-course study using TaqMan polymerase chain reaction." Avian Pathol **37**(3): 307-310.
Yang, C., J. Li, Q. Li, L. Li, M. Sun, H. Li, Y. Xia, H. Yang and K. Yu (2015). "Biological properties of a duck enteritis virus attenuated via serial passaging in chick embryo fibroblasts." Arch Virol **160**(1): 267-274.
Yang, F. L., W. X. Jia, H. Yue, W. Luo, X. Chen, Y. Xie, W. Zen and W. Q. Yang (2005). "Development of quantitative real-time polymerase chain reaction for duck enteritis virus DNA." Avian Dis **49**(3): 397-400.
Yang, J., R. Yan, A. Roy, D. Xu, J. Poisson and Y. Zhang (2015). "The I-TASSER Suite: protein structure and function prediction." Nat Methods **12**(1): 7-8.
Yaqoob, P. (2009). "The nutritional significance of lipid rafts." Annu Rev Nutr **29**: 257-282.
Yogev, O., D. Lagos, T. Enver and C. Boshoff (2014). "Kaposi's sarcoma herpesvirus microRNAs induce metabolic transformation of infected cells." PLoS Pathog **10**(9): e1004400.
Yu, S., C. Yin, K. Song, S. Li, G. L. Zheng, L. F. Li, J. Wang, Y. Li, Y. Luo, Y. Sun and H. J. Qiu (2019). "Engagement of cellular cholesterol in the life cycle of classical swine fever virus: its potential as an antiviral target." J Gen Virol **100**(2): 156-165.
Yuan, G. P., A. C. Cheng, M. S. Wang, F. Liu, X. Y. Han, Y. H. Liao and C. Xu (2005). "Electron microscopic studies of the morphogenesis of duck enteritis virus." Avian Dis **49**(1): 50-55.
Zhang, Q., H. Ke, A. Blikslager, T. Fujita and D. Yoo (2018). "Type III Interferon Restriction by Porcine Epidemic Diarrhea Virus and the Role of Viral Protein nsp1 in IRF1 Signaling." J Virol **92**(4).
Zhang, Y. and J. Skolnick (2004). "SPICKER: a clustering approach to identify near-native protein folds." J Comput Chem **25**(6): 865-871.

Zhang, Y. and J. Skolnick (2005). "TM-align: a protein structure alignment algorithm based on the TM-score." Nucleic Acids Res **33**(7): 2302-2309.
Zhou, H., S. Chen, M. Wang and A. Cheng (2014). "Interferons and their receptors in birds: a comparison of gene structure, phylogenetic analysis, and cross modulation." Int J Mol Sci **15**(11): 21045-21068.
Zhu, H., J. P. Cong and T. Shenk (1997). "Use of differential display analysis to assess the effect of human cytomegalovirus infection on the accumulation of cellular RNAs: induction of interferon-responsive RNAs." Proc Natl Acad Sci U S A **94**(25): 13985-13990.
Zhu, L., X. Ding, J. Tao, J. Wang, X. Zhao and G. Zhu (2010). "Critical role of cholesterol in bovine herpesvirus type 1 infection of MDBK cells." Vet Microbiol **144**(1-2): 51-57.
Zhu, X., J. Y. Lee, J. M. Timmins, J. M. Brown, E. Boudyguina, A. Mulya, A. K. Gebre, M. C. Willingham, E. M. Hiltbold, N. Mishra, N. Maeda and J. S. Parks (2008). "Increased cellular free cholesterol in macrophage-specific Abca1 knock-out mice enhances pro-inflammatory response of macrophages." J Biol Chem **283**(34): 22930-22941.
Zhu, X., M. M. Westcott, X. Bi, M. Liu, K. M. Gowdy, J. Seo, Q. Cao, A. K. Gebre, M. B. Fessler, E. M. Hiltbold and J. S. Parks (2012). "Myeloid cell-specific ABCA1 deletion protects mice from bacterial infection." Circ Res **111**(11): 1398-1409.
Ziedler, K. and A. Hlinak (1992). "The occurrence of virus enteritis (duck plague) in wild birds." Berl Munch Tierarztl Wochenschr **105**(4): 122-125.

Research Achievements
Publications

Thesis

1. **Shah M**, Kumar S. Adaptation and characterization of Anatid herpesvirus 1 in different permissible cell lines; *Biologicals*; 2021 Apr; 70:1-6.
2. **Shah M,** Kumar S. Role of cholesterol in anatid herpesvirus 1 infections in vitro. *Virus Research*; 2020 Dec; 290:198174.
3. **Shah M,** Bharadwaj MSK, Gupta A, Kumar R, Kumar S. Chicken viperin inhibits Newcastle disease virus infection in vitro: A possible interaction with the viral matrix protein. *Cytokine*; 2019 Aug; 120:28-40.

Others

4. Sarmah H, **Shah M,** Pathak M, Barman NN, Koul M, Gupta A, Sahariah PJ, Neher S, Das SK, Gogoi SM, Kumar S. Pathodynamics of Circulating Strains of Duck Enteritis Virus: A Step Forward to Understand Its Pathogenesis; *Avian Diseases*. 2020 Jun; 64(2):166-173. **(Equal Contribution)**.
5. Ganar K, **Shah M**, Kamdi BP, Kurkure NV, Kumar S. Molecular characterization of chicken anemia virus outbreaks in Nagpur province, India from 2012 to 2015. *Microbial Pathogenesis*. 2017 Jan; 102:113-119.
6. Morla S, **Shah M**, Kaore M, Kurkure NV, Kumar S. Molecular characterization of genotype XIIIb Newcastle disease virus from central India during 2006-2012: Evidence of its panzootic potential. *Microbial Pathogenesis*. 2016 Oct; 99:83-86.
7. Mondal S, Kumar V, Chowdhury SR, Shah M, Gaur A, Kumar S, and Iyer PK. Template-Mediated Detoxification of Low-Molecular-Weight Amyloid Oligomers and Regulation of Their Nucleation Pathway. *ACS Applied Bio Materials*. 2019 2 (12), 5306-5312.
8. Akhtar N, Pradhan N, Saha A, Kumar V, Biswas O, Dey S, **Shah M**, Kumar S, Manna D. Tuning the Solubility of the Ionophores: Glutathione-Mediated Transport of Chloride Ion across the Membranes. *Chemical Communication*. 2019, 55, 8482-8485.
9. Mondal S, Chowdhury SR., **Shah M**, Kumar V, Kumar S, and Iyer PK. Nanoparticle Assisted Regulation of Nucleation Pathway of Amyloid Tetramer and Inhibition of Their Fibrillation Kinetics. *ACS Applied Bio Material*. 2019, 2, 5, 2137–2142.
10. Patwa R, Soundararajan N, Mulchandani N, Bhasney SM, **Shah M**, Kumar S, Kumar A, Katiyar V. Silk nano-discs: A natural material for cancer therapy. *Biopolymers*. 2018 Nov;109(11): e23231.
11. Gupta A, Mulchandani N, **Shah M**, Kumar S, Katiyar V. Functionalized chitosan mediated stereocomplexation of poly (lactic acid): Influence on crystallization, oxygen permeability, wettability and biocompatibility behavior. *Polymer*. 2017, 142: 196-208.
12. Gupta A, Prasad A, Mulchandani N, Shah M, Sankar MR, Kumar S, and Katiyar V. Multifunctional Nanohydroxyapatite-Promoted Toughened High-Molecular-Weight Stereocomplex Poly (lactic acid)-Based Bionanocomposite for Both 3D-Printed Orthopedic Implants and High-Temperature Engineering Applications. *ACS Omega*. 2017 2 (7), 4039-4052.

13. Kalita S, Kalita S, Paul A, **Shah M**, Kumar S, Mandal B. Site-Specific Single Point Mutation by Anthranilic Acid in hIAPP8-37 Enhances Anti-Amyloidogenic Activity. *RSC Chemical Biology*. 2021 2:266-273.
14. Shokeen K, Pandey S, **Shah M**, Kumar S. Insight towards the effect of the multibasic cleavage site of SARS-CoV-2 spike protein on cellular proteases. *bioRxiv* 2020.04.25.061507.

GeneBank Submissions:

- NCBI GenBank Accession number **KY856894** - *Gallus gallus* viperin mRNA, complete CDS. 2019
- NCBI GenBank Accession number **KX377124-KX377130** – Complete genome sequence of seven chicken anemia virus isolated from Nagpur, India. 2017

Conference Proceedings

1. **Research Conclave Indian Institute of Technology Guwahati, Assam.** 2019
   Shah, M., et al. Chicken viperin inhibits Newcastle Disease virus infection: A possible interaction with viral matrix protein
2. **27th International Conference of Virology INTERVIROCON, PGIMER, Chandigarh.** 2018
   Shah, M., et al. Chicken viperin inhibits Newcastle Disease virus infection: A possible interaction with viral matrix protein.
3. **International Conference on "Global Perspectives in Virus Diseases Management" VIROCON, IIHR, Bengaluru** 2016
   Shah, M., et al. Viperin: A potential target for Newcastle Disease virus infection.
4. **57th Annual conference of Association of Microbiologists of India, Gauhati University, Guwahati, Assam.** 2016
   Shah, M., et al. Viperin: A potential target for Newcastle Disease virus infection.

Workshop Attended and organized

1. International Seminar cum Workshop on "Computer-aided drug design for human pathogen (CADDHP), Tezpur University, Assam. 2018
2. 9th Flow cytometry workshop on flow application in basics, applied and clinical biology, IIT Guwahati, Assam. 2016
3. Organized Workshop on Diagnostic Approaches in Virology: Recent Advancements, IIT Guwahati, Assam 2018-20